

**ENGINEERING OF POLYMERS TO THICKEN CARBON DIOXIDE:  
A SYSTEMATIC APPROACH**

by

**Sevgi Kilic**

BS, Chemical Engineering, Hacettepe University, 1994

MS, Chemical Engineering, The Pennsylvania State University, 1998

Submitted to the Graduate Faculty of  
the School of Engineering in partial fulfillment  
of the requirements for the degree of  
Doctor of Philosophy

University of Pittsburgh

2003

**UNIVERSITY OF PITTSBURGH**

**SCHOOL OF ENGINEERING**

This dissertation was presented

by

**Sevgi Kilic**

It was defended on

October 9, 2003

and approved by

Robert M. Enick, Professor, Chemical and Petroleum Engineering Department

J. Karl Johnson, Associate Professor, Chemical and Petroleum Engineering Department

Toby Chapman, Associate Professor, Department of Chemistry

Dissertation Director: Eric J. Beckman, Chairman and Professor, Chemical and Petroleum  
Engineering Department

**ENGINEERING OF POLYMERS TO THICKEN CARBON DIOXIDE:  
A SYSTEMATIC APPROACH**

Sevgi Kilic, Ph.D.

University of Pittsburgh, 2003

Carbon dioxide (CO<sub>2</sub>) is one of the potential displacing fluids used in Enhanced Oil Recovery (EOR). However, the effective use of CO<sub>2</sub> in EOR is hindered by its low viscosity, resulting in CO<sub>2</sub> to “finger” towards production well and thus low sweep efficiency. The current research has aimed to bring the viscosity of CO<sub>2</sub> to a level comparable to that of oil via dissolution of polymeric materials (thickeners) to suppress early breakthrough of CO<sub>2</sub> in EOR. A series of fluoroacrylate-aromatic acrylate copolymers was designed and tested for their miscibility and viscosity enhancement in CO<sub>2</sub> at 295 K. The change in the series was created by changing either the spacer length or the size of aromatic rings in the aromatic acrylate unit of the copolymer. Aforementioned copolymers were found to be highly miscible with CO<sub>2</sub> and to impart enhancement in the viscosity of CO<sub>2</sub>, depending on the type and content of the aromatic acrylate unit in the copolymer. Increase in the viscosity was attributed to association of aromatic rings by stacking.

Feasibility of EOR process depends also on the factors associated with economic and environmental issues. The current research, therefore, also aimed to explore the generation of low-cost, non-fluorous polymers to replace high cost fluoroacrylate moiety. The polymers were designed hypothesizing that a CO<sub>2</sub>-philic polymer should possess inherently low cohesive energy density, low glass transition temperature (i.e. high chain flexibility and free volume) and a number of Lewis base groups to promote cross interactions with CO<sub>2</sub>. Polymers were prepared, where possible, via modification of an existing polymer with a precursor containing Lewis base group to eliminate the effect of chain length on the phase behavior. Modifications were performed basically on silicone, polyether or hydrocarbon backbone (vinyl and allyl). The phase behavior results showed that there is a delicate balance between the forces working to increase the miscibility pressures (e.g. high cohesive energy density) or factors suppressing the entropy of mixing, and those working to lower miscibility pressures, such as enhanced specific interactions with CO<sub>2</sub> and increased free volume or chain flexibility.

## TABLE OF CONTENTS

ACKNOWLEDGMENTS .....	xvi
1.0 INTRODUCTION .....	1
1.1 CARBON DIOXIDE AS A FLOODING AGENT IN ENHANCED OIL RECOVERY ..	1
2.0 BACKGROUND .....	5
2.1 PREVIOUS ATTEMPTS TO DECREASE THE MOBILITY OF CO <sub>2</sub> .....	5
2.2 MILESTONES IN THE DEVELOPMENT OF CO <sub>2</sub> -PHILIC MATERIALS .....	10
3.0 RESEARCH OBJECTIVE AND APPROACH .....	15
3.1 RESEARCH OBJECTIVE .....	15
3.2 RESEARCH APPROACH FOR CO <sub>2</sub> -THICKENERS .....	17
3.2.1 Stacking of Aromatic Rings:.....	17
3.2.2 Design Strategy for CO <sub>2</sub> -Direct Thickeners: .....	20
3.3 RESEARCH APPROACH FOR CO <sub>2</sub> -PHILIC POLYMERS .....	22
3.3.1 Heuristics on Miscibility of Materials with CO <sub>2</sub> : .....	22
3.3.2 Design Strategy for CO <sub>2</sub> -Philic Polymers: .....	28
4.0 ACRYLATE COPOLYMERS AS CO <sub>2</sub> -DIRECT THICKENERS .....	30
4.1 EXPERIMENTAL PROTOCOL.....	30
4.1.1 Materials: .....	30
4.1.2 Synthesis of Copolymers of Styrene with Fluoroacrylate and its Sulfonation: .....	31
4.1.3 Synthesis of Aromatic Acrylate Monomers:.....	32

4.1.4	Synthesis of Copolymers of Aromatic Acrylates with Fluoroacrylate:.....	34
4.1.5	Synthesis of Copolymers of Cyclohexyl Acrylate with Fluoroacrylate: .....	35
4.1.6	Structural Characterization: .....	35
4.1.7	Phase Behavior Measurements: .....	38
4.1.8	Solution Relative Viscosity Measurements: .....	40
4.2	PHASE BEHAVIOR RESULTS OF COPOLYMERS IN DENSE CO <sub>2</sub> .....	44
4.3	VISCOSITY BEHAVIOR RESULTS OF COPOLYMERS IN DENSE CO <sub>2</sub> .....	54
4.4	CONCLUSIONS.....	70
5.0	EFFECT OF GRAFTED LEWIS BASE GROUPS ON THE PHASE BEHAVIOR OF MODEL POLY (DIMETHYL SILOXANES) IN CO <sub>2</sub> .....	73
5.1	INTRODUCTION .....	73
5.2	EXPERIMENTAL PROTOCOL.....	74
5.2.1	Materials: .....	74
5.2.2	Synthesis of Lewis Base Grafted Siloxane Polymers:.....	75
5.2.3	Structural Characterization: .....	76
5.2.4	Phase Behavior Measurements: .....	77
5.3	PHASE BEHAVIOR RESULTS OF LEWIS BASE GRAFTED SILOXANE POLYMERS .....	79
5.4	CONCLUSIONS.....	95
6.0	EVALUATION OF PHASE BEHAVIOR OF NITROGEN CONTAINING POLYMERS IN CO <sub>2</sub> .....	97
6.1	INTRODUCTION .....	97
6.2	EXPERIMENTAL PROTOCOL.....	98

6.2.1 Materials: .....	98
6.2.2 Polymerization of N,N-dimethylacrylamide:.....	98
6.2.3 Synthesis of Poly(propylethyleneimine):.....	99
6.2.4 Preparation of Poly(propylmethylacrylate ethyleneimines): .....	101
6.2.5 Phase Behavior Measurements: .....	101
6.3 PHASE BEHAVIOR RESULTS OF NITROGEN CONTAINING POLYMERS .....	102
7.0 EFFECT OF BACKBONE TYPE AND ETHER OXYGEN ON PHASE BEHAVIOR OF POLYMERS IN CO <sub>2</sub> .....	108
7.1 INTRODUCTION .....	108
7.2 EXPERIMENTAL PROTOCOL.....	109
7.2.1 Materials: .....	109
7.2.2 Synthesis of Poly(allyl alcohol) via Reduction:.....	109
7.2.3 Synthesis of Poly(allyl acetate):.....	111
7.2.4 Synthesis of Partially Sulfinate-functionalized Poly(propylene glycol):.....	111
7.2.5 Synthesis of Poly(propylene oxide)-dimethyl ether: .....	113
7.2.6 Phase Behavior Measurements: .....	115
7.3 PHASE BEHAVIOR RESULTS OF THE POLYMERS IN CO <sub>2</sub> .....	115
7.4 CONCLUSIONS.....	130
8.0 SUMMARY .....	131
9.0 FUTURE WORK.....	134
A <sup>1</sup> H-NMR SPECTRA OF COPOLYMERS IN CHAPTER 4 .....	143
B <sup>1</sup> H-NMR AND FT-IR SPECTRA OF SILICONE POLYMERS (CHAPTER 5) .....	146
C <sup>1</sup> H-NMR SPECTRA OF NITROGEN CONTAINING POLYMERS (CHAPTER 6) .....	150

D	<sup>1</sup> H-NMR SPECTRA OF THE POLYMERS IN CHAPTER 7.....	154
	BIBLIOGRAPHY .....	157

## LIST OF TABLES

Table 4.1 General Structure of the Fluoroacrylate-Aromatic Acrylate copolymers.....	37
Table 4.2 Number of “m” and “n” in the aromatic acrylates used in this study .....	46
Table 5.1 Methylhydrosiloxane-dimethylsiloxane copolymers <sup>(a)</sup> used in this study.....	74
Table 6.1 Structure of Polymers Possessing Nitrogen.....	106
Table 7.1 Surface tension and glass transition temperature of the polymers used to assess .....	122

## LIST OF FIGURES

Figure 1.1 Change of viscosity of CO <sub>2</sub> with temperature at different pressures. ....	3
Figure 1.2 CO <sub>2</sub> Flooding in EOR: (a) Ideal case, (b) Actual behavior. ....	4
Figure 3.1 Packing of molecules in crystalline benzene, showing: a. a stereoview of the overall structure; b. the shortest C-H distances in A <sup>o</sup> (representative of an H $\cdots$ p interactions ..... 19	19
Figure 3.2 Structure of fluoroacrylate monomer .....	20
Figure 3.3 General Structure of Aromatic Acrylate-Fluoroacrylate Copolymers .....	22
Figure 4.1 Phase Behavior of Sulfonated and Unsulfonated Styrene-Fluoroacrylate Copolymer in CO <sub>2</sub> at T=295 K (St: Styrene, FA: Fluoroacrylate, S.St: Sulfonated Styrene) 1) 11%St-89%FA, 2) 0.1%S.St -10.9%St-89%FA .....	45
Figure 4.2 Phase Behavior of PHA-FA Copolymer in CO <sub>2</sub> at T=295 K (PHA: Phenyl Acrylate, n=0, m=1; FA: Fluoroacrylate) 1) 31%PHA-69%FA, 2) 29%PHA-71%FA, 3) 26%PHA-74%FA, 4) 23%PHA-77%FA. ....	47
Figure 4.3 Phase Behavior of BEA-FA Copolymer in CO <sub>2</sub> at T=295 K (BEA: Benzyl Acrylate, n=1, m=1; FA: Fluoroacrylate), 1) 54%BEA-46%FA, 2) 38%BEA-62%FA, 3) 27%BEA-73%FA, 4) 29%BEA-71%FA, 5) 18%BEA-82%FA, 6) 21%BEA-79%FA .....	48
Figure 4.4 Phase Behavior of PEA-FA Copolymer in CO <sub>2</sub> at T=295 K (PEA: Phenyl ethyl acrylate, n=2, m=1; FA: Fluoroacrylate), 1) 36%PEA-64%FA, 2) 24%PEA-76%FA, 3) 26%PEA-74%FA, 4) 25%PEA-75%FA, 5) 29%PEA-71%FA.....	49
Figure 4.5 Effect of spacer length on the phase behavior of copolymers in CO <sub>2</sub> at T=295 K (PHA: Phenyl acrylate, n=0, m=1; BEA: Benzyl acrylate, n=1, m=1; PEA: Phenyl ethyl acrylate, n=2, m=1; FA: Fluoroacrylate), 1) 29%PHA-71%FA, 2) 29%BEA-71%FA, 3) 29%PEA-71%FA. ....	50

Figure 4.6 Phase Behavior of NA-FA Copolymer in CO <sub>2</sub> at T=295 K (NA: Naphthyl acrylate, n=0, m=2; FA: Fluoroacrylate), 1) 32%NA-68%FA, 2) 17%NA-83%FA, 3) 22%NA-78%FA, 4) 19%NA-81%FA .....	51
Figure 4.7 Phase Behavior of NA-FA and PHA-FA Copolymers in CO <sub>2</sub> at T=295 K (NA: Naphthyl acrylate; n=0, m=2; PHA: Phenyl acrylate, n=0, m=1, FA: Fluoroacrylate), 1) 32%NA-68%FA, 2) 31%PHA-69%FA, 3) 22%NA-78%FA, 4) 23%PHA-77%FA .....	52
Figure 4.8 Phase Behavior of NA-FA, CHA-FA and PHA-FA Copolymers in CO <sub>2</sub> at T=295 K (CHA: Cyclohexyl acrylate, NA: Naphthyl acrylate; n=0, m=2; PHA: Phenyl acrylate, n=0, m=1, FA: Fluoroacrylate), 1) 22%NA-88%FA, 2) 22%CHA-78%FA, 3) 23%PHA-77%FA .....	53
Figure 4.9 Relative viscosity of Sulfonated and Unsulfonated Styrene-Fluoroacrylate Copolymer Solutions in CO <sub>2</sub> as a function of concentration at T=295 K and P=41.4 MPa (St: Styrene, FA: Fluoroacrylate, S.St: Sulfonated Styrene), 1) 0.1%S.St-10.9%St-89%FA, 2) 11%St-89%FA.....	55
Figure 4.10 Relative viscosity of x%PHA-y%FA copolymer solutions in CO <sub>2</sub> as a function of concentration at T=295 K at varying copolymer composition, P=41.4 MPa, (PHA: Phenyl Acrylate, n=0, m=1; FA: Fluoroacrylate), 1) 29%PHA-71%FA, 2) 26%PHA-74%FA, 3) 23%PHA-77%FA, 4) 31%PHA-69%FA.....	56
Figure 4.11 Relative viscosity of x%BEA-y%FA copolymer solutions in CO <sub>2</sub> as a function of concentration at T=295 K at varying copolymer composition, P=41.4 MPa, (BEA: Benzyl Acrylate, n=1, m=1; FA: Fluoroacrylate), 1) 18%BEA-82%FA, 2) 21%BEA-79%FA, 3) 27%BEA-73%FA, 4) 29%BEA-71%FA, 5) 38%BEA-62%FA, 6) 54%BEA-46%FA.....	57
Figure 4.12 Relative viscosity of x%PEA-y%FA copolymer solutions in CO <sub>2</sub> as a function of concentration at T=295 K at varying copolymer composition, P=41.4 MPa, (PEA: Phenyl ethyl acrylate, n=2, m=1; FA: Fluoroacrylate), 1) 24%PEA-76%FA, 2) 36%PEA-64%FA, 3) 25%PEA-75%FA, 4) 26%PEA-74%FA, 5) 29%PEA-71%FA .....	58
Figure 4.13 Effect of spacer length on CO <sub>2</sub> -viscosity enhancement of copolymer solutions as a function of concentration at T=295 K and P= 41.4 MPa, (BEA: Benzyl Acrylate, n=1, m=1; PHA: Phenyl acrylate, n=0, m=1; PEA: Phenyl ethyl acrylate, n=2, m=1; FA: Fluoroacrylate), 1) 29%PHA-71%FA, 2) 29%PEA-71%FA, 3) 29%BEA-71%FA .....	60
Figure 4.14 The effect of pressure on relative viscosity of 29%PHA-71%FA copolymer solutions in CO <sub>2</sub> as a function of concentration at T=295 K (PHA: Phenyl Acrylate, n=0, m=1; FA: Fluoroacrylate), 1) P=41.4 MPa, 2) P=34.5 MPa, 3) P=27.6 MPa, 4) P=20.7 MPa. ....	62

Figure 4.15 Comparison of aromatic and non-aromatic rings on CO <sub>2</sub> -viscosity enhancement at similar compositions at T=295 K and P=41.4 MPa as a function of concentration (PHA: Phenyl Acrylate; CHA: Cyclohexyl Acrylate; FA: Fluoroacrylate), 1) 26%PHA-74%FA, 2) 27%CHA-73%FA. ....	63
Figure 4.16 Comparison of aromatic and non-aromatic rings on CO <sub>2</sub> -viscosity enhancement at their optimum composition at T=295 K and P=41.4 MPa as a function of concentration (PHA: Phenyl Acrylate; CHA: Cyclohexyl Acrylate; FA: Fluoroacrylate), 1) 29%PHA-71%FA, 2) 16%CHA-84%FA. ....	64
Figure 4.17 Comparison of effect of size of aromatic rings on viscosity enhancement ability of CO <sub>2</sub> at similar compositions at T=295 K and P=41.4 MPa as a function of concentration (PHA: Phenyl acrylate; NA: Naphthyl acrylate; FA: Fluoroacrylate), 1) 23%PHA-77%FA, 2) 22%NA-78%FA. ....	65
Figure 4.18 Comparison of effect of size of aromatic rings on viscosity enhancement ability of CO <sub>2</sub> at their optimum compositions at T=295 K and P= 41.4 MPa as a function of concentration (PHA: Phenyl acrylate; NA: Naphthyl acrylate; FA: Fluoroacrylate), 1) 29%PHA-71%FA, 2) 32%NA-68%FA. ....	66
Figure 4.19 Relative viscosity of x%NA-y%FA copolymer solutions in CO <sub>2</sub> as a function of concentration at T=295 K at varying copolymer composition, and P=41.4 MPa, (NA: Naphthyl Acrylate, n=0, m=2; FA: Fluoroacrylate), 1) 32%NA-68%FA, 2) 19%NA-81%FA, 3) 17%NA-83%FA, 4) 22%NA-78%FA. ....	69
Figure 4.20 The effect of pressure on relative viscosity of 32%NA-68%FA copolymer solutions in CO <sub>2</sub> as a function of concentration at T=295 K (NA: Naphthyl Acrylate, n=0, m=2; FA: Fluoroacrylate), 1) 41.4 MPa, 2) 34.5 MPa, 3) 27.6 MPa, 4) 20.7 MPa. ..	70
Figure 5.1 Phase behavior of functionalized (z=5) siloxane copolymers, 1) methyl butyrate (MB), 2) propyl acetate (PA), at 295 K. ....	81
Figure 5.2 Phase behavior of functionalized (z=5) siloxane copolymers 1) butyl methyl ketone (BMK), 2) propyl acetate (PA), at 295 K. ....	82
Figure 5.3 CO <sub>2</sub> -carbonyl interactions having a) C <sub>2v</sub> b) C <sub>s</sub> symmetry. ....	84
Figure 5.4 Phase behaviors of functionalized (z=5) siloxane copolymers, 1) propyl methyl carbonate (PMC), 2) propyl acetate (PA) at 295 K. ....	86
Figure 5.5 Comparison of phase behaviors of hydromethyl-dimethyl siloxane copolymers at varying functionality with a total of 25 repeat units, at 295 K, 1) z=2, 2) z=0, 3) z=1. ....	87
Figure 5.6 Phase behavior of propyl acetate (PA)-functionalized siloxane copolymers at different degree of substitution 1) z=11, 2) z=1, 3) z=2, 4) z=5, at 295 K. ....	88

Figure 5.7 Phase behaviors of methyl butyrate (MB)- functionalized siloxane copolymers at different degree of substitution 1) $z=11$ , 2) $z=2$ , 3) $z=5$ , 4) $z=1$ , at 295 K. ....	89
Figure 5.8 Phase behavior of propyl ethyl ether- functionalized siloxane copolymers at different degree of substitution 1) $z=11$ , 2) $z=5$ , 3) $z=1$ , 4) $z=2$ , at 295 K. ....	89
Figure 5.9 Phase behaviors of ( $z=2$ ) functional siloxane copolymers with 1) Propyl acetate (PA), 2) Butyl methyl ketone (BMK), 3) Propyl ethyl ether (PEE) at 295 K.....	92
Figure 5.10 Phase behaviors of ( $z=5$ ) functional siloxane copolymers with 1) Propyl ethyl ether (PEE), 2) Butyl methyl ketone (BMK), 3) Propyl acetate (PA), at 295 K.....	93
Figure 5.11 Comparison of phase behaviors of 1) ( $z=1$ ) propyl dimethyl amine- functional (PDA), 2) ( $z=5$ ) propyl acetate (PA)- functional siloxane copolymers at 295 K. ....	94
Figure 7.1 Schematic for reduced and functionalized poly(epichlorohydrin) (PECH) .....	117
Figure 7.2 Schematic for hypothesized steric hindrance in ether- functionalized PPO's (repulsive effects indicated by arrows) .....	118
Figure 7.3 Structure of poly(allyl acetate) .....	119
Figure 7.4 Phase behavior of 1) PP-425, <sup>124</sup> 2) Poly(propylene glycol)- monomethylether, $M_w=1000$ , at 295 K. ....	123
Figure 7.5 Effect of location of oxygen (backbone versus side chain) in the polymer on phase behavior: 1) PPO-DME 3500, 2) PVME -3850 at 295 K. ....	124
Figure 7.6 Effect of length of side chain on phase behavior in vinyl ether polymers, 1) PVME 3850, 2) PVEE-3800, <sup>124</sup> at 295 K.....	126
Figure 7.7 Phase behavior of (1) PPO-DME 3500 (2) PVEE 3800 <sup>124</sup> at 295 K.....	127
Figure 7.8 Comparison of phase behavior of 1) PVAc-7700, <sup>56</sup> 2) PVEE-3800, <sup>124</sup> 3) PVAc-3090, <sup>56</sup> at 295 K.....	129
Figure 9.1 (a) Poly(vinyl acetate-co-aromatic acrylate), (b) Poly(vinyl acetate-co-aromatic acetate) .....	135
Figure 9.2 Structure of poly(isobutylene oxide) .....	136
Figure 9.3 Structure of (a) poly(vinyl acetate-co-vinyl ethyl ether), (b) poly(vinyl acetate-co-isobutylene oxide). ....	137
Figure 9.4 Structure of Poly(vinyl sulfonate) .....	138

Figure 9.5 Structure of (a) Poly(vinyl sulfonate-co-vinyl ethyl ether), (b) Poly(vinyl sulfonate-co-isobutylene oxide). .....	138
Figure 9.6 Poly(vinyl ethyl ketone) .....	139
Figure 9.7 Reaction scheme for synthesis of substituted poly(oxetane)s. ....	140
Figure 9.8 Structure of Poly(oxetane).....	140
Figure 9.9 Poly(methylated ethyleneimine-co-acetylated ethyleneimine) .....	141
Figure A.1 <sup>1</sup> H-NMR spectrum of St-FA Copolymer in Freon. ....	143
Figure A.2 <sup>1</sup> H-NMR spectrum of 29%PHA-71% Copolymer in Freon.....	143
Figure A.3 <sup>1</sup> H-NMR spectrum of 21%BEA-79%FA Copolymer in Freon.....	144
Figure A.4 <sup>1</sup> H-NMR spectrum of 29%PEA-71%FA Copolymer in Freon .....	144
Figure A.5 <sup>1</sup> H-NMR spectrum of 17%NA-83%FA Copolymer in Freon.....	145
Figure A.6 <sup>1</sup> H-NMR spectrum of 27%CHA-73%FA Copolymer in Freon.....	145
Figure B.1 FT-IR spectrum for a) methylhydrosiloxane (16.5mole %)-dimethylsiloxane (83.5mole%) copolymer, b) Propyl acetate functionalized siloxane copolymer. The peak at 2157 cm <sup>-1</sup> in Figure 1.a corresponds to Si-H stretching. ....	146
Figure B.2 <sup>1</sup> H NMR spectrum (300 MHz, CDCl <sub>3</sub> ) of a) MethylHydrosiloxane (16.5mole %) - Dimethylsiloxane (83.5mole%) copolymer, The peak at 4.7 ppm corresponds to Si-H. b) (z=5) PA-functionalized siloxane copolymer .....	147
Figure B.3 <sup>1</sup> H-NMR spectrum of (z=5) MB-functional siloxane copolymer in CDCl <sub>3</sub> .....	148
Figure B.4 <sup>1</sup> H-NMR spectrum of (z=5) PMC-functional siloxane copolymer in CDCl <sub>3</sub> .....	148
Figure B.5 <sup>1</sup> H-NMR spectrum of (z=5) PDA-functional siloxane copolymer in CDCl <sub>3</sub> .....	149
Figure C.1 <sup>1</sup> H-NMR Spectrum of Poly(N,N-dimethyl acrylamide) in C <sub>6</sub> D <sub>6</sub> .....	150
Figure C.2 FT-IR spectrum of Poly(2-ethyl-2-oxazoline), Mw=5000 (Scientific Polymers, Inc.) .....	151
Figure C.3 FT-IR spectrum of Poly(propylethyleneimine) .....	151
Figure C.4 <sup>1</sup> H-NMR spectrum of Poly(2-ethyl-2-oxazoline), Mw=5000 (SP <sup>2</sup> Inc.).....	152

Figure C.5 $^1\text{H-NMR}$ spectrum of Poly(propylethyleneimine) in $\text{CDCl}_3$ .....	152
Figure C.6 $^1\text{H-NMR}$ spectrum of PPMAEI in $\text{CDCl}_3$ .....	153
Figure D.1 $^1\text{H-NMR}$ spectrum of poly(allyl alcohol) in $\text{D}_2\text{O}$ .....	154
Figure D.2 $^1\text{H-NMR}$ spectrum of poly(allyl acetate) in $\text{C}_6\text{D}_6$ .....	154
Figure D.3 FT-IR spectrum of poly(propylene glycol), $M_w=3500$ (Aldrich) .....	155
Figure D.4 FT-IR spectrum of poly(propylene oxide) dimethylether .....	155
Figure D.5 $^1\text{H-NMR}$ ( $\text{CDCl}_3$ ) spectrum of poly(propylene glycol), $M_w=3500$ .....	156
Figure D.6 $^1\text{H-NMR}$ ( $\text{CDCl}_3$ ) spectrum of poly(propylene oxide) dimethylether .....	156

## ACKNOWLEDGMENTS

It is a great pleasure that I have now the opportunity to express my gratitude to the people who contributed their efforts in accomplishment of this work. First, I would like to thank Dr. Eric Beckman, my Ph.D. advisor, for his valuable suggestions, creative discussions and encouragement during the course of this study. I appreciate his efforts to teach his students to see the “big picture” and his respect to other’s ideas.

Special thanks to all my friends for their moral support and the fun times we shared together. I also would like to thank Yang Wang for the ab initio calculation results. Many thanks are also in order for the staff of the chemical engineering department for their behind-the-scenes work.

I would like to thank the committee members, Dr. R. Enick, Dr. K. Johnson, and Dr. T. Chapman, for serving in my doctoral committee and for their helpful comments and suggestions.

I would like to thank the US Department of Energy and National Science Foundation for the financial support.

Lastly, but not the least, I would like to express my deep gratitude to my husband, Ekrem, for his constant genuine support, love and understanding, and to my parents for their unlimited love, sacrifices, and continuous support from overseas.

## **1.0 INTRODUCTION**

### **1.1 CARBON DIOXIDE AS A FLOODING AGENT IN ENHANCED OIL RECOVERY**

After application of primary (recovery under natural reservoir pressure) and secondary production (recovery by artificial maintenance of pressure by water, called waterflooding) of petroleum, much of the oil still remains behind in place due to inefficiency of these recovery processes. With the increasing demand for petroleum versus limited resources, the discovery of more advanced techniques is needed. Newly developed techniques fall under the broad heading of Enhanced Oil Recovery (EOR). The aim in EOR is to increase the production of crude oil beyond the limit recoverable by primary and secondary production methods. CO<sub>2</sub>, being as the second least expensive flooding fluid after water, has been used in Enhanced Oil Recovery for many years. CO<sub>2</sub> is non-flammable, non-toxic, capable of developing miscibility with crude oil and classified as non-volatile organic compound. As well as the above features, its low cost, availability in large quantities from natural reservoirs and environmentally benign nature have maintained its popularity as an EOR fluid. Advantageously, it is in the gaseous state at atmospheric conditions. Therefore, CO<sub>2</sub> can be separated from the oil by simply releasing the pressure after the recovery.

In CO<sub>2</sub> flooding (also called CO<sub>2</sub> miscible displacement), carbon dioxide is injected into the oil-bearing porous media at reservoir temperature, which is usually between 25 °C and 120 °C. The pressure of CO<sub>2</sub> is maintained above the minimum miscibility pressure to ensure its solvency with oil. Thus, unlike water flooding in secondary oil recovery, CO<sub>2</sub> can dynamically develop effective miscibility with petroleum oil and therefore displace the oil left behind by waterflooding.

The foremost disadvantage of CO<sub>2</sub> as an oil-displacing agent is its low viscosity, 0.03-0.10 cP at reservoir conditions (Figure 1.1) while the oil to be displaced has viscosity of 0.1-50 cP. The low viscosity of CO<sub>2</sub> results in its higher mobility (defined as permeability/viscosity of that fluid in porous media) compared to that of reservoir oil, causing the mobility ratio (defined as the ratio of mobility of displacing fluid to the fluid which is being displaced) to be greater than one. High values of the mobility ratio means that displacing fluid, i.e. CO<sub>2</sub>, moves more easily than the displaced fluid. As a result, the carbon dioxide tends to “finger” towards production wells without contacting much of the oil in the reservoir, resulting in low sweep efficiency (Figure 1.2). Even though high displacement efficiency is attained for the oil contacted, because of the fingering, much of the oil is by-passed. For maximum displacement efficiency, the mobility ratio should be  $\leq 1$ . The mobility ratio can be made smaller, i.e. improved, by lowering the viscosity of oil, increasing the viscosity of the displacing fluid CO<sub>2</sub>, increasing the effective permeability to oil, or decreasing the effective permeability to the displacing fluid CO<sub>2</sub>. The most feasible way to lower the mobility ratio is to co-inject water and CO<sub>2</sub>, thereby lowering the relative permeability of CO<sub>2</sub> by decreasing its saturation. This technique prolongs the duration of the CO<sub>2</sub> flood. Further, the high water saturation results in mass transfer limitations of CO<sub>2</sub>

contacting oil. We proposed to eliminate the need to co-inject water by increasing the viscosity of displacing fluid CO<sub>2</sub>.

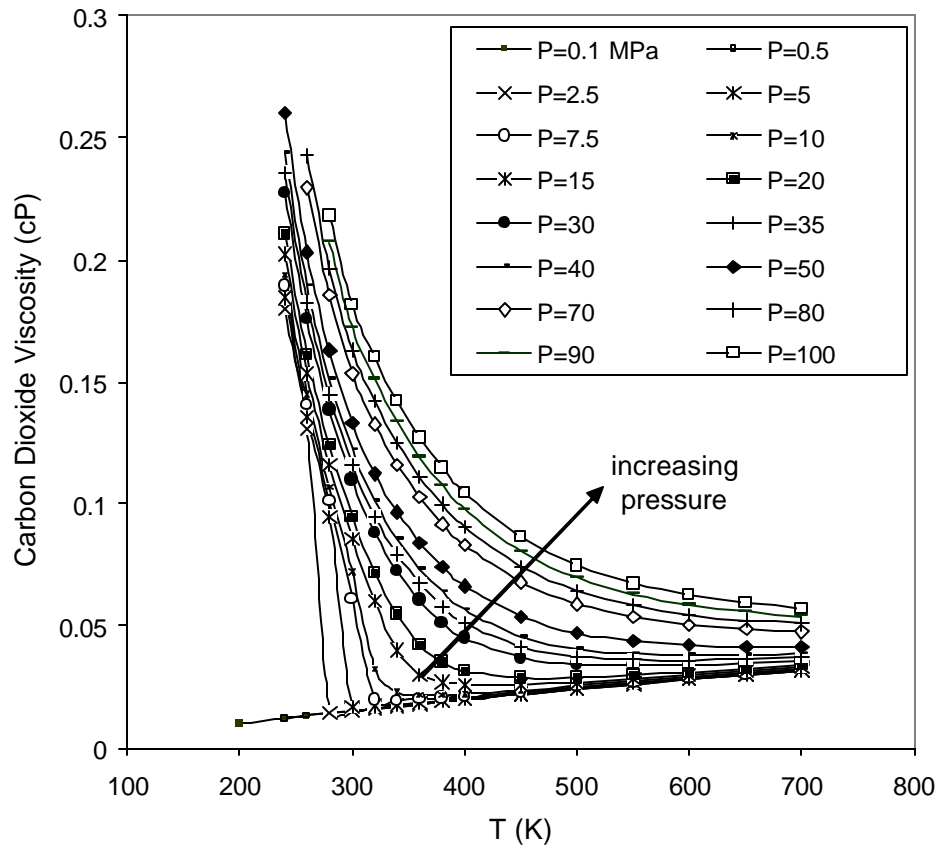
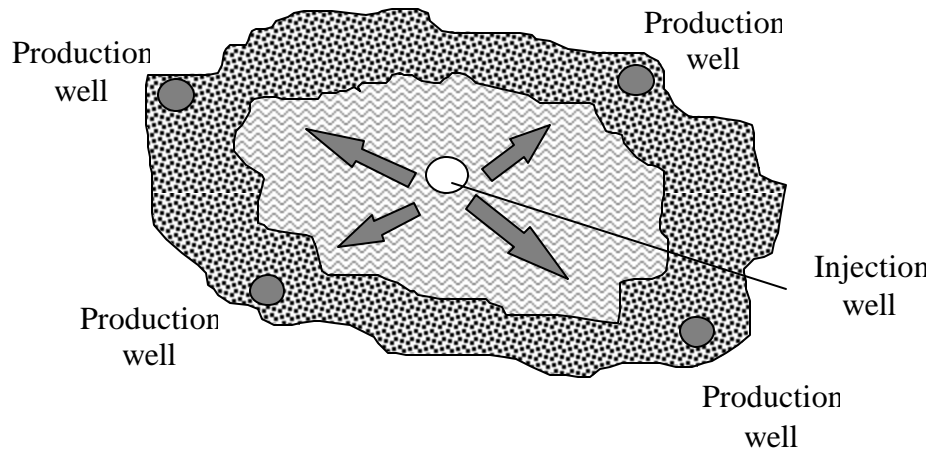
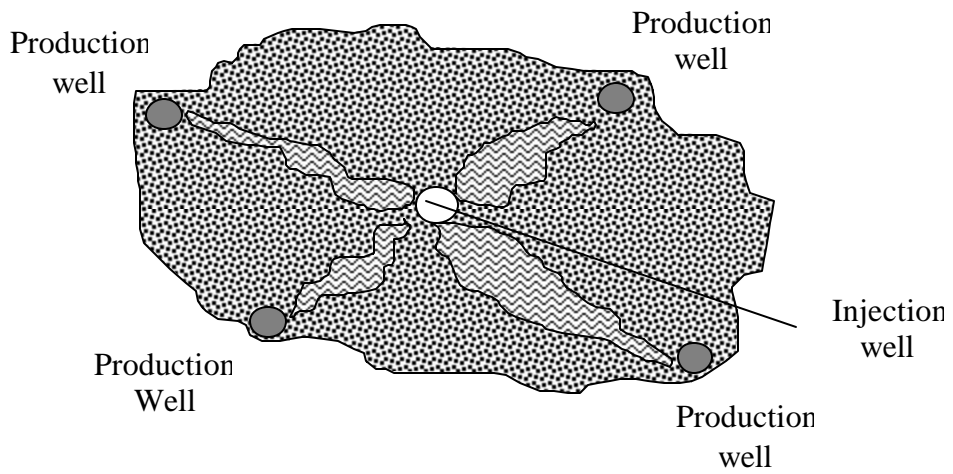


**Figure 1.1** Change of viscosity of CO<sub>2</sub> with temperature at different pressures.<sup>1</sup>



(a) CO<sub>2</sub> Flooding: Ideal Case



(b) CO<sub>2</sub> Flooding: Actual Behavior

**Figure 1.2** CO<sub>2</sub> Flooding in EOR: (a) Ideal case, (b) Actual behavior.<sup>2</sup>

## **2.0 BACKGROUND**

### **2.1 PREVIOUS ATTEMPTS TO DECREASE THE MOBILITY OF CO<sub>2</sub>**

In last two decades, a number of attempts have been made to identify a thickener for carbon dioxide to decrease its mobility and thus increase greatly the quantity of producible oil during EOR. A thickener that would be considered as a candidate for EOR should be inexpensive, safe and stable at reservoir conditions. Furthermore, it should remain in the CO<sub>2</sub>-rich phase rather than partitioning into the brine or oil or absorbing onto the porous media while the level of viscosity increase is easily controlled by the concentration of the thickening agent.

Heller et al. were the first group to study and report data on use of direct thickeners for dense CO<sub>2</sub>. They evaluated the effect of viscosity increasing capability of commercially available polymers.<sup>3,4,5</sup> None of the polymers that they tested was successful enough to induce viscosity enhancement in CO<sub>2</sub> due to extremely low solubility of these polymers. Nevertheless, they made some generalizations for features of polymers soluble in CO<sub>2</sub>. They have found that for a polymer to be able to dissolve in CO<sub>2</sub>, the polymer should be amorphous and irregular in structure to maximize the entropy of mixing. Taking these findings into consideration, they subsequently synthesized polymers with various molecular weights in their laboratory. Although

they were slightly more soluble, these polymers did not promote any significant increase in the viscosity. One important result that they reported, however, was that higher molecular weight polymers are much more effective in viscosifying CO<sub>2</sub> than equivalent mass concentrations of lower molecular weight polymers.

Heller and co-workers also studied the possibility of using hydrocarbon based telechelic ionomers as effective thickeners for dense CO<sub>2</sub>. Telechelic ionomers are polymers with low molecular weight and ionic groups at each end of the polymer chain. These compounds are known to have a thickening ability in light alkanes via association of ionic groups forming a pseudo-network structure. However, their effort to thicken CO<sub>2</sub> via sulfonated polyisobutylene failed due to the low solubility of alkyl based ionomers in dense CO<sub>2</sub>, leading to no increase in viscosity.<sup>6</sup>

Carbon dioxide exhibits miscibility with the light components of crude oil, but CO<sub>2</sub> can be immiscible with the higher molecular weight species of crude oil. Therefore, miscibility is developed as CO<sub>2</sub> strips the light oils from the crude near the injection well. This enriched fluid can exhibit miscibility with oil in the reservoir. Llave et al. developed the idea of adding an entrainer to CO<sub>2</sub>.<sup>7,8</sup> The entrainer serves as a miscible additive (co-solvent) that modifies the phase behavior of carbon dioxide and enhances the solubility of viscous crude oil components in the CO<sub>2</sub>-rich phase. The presence of the entrainer itself increases the density and viscosity of the gas phase. This would result in a more rapid development of miscibility providing further improvement in the mobility. Although the viscosity increased substantially with the addition of entrainer, i.e. 1565 % at 44 mole % 2-ethylhexanol, this much cosolvent is not economically

acceptable for EOR. The increase at low concentration of entrainer was very low; for example, 6 % viscosity increase with 0.5 mole % of 2-ethylhexanol.

Irani and co-workers considerably increased the viscosity of CO<sub>2</sub> by using commercially available silicone polymers.<sup>9,10,11</sup> However, large amounts of toluene had to be introduced as a cosolvent to enable the polymer to dissolve. For example, they reported that the increase in viscosity is around 90-fold for neat CO<sub>2</sub> with a mixture of 6-wt% polymer, namely polydimethyl siloxane, 20 wt % toluene and 74 wt % CO<sub>2</sub> at 130 °F and 2500 psi. In their published work, they demonstrated that the use of viscous CO<sub>2</sub> in corefloods accelerated oil recovery and delayed the early breakthrough of CO<sub>2</sub>.

Normal micelles and microemulsions in aqueous solutions are known to be capable of increasing solution viscosity. Enick et al. extended this idea to CO<sub>2</sub> solutions and attempted to increase the viscosity by using commercially available surfactants.<sup>12,13,14,15</sup> None of the commercially available surfactants were found to be soluble in CO<sub>2</sub>.

In the literature, it was also reported that low molecular weight compounds could associate in solution via secondary forces to form a pseudo network structure, resulting in significant increase in the viscosity of the solvent. Dunn and Oldfield reported that tri-n-butyltin fluoride could increase the viscosity of light alkanes by forming linear polymer chains via dipole-dipole interactions between the fluorine and tin of adjacent molecules.<sup>16</sup> Disappointingly, this compound was only very slightly soluble in CO<sub>2</sub> (<2 wt.%) and it did not have any effect on viscosity. In order to enhance its solubility in CO<sub>2</sub>, pentane was used as cosolvent. Several orders

of magnitude CO<sub>2</sub>-viscosity enhancement was obtained using 1 wt % tri-n-butyltin fluoride, but only using large amounts (~50 mole %) of pentane.<sup>12</sup>

Enick et al. showed that the CO<sub>2</sub>-solubility of a hydrocarbon compound can be improved by fluorination of an alkane or alkyl chain.<sup>17</sup> Semifluorinated alkanes were demonstrated to be good gelation agents for alkanes, forming microfibrillar networks. Several CO<sub>2</sub>/semifluorinated alkane systems were tested for gel formation, yet the resulting gels were not single, viscous, transparent phases, but rather semifluorinated alkane microfibers, with the liquid CO<sub>2</sub> filling the cavities. This type of gelling agent is not desirable for flow in porous media,<sup>17</sup> where a stable, transparent, single phase of high viscosity is required.

Heller and co-workers presented the gelation results of a variety of organic fluids and supercritical CO<sub>2</sub> with 12-hydroxystearic acid (HSA). In the absence of any cosolvent, HSA is insoluble in dense CO<sub>2</sub>. However, with the addition of a significant amount of cosolvent, such as 10-15 % ethanol, HSA was found to be completely soluble in CO<sub>2</sub>, while forming translucent or opaque gels.<sup>18</sup>

Terry et al. attempted to increase the viscosity of CO<sub>2</sub> by in-situ polymerization of monomers miscible with CO<sub>2</sub>. Authors polymerized the light olefins in an environment of supercritical CO<sub>2</sub> using commonly available initiators. However, the resultant polymers were insoluble in CO<sub>2</sub>.<sup>19</sup>

In summary, it is clear that none of the traditional hydrocarbon thickeners or commercially available compounds are good candidates for CO<sub>2</sub> thickening. Success has been hindered due to insolubility of these compounds in dense CO<sub>2</sub> or the requirement of a large amount of co-solvent. Economically and environmentally, it is desirable to have the thickener dissolved in dense CO<sub>2</sub> without a need for a cosolvent. Therefore, these results prompted researchers to design and synthesize thickeners specifically for CO<sub>2</sub>. For a polymer to be able to be a good candidate for thickening, solubility in CO<sub>2</sub> is first needed.

In the last decade, with the identification of CO<sub>2</sub>-philic functionalities, successful design of CO<sub>2</sub> thickeners became possible. DeSimone and coworkers reported that silicones and fluoropolymers exhibit higher degree of solubility in CO<sub>2</sub> at moderate pressures and temperatures than other non-fluorous polymers.<sup>20,21,22</sup> In a subsequent publication, they reported that solubility of a CO<sub>2</sub>-phobic polymer could also be achieved if a certain amount of CO<sub>2</sub>-philic character is introduced in the polymer chain.<sup>23</sup> Not long ago, DeSimone published the first work in the literature for CO<sub>2</sub> direct thickener without a need for a cosolvent. They observed that approximately 5-10 wt % of fluoroacrylate polymer, namely poly (1,1-dihydroperfluorooctyl acrylate), caused 3-8 fold increase in CO<sub>2</sub>-viscosity as measured with a falling cylinder viscometer.<sup>24</sup>

Shi et al. synthesized CO<sub>2</sub>-soluble fluorinated polyurethane telechelic disulfates with molecular weights up to 29,900. Their results showed that a concentration of 4 wt % of the aforementioned polymer increases the solution viscosity 2.7 fold relative to neat CO<sub>2</sub> at room

temperature and 34.5 MPa. Above 4 wt %, the polymer, however, was found to be insoluble in CO<sub>2</sub>.<sup>25</sup>

Fluoroacrylate-styrene random copolymers create a greater increase in CO<sub>2</sub>-viscosity.<sup>26</sup> The increase in viscosity was attributed to stacking of aromatic rings of the styrene repeats (aromatic ring association). The increase in viscosity was found to depend on the composition of the copolymer, where a 29 mole% styrene-71mole% fluoroacrylate copolymer was found as the optimum composition for maximum viscosity increase. Further increases in composition decreased viscosity due likely to intramolecular interactions rather than intermolecular interactions being formed. The maximum increase at this optimum composition was found to be 250 fold at a concentration of 5-wt% copolymer at room temperature and 34.5 MPa. However, 10-100 folds increase in viscosity at dilute polymer concentrations and low shear rates, which is our target, remain as a challenge to be investigated.

## **2.2 MILESTONES IN THE DEVELOPMENT OF CO<sub>2</sub>-PHILIC MATERIALS**

The possibility for the use of carbon dioxide as a process solvent has been widely investigated because CO<sub>2</sub> is an environmentally benign, inexpensive and abundant material. Solubility parameter studies using equation of state data once suggested that CO<sub>2</sub> possesses the solvent power of short n-alkanes,<sup>27</sup> and it was hoped that CO<sub>2</sub> could be used to replace an array of environmentally unfriendly non-polar organic solvents. Although CO<sub>2</sub> initially looked to be useful only for non-polar materials, it was thought that polar materials could be brought into

solution by adding conventional alkyl-functional surfactants to the mixture. However, early attempts to put these surfactants to use were hindered due to the poor solubility of the amphiphiles in CO<sub>2</sub>. The fact that these amphiphiles showed adequate solubility in short alkanes such as ethane and propane and were quite insoluble in CO<sub>2</sub><sup>28</sup> revealed a gap between theoretical models and experimental data for CO<sub>2</sub> solubility. Johnston and colleagues suggested polarizability/free volume as a better method of evaluating solvent power,<sup>29,30</sup> and by this method CO<sub>2</sub> is seen to be a very poor solvent when compared to short n-alkanes.

The solvent quality of CO<sub>2</sub> has also been investigated experimentally. Francis tested the phase behavior of more than 250 compounds in ternary systems containing liquid CO<sub>2</sub>.<sup>31</sup> Hyatt presented an extensive study of phase behavior of more than 30 organic compounds in liquid CO<sub>2</sub> to attempt to draw comparisons between CO<sub>2</sub> and organic solvents.<sup>32</sup> Phase behavior studies showed that CO<sub>2</sub> is a reasonably good solvent for aldehydes, ketones, esters and low alcohols, but higher alcohols (C>10), aromatic alcohols, polar compounds such as amides, ureas, urethanes exhibit poor solubility in CO<sub>2</sub>. Hydroquinone and multihydroxy compounds were found to be insoluble in the aforementioned study. Heller and coworkers evaluated, the miscibility of commercially available polymers with CO<sub>2</sub> in an attempt to find a polymer to control the mobility of CO<sub>2</sub> during Enhanced Oil Recovery (EOR) operations.<sup>4</sup> They reported that tacticity plays an important role in determining the miscibility of a polymer in CO<sub>2</sub>. For example, they found that although atactic poly(butene) and poly(propylene oxide) are miscible with CO<sub>2</sub>, isotactic polymers are not. It was also found that the presence of aliphatic side chains reduces the miscibility pressures significantly, but on the other hand, the presence of aromatic groups in a polymer raises miscibility pressures drastically. They also reported that the presence of amide,

carbonate, ester and hydroxyl groups in the polymer imparts immiscibility to a polymer with CO<sub>2</sub>, while ester and ether groups in the side chain do not have a detrimental effect on miscibility.

A number of groups continued the search for materials that would be soluble in CO<sub>2</sub> at significantly lower pressures than similarly sized alkyl-functional equivalents, and it was found that some fluorinated materials were miscible with CO<sub>2</sub> at relatively low pressures.<sup>33,34,35,36,37</sup> Harrison et al. synthesized a hybrid alkyl/fluoroalkyl surfactant that dissolved in CO<sub>2</sub> and solubilized a significant amount of water.<sup>22</sup> Through fluorination, even CO<sub>2</sub>-insoluble hydrocarbon polymers could be rendered miscible with CO<sub>2</sub>.<sup>13,38</sup> In addition, dispersion polymerization of methyl methacrylate in CO<sub>2</sub> was supported by block polymers containing fluorinated acrylate monomers,<sup>39</sup> leading to the generation of monodisperse, micron-sized spheres. Other developments using fluoro-functional amphiphiles followed, including emulsion polymerization,<sup>40</sup> protein extraction,<sup>41,42</sup> and heavy metal extraction from soil and water.<sup>43</sup>

Without question, perfluoropolyacrylates are the most CO<sub>2</sub>-philic polymers discovered to date. Their thermodynamic compatibility with CO<sub>2</sub> might be attributed to their low cohesive energy density and relatively low glass transition temperature. McHugh et al have conducted extensive studies on the impact of fluorination on the CO<sub>2</sub>-solubility of macromolecules.<sup>44</sup> They argue that fluorination itself does not ensure the miscibility of a polymer with CO<sub>2</sub> at moderately low temperatures and pressures. They found, for example, that poly(vinylidene fluoride-co-22.0 mol% hexafluoropropylene) is miscible with CO<sub>2</sub> at substantially lower pressures than poly(tetrafluoroethylene-co-19.3 mol% hexafluoropropylene). Because poly(vinylidene fluoride-

co-22.0 mol% hexafluoropropylene) contains a polar vinylidene unit, they concluded that a polymer should exhibit polarity upon fluorination, to create favorable dipole-quadrupole interactions, thus shielding quadrupole-quadrupole interactions between two CO<sub>2</sub> molecules.<sup>36</sup> In a recent paper, McHugh et al. suggested again that solubility of fluorinated polybutadiene and polyisoprene in CO<sub>2</sub> is possible not only due to fluorination, but due to induced polarity created by incorporating CF<sub>2</sub> moieties across the double bonds of the polymers.<sup>45</sup> In another recent paper, they examined the effect various side chains on miscibility pressures of siloxane polymers in CO<sub>2</sub>.<sup>46</sup> It was found that, although poly(dimethylsiloxane) is miscible with CO<sub>2</sub> at 40 °C and 300 bar, poly(methylpropoxynonyl siloxane) was not miscible below 1200 bar at 200 °C, despite the polar character gained by the propenoxy group. They ascribed this result to a reduction in polarity of the polymer due to the long alkyl tail of the side chain, and unfavorable interactions between the alkyl chain and CO<sub>2</sub>. It was also found that, not unexpectedly, fluorinating the siloxane polymer dramatically lowers the pressures needed to maintain the single phase.

The addition of carbonyl groups to lower miscibility pressures of materials in CO<sub>2</sub> has been of considerable interest. Kazarian et al. used FT-IR spectroscopy to show that carbonyl groups in polymers exhibit specific interactions with CO<sub>2</sub>.<sup>47</sup> Carbonyl-CO<sub>2</sub> interactions were calculated at the molecular level for small molecules,<sup>48,49</sup> which showed that the strength of the CO<sub>2</sub>-carbonyl interactions depends on the geometry of the interaction. Sarbu et al. hypothesized that addition of carbonyl groups to polyethers might lower miscibility pressures with CO<sub>2</sub>; results with ether-carbonate copolymers showed that addition of carbonyl groups lowered miscibility pressures to a point lower than those of fluoroether polymers of equivalent chain

length.<sup>50,51</sup> However, the miscibility pressures of perfluoroacrylate polymers in CO<sub>2</sub> are still substantially lower than those of the ether-carbonate copolymers. Recently, Xiao and colleagues showed that addition of carbonyl groups to triphenyl phosphine ligands allowed the creation of CO<sub>2</sub>-soluble organometallic catalysts.<sup>52</sup> Wallen and colleagues,<sup>53</sup> as well as Hamilton et al.,<sup>54</sup> showed that peracetylated monosaccharides and cyclodextrins are also miscible with CO<sub>2</sub>, although miscibility pressures for the cyclodextrins are substantially higher than those of the simple sugars.

Although addition of carbonyl groups might appear to be a general strategy for lowering miscibility pressures of materials in CO<sub>2</sub>, effects other than strength of interaction between carbonyls and CO<sub>2</sub> must also be considered. For example, Rindfleisch et al.,<sup>55</sup> as well as Enick and colleagues,<sup>56</sup> noted that the miscibility pressures of poly(vinyl acetate) and poly(methyl acrylate) differ by 100's to thousands of atmospheres, despite the fact that these materials are isomers. Topology clearly plays a role in determining the phase boundary of a material mixed with CO<sub>2</sub>.

### 3.0 RESEARCH OBJECTIVE AND APPROACH

#### 3.1 RESEARCH OBJECTIVE

The research objective is to design and synthesize polymers which can increase the viscosity of CO<sub>2</sub> and thus lower the mobility ratio during CO<sub>2</sub>-flooding. The ultimate goal is to increase the viscosity 10-100 fold at low shear rates of 1-10 s<sup>-1</sup> and at concentrations less than 1 wt% of polymer, while considering environmental and economical aspect of the polymer applied in EOR application. The key in designing a thickener is that the polymer should be miscible with CO<sub>2</sub>, plus should possess a number of functional groups that can exhibit attractive intermolecular associations between the polymer chains in CO<sub>2</sub> and thus form higher order architectures, promoting enhancement in the CO<sub>2</sub> viscosity.

Due to the poor solvent power of dense CO<sub>2</sub>, traditional hydrocarbon based polymers fail to dissolve in CO<sub>2</sub>, and thus, induce any significant viscosity increase. To date, fluoroacrylate polymers have proven to be highly CO<sub>2</sub>-philic. Their presence in any molecular structure at sufficient amount has the capability of “pulling” even highly CO<sub>2</sub>-phobic material into the CO<sub>2</sub> phase. Unfortunately, a homopolymer of fluoroacrylate does not give rise to considerable increase in viscosity of CO<sub>2</sub> (3-8 fold at 5-10 wt%).<sup>24</sup> This is due to the lack of any associating group in the body of fluoroacrylates homopolymer. Therefore, in order to find appropriate

functional groups for the design of a CO<sub>2</sub>-direct thickener, the fluoroacrylates were chosen to be included in the body of the polymer to eliminate the miscibility problem and copolymerized with another monomer which can promote association among the polymer chains.

Using CO<sub>2</sub> in EOR as a displacing fluid has a lot of advantages, if the sweep efficiency of CO<sub>2</sub> is high. These advantages include low-cost, non-toxicity, non-flammability, and natural abundance. However, if the thickening agent applied is high-priced, as with fluoroacrylate polymers, and environmentally suspicious, then, any economic and environmental advantages gained with the use of CO<sub>2</sub> are lost. Thus, one should also consider the cost and “greenness” of the polymer employed in the EOR process. Therefore, in the current study, substitution of fluoroacrylate polymer with inexpensive, environmentally friendly CO<sub>2</sub>-philic polymers (composed of only C, H, O, N, and S) was also aimed to enhance the viability of EOR application. In the design of these polymers, it was aimed that newly designed polymers would exhibit miscibility in CO<sub>2</sub> at as low temperatures and pressures as fluoroacrylate polymers.

## 3.2 RESEARCH APPROACH FOR CO<sub>2</sub>-THICKENERS

### 3.2.1 Stacking of Aromatic Rings:

Stacking of aromatic rings is a noncovalent interaction and has been known for many years.<sup>57,58</sup> Application of these interactions to synthetic polymers allows the creation of higher order architecture. In stacking of aromatic rings, equilibrium structure corresponds to a balance between attractive and repulsive forces.

The generally accepted picture of stacking involves the delocalization of electrons on the carbon atoms of benzene and slight residual positive charges on the hydrogen atoms. This inherent polarity of benzene, an electron-rich central core being surrounded by an electron-poor periphery of hydrogens, gives rise to T-shaped arrangement (Figure 3.1). In other words, this electrostatic description energetically favors the T-shaped (edge-to-face) arrangement.<sup>57,59,60,61,62</sup> The hydrogen atoms are attracted to the more electron rich carbon atoms to give a herring-bone arrangement of molecules. In the figure, two adjacent CH-bonds of the first molecule point towards to the core of the neighboring benzene molecule, and a shift of the center of the first from the normal centered on the second molecule is observed so that one hydrogen of the first is located above the centre of the second molecule, but note that the corresponding C-H bond direction does not point towards to ring center.<sup>57</sup> Since polycyclic aromatic hydrocarbons do not have any significant dipole moment, this electrostatic interaction between rings is attributed to their quadruple-quadrupole interactions.<sup>63,64</sup>

As the polycyclic aromatic hydrocarbon becomes larger, the carbon-to-hydrogen ratio increases. The expected result is that larger polycyclic aromatic hydrocarbon molecules stack one above the other more strongly.<sup>57,62,65</sup>

The energy of interaction between two stacking molecules in solution includes association of the two molecules and displacement of solvent. Hunter and Sanders declared that in nonpolar organic solvents, the electrostatic interactions with the solvent will be negligible, and so the dominant electrostatic interaction would come from the association energy.<sup>58</sup> In addition, aromatic solvents are known to significantly disrupt stacking interactions because the solvent molecules effectively solvate the solute opening up stacked conformations. Indeed, for any solute molecules to associate in solution to form higher order structure, solvent molecules are required not to interfere with solute molecules so that stable higher order architecture can be attained in the solution.

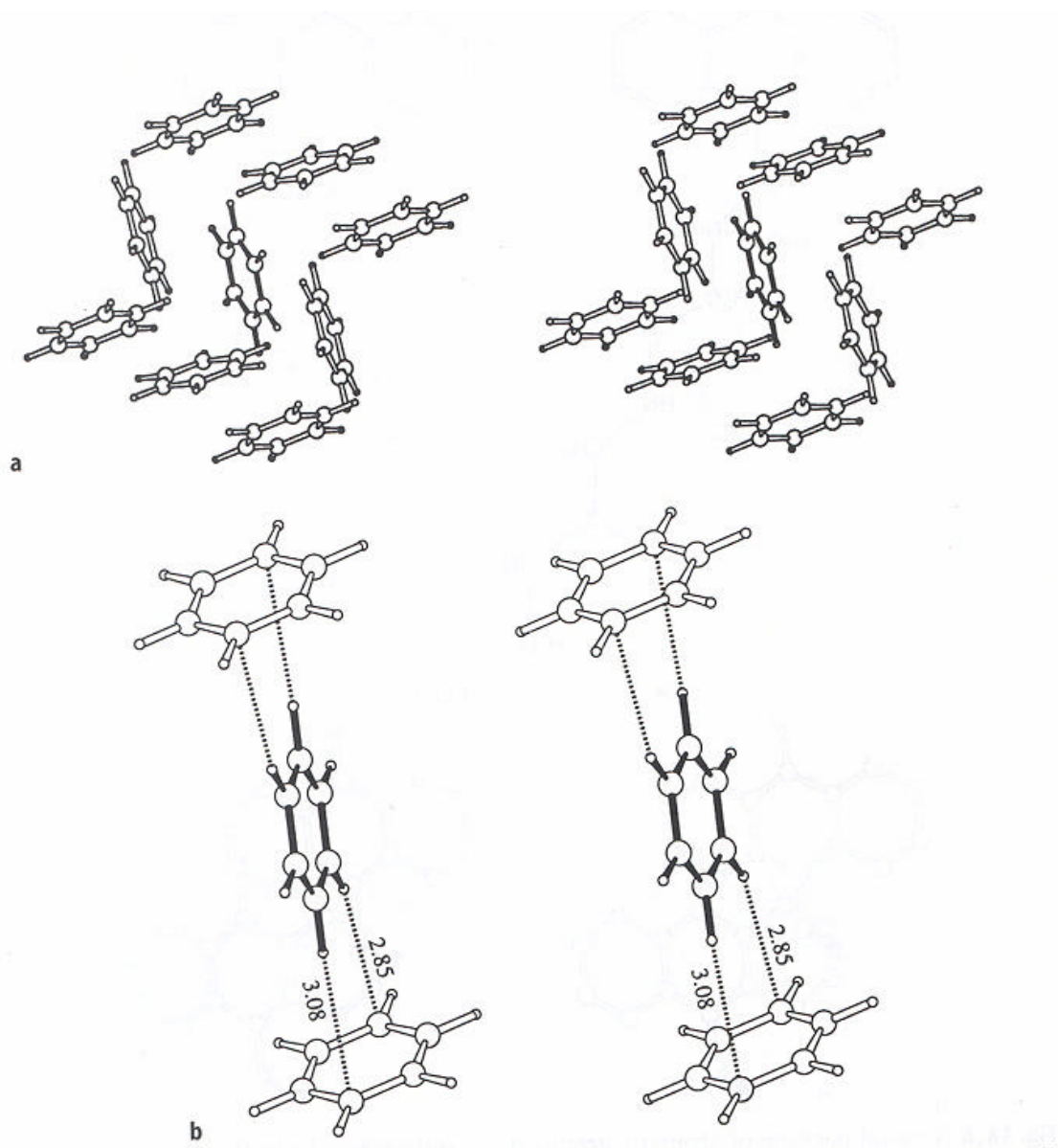


**Figure 3.1** Packing of molecules in crystalline benzene, showing: a. a stereoview of the overall structure; b. the shortest C...H distances in Å (representative of an H... $\pi$  interactions)<sup>62</sup>



copolymer. The second monomer should impart some sort of attractive intermolecular association among the polymer chains in CO<sub>2</sub> forming higher order architectures in order to promote enhancement in viscosity of CO<sub>2</sub>. Having known that aromatic rings can associate by forming noncovalent bonds via stacking, and thus result in enhancement in viscosity,<sup>26</sup> the second monomer included aromatic rings. Given that carbonyl groups exhibit favorable Lewis acid-Lewis base interactions with CO<sub>2</sub> towards miscibility, carbonyl group was also included in the designed second monomer. All these led to generation of an aromatic acrylate monomer. In the generation of potential CO<sub>2</sub>-thickeners, it was hypothesized that, by separation of aromatic ring(s) from the rigid polymer backbone by a spacer unit, the aromatic group(s) can relax to optimum geometrics to achieve the strongest interactions. In the stacking profile of aromatic rings, the hydrogen atoms are attracted to the more electron rich carbon atoms to give herringbone arrangements of molecules. Therefore, it was hypothesized that one can obtain higher viscosity enhancement in CO<sub>2</sub> by increasing the surface area of overlap, given that as the polycyclic aromatic hydrocarbons becomes larger, the-carbon-to-hydrogen ratio increases in the ring, resulting in stronger interaction. The general structure of the proposed Aromatic Acrylate-Fluoroacrylate copolymers is shown in Figure 3.3.

In the current work, the optimum conditions (x,y,n,m) resulting in maximum increase in viscosity at minimum concentration in CO<sub>2</sub> were examined. Knowing the fact that fluorinated thickeners are not applicable in EOR because of their high-cost and immiscibility with crude oil, the design of low-cost, environmentally friendly, non-fluorous polymers as a substitution to fluoroacrylate moiety was also investigated.

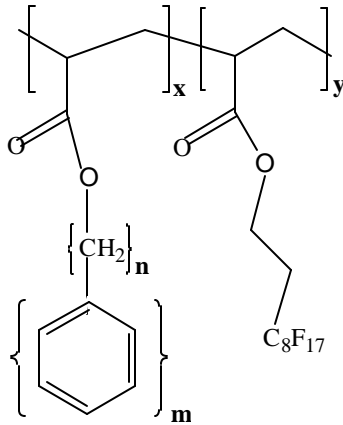


**Figure 3.3** General Structure of Aromatic Acrylate-Fluoroacrylate Copolymers

### 3.3 RESEARCH APPROACH FOR CO<sub>2</sub>-PHILIC POLYMERS

#### 3.3.1 Heuristics on Miscibility of Materials with CO<sub>2</sub>:

The successful design and synthesis of CO<sub>2</sub>-thickeners (polymers) requires miscibility of the polymeric materials in CO<sub>2</sub>. In order for a polymeric material or any other solute to dissolve in a given solvent, Gibbs free energy of mixing,  $\Delta G_{\text{mix}}$ , must be negative and at a minimum. The Gibbs free energy of mixing is given by

$$\Delta G_{\text{mix}} = \Delta H_{\text{mix}} - T\Delta S_{\text{mix}} \quad (3.1)$$

where  $\Delta H_{\text{mix}}$  and  $\Delta S_{\text{mix}}$  are the change of enthalpy and entropy, respectively, on mixing. The enthalpic interactions depend predominately on solution density, and polymer segment-segment, solvent-solvent and polymer segment-solvent interaction energies.  $\Delta S_{\text{mix}}$  depends on the combinatorial (or configurational) and noncombinatorial contributions. Because the entropy and enthalpy of mixing are coupled, it is not an easy task to treat them separately.

Carbon dioxide is a relatively nonpolar solvent with a low dielectric constant and large quadrupole moment, and it is not strongly involved in van der Waals interactions.<sup>66</sup> Therefore,  $\text{CO}_2$  is considered to be a feeble solvent for many polar and high-molecular weight materials, although it can solubilize low-molecular weight, volatile compounds. The solvent character of  $\text{CO}_2$  has been investigated for more than two decades. Its solvation power was first likened to hexane given its calculated thermodynamic solubility parameter.<sup>67</sup> However, this concept was discarded over the years as many materials that are soluble in hexane were reported to be insoluble in  $\text{CO}_2$  and vice versa.<sup>68</sup> The large quadrupole moment of  $\text{CO}_2$  was suggested to be responsible for its weak solvency character.<sup>44,69</sup>  $\text{CO}_2$  was also likened to fluorocarbons owing to its low “polarizability per volume”, which is a measure of the strength of van der Waals interactions. It was reported that  $\text{CO}_2$  has a lower polarizability/volume, and hence weaker solvent power towards nonpolar hydrocarbons, than either ethane or ethylene.<sup>68</sup>

The fact that some fluorinated alkane, acrylate and ether polymers are much more miscible with  $\text{CO}_2$  than their non-fluorous counterparts has been known since early 1990s.<sup>22,38,70</sup> Because these polymers exhibit miscibility in  $\text{CO}_2$  under mild conditions (temperatures and pressures less than 100 °C and 200 bar, respectively), they are called  $\text{CO}_2$ -philic polymers. The

origin of favorable miscibility of fluorinated polymer has been closely scrutinized by researchers to try to shed light onto design of new CO<sub>2</sub>-philic materials. However, there is a considerable controversy in the literature for the high miscibility of fluorinated polymers in CO<sub>2</sub>.

To explain the CO<sub>2</sub>-philic character of fluorinated polymers, efforts have focused on both spectroscopic and theoretical studies. The main focus was whether there exists any specific interactions between CO<sub>2</sub> and these molecules, and if there is, what the nature of these interactions would be. For example, Yee et al. used FTIR to investigate the possibility of specific interactions between CO<sub>2</sub> and hexafluoroethane (C<sub>2</sub>F<sub>6</sub>).<sup>71</sup> They found no evidence of specific attractive interactions between the F atoms and CO<sub>2</sub>, and in fact, CO<sub>2</sub> was found to be more repulsive to C<sub>2</sub>F<sub>6</sub> than C<sub>2</sub>H<sub>6</sub>. Therefore, the authors attributed the enhanced solubility of fluorocarbons to the highly repulsive nature of fluorocarbon-fluorocarbon interactions, making the solute-solute interactions less favorable than solute-solvent interactions. Possible specific interactions between F and CO<sub>2</sub> were also investigated using NMR spectroscopy. Dardin et al. have compared <sup>1</sup>H and <sup>19</sup>F NMR chemical shifts of n-hexane (C<sub>6</sub>H<sub>14</sub>) and perfluoro-n-hexane (C<sub>6</sub>F<sub>14</sub>) in CO<sub>2</sub>.<sup>72</sup> They reported that no extraordinary solvent-solute interactions were present between C<sub>6</sub>H<sub>14</sub> and CO<sub>2</sub> while they observed a chemical shift, which they ascribe to C<sub>6</sub>F<sub>14</sub>-CO<sub>2</sub> van der Waals interactions.<sup>73</sup> On the contrary, using <sup>1</sup>H and <sup>19</sup>F NMR, Yonker et al. showed that neither fluoromethane (CH<sub>3</sub>F) nor trifluoromethane (CHF<sub>3</sub>) exhibit significant specific attractive interactions with CO<sub>2</sub>.<sup>74</sup> Taylor et al. attributed the discrepancy in the NMR results to the electronic and structural difference between the molecules in comparison.<sup>66</sup>

Theoretical studies have also resulted in contradictory findings. Based on restricted Hartree-Fock level ab initio calculations, Cece et al. suggested that there exist specific interactions between CO<sub>2</sub> and fluorine of C<sub>2</sub>F<sub>6</sub>, unlike between CO<sub>2</sub> and C<sub>2</sub>H<sub>6</sub>.<sup>75</sup> Han and Jeong, however, disagreed with these results, stating that Cece et al. did not take into account basis set superposition error (BSSE) corrections in their calculations. Using similar ab initio calculations, but accounting for BSSE corrections, Diep et al. reported no evidence to support CO<sub>2</sub>-F interactions to explain the superior solubility of fluorocarbons versus hydrocarbons. Furthermore, interactions between hydrocarbons and CO<sub>2</sub> were found to be even stronger than those between fluorocarbon analogues and CO<sub>2</sub>.<sup>76</sup> Raveendran and Wallen computationally investigated the effect of stepwise fluorination on the CO<sub>2</sub>-philicity of methane in an effort to address the existence/nonexistence of F-CO<sub>2</sub> interactions, and to explain the fundamental difference in the nature of interactions of fluorocarbons and hydrocarbons with CO<sub>2</sub>. Their calculations showed that there is an optimum degree of fluorination for maximum CO<sub>2</sub>-philicity. Their results for comparison of methane (CH<sub>4</sub>) and perfluoromethane (CF<sub>4</sub>) indicated that CO<sub>2</sub>-fluorocarbon and CO<sub>2</sub>-hydrocarbon interactions are energetically comparable; however, they are different in nature. In partially fluorinated systems, the fluorine atom acts as a Lewis base towards electron deficient carbon atom of CO<sub>2</sub>, and the hydrogen atoms, having increased positive charge due to the neighboring fluorine, act as Lewis acids towards the electron rich oxygen atoms of CO<sub>2</sub>.<sup>77</sup>

A different scenario emerges from a recent study by Fried and Hu, who used second order Møller-Plesset (MP2) perturbation calculations (6-311++G\* \* basis set) in an effort to identify the nature of specific interactions between CO<sub>2</sub> and the fluorinated substituent groups of

polymers.<sup>78</sup> These authors investigated interactions of CO<sub>2</sub> with three fluoroalkanes (CF<sub>4</sub>, CF<sub>3</sub>CH<sub>3</sub>, CF<sub>3</sub>CH<sub>2</sub>CH<sub>3</sub>) and alkanes (CH<sub>4</sub>, CH<sub>3</sub>CH<sub>3</sub>, CH<sub>3</sub>CH<sub>2</sub>CH<sub>3</sub>). They reported that the quadrupole-dipole interaction is an important contribution to the total energy of interaction, with CF<sub>3</sub>CH<sub>2</sub>CH<sub>3</sub> having the maximum quadrupole-dipole interaction energy of 11.5 kJ/mol, while the interaction energy between propane and CO<sub>2</sub> is 6.88 kJ/mol. They attributed the interaction between propane and CO<sub>2</sub> to dispersion forces and other interactions. Furthermore, in experimental studies by McHugh et al., the favorable miscibility of fluorocarbons has been attributed to polar-quadrupole interactions between fluorinated polymers and CO<sub>2</sub>, given that CO<sub>2</sub> has a large quadrupole moment.<sup>44,79</sup> These authors suggest that the large quadrupole moment works against solubilizing predominantly nonpolar polymers since the CO<sub>2</sub> quadrupole interactions dominate, especially at low temperatures. The authors also noted that fluorination imparts solubility to the polymer provided that polarity is also introduced to the polymer via fluorination. However, it was suggested that a high level of fluorination shows an adverse effect on miscibility due to dipole-dipole interactions between the polymer chains.<sup>44,79</sup>

Specific attractive interactions between CO<sub>2</sub> and a material favor miscibility from the enthalpic point of view. As mentioned before, the enthalpy of mixing is a strong function of the strength of interaction of solute-solute, solvent-solvent and solute-solvent contacts. Thus, for a material to be considered CO<sub>2</sub>-philic, cross interactions should dominate over self interactions. Due to its large quadrupole moment, CO<sub>2</sub> has a partial positive charge on the carbon atom, and partial negative charges on the oxygen atoms. In mid-1990s, using FT-IR, Kazarian and coworkers reported the existence of specific interactions between partially positively charged carbon atom of CO<sub>2</sub> and lone pairs on the oxygen of a carbonyl moiety. They argued that this

complex formation is most probably of a Lewis acid-Lewis base nature.<sup>47</sup> The Lewis acid character of CO<sub>2</sub> has also been shown by FT-IR in a number of studies.<sup>80,81</sup> The interaction of CO<sub>2</sub> with various carbonyl containing compounds was also found computationally by a number of researchers.<sup>48,49</sup> In these studies, it was shown that the carbonyl oxygen interacts with the carbon atom of CO<sub>2</sub>, but the geometry and strength of the interaction may vary depending on adjacent groups. Experimental findings also revealed that one can achieve miscibility of an otherwise immiscible polymer in CO<sub>2</sub> via incorporation of carbonyl groups.<sup>50,51</sup> In the aforementioned studies, it was shown that placement and extent of carbonyl substitution are the key factors to maximize miscibility. In mid-1990s, using FT-IR, Meredith et al. reported that CO<sub>2</sub> can also interact with other Lewis base groups, such as tributyl phosphate and a tertiary alkyl amine.<sup>82</sup> Recently, Wallen and co-workers reported the presence of attractive specific interactions between CO<sub>2</sub> and the S=O group in dimethylsulfoxide based on ab initio calculations.<sup>49</sup> However, the effect of these groups on miscibility behavior in CO<sub>2</sub> hasn't been probed yet.

Because CO<sub>2</sub> is a weak solvent, O'Neill et al. hypothesized that a CO<sub>2</sub>-philic material should exhibit weak self interactions.<sup>68</sup> O'Neill has shown that many of the compounds exhibiting CO<sub>2</sub>-philic character (e.g. fluoroacrylates, siloxane polymers, polyethers) have low surface tension and thus low cohesive energy density (a measure of strength of the intermolecular forces keeping the chain molecules together). Materials with relatively weak self interaction indeed possess low cohesive energy density, and hence, low surface tension and solubility parameter.

Concerning the contributions from entropy of mixing in determining CO<sub>2</sub>-philicity of a material, one needs to design polymeric materials in such a way so as to high free volume and high chain flexibility. High free volume and flexibility would consequently cause a low glass transition temperature of the polymer ( $T_g$ ). In general, the glass transition temperature is lowered with increasing number of rotational degrees of freedom in side chain groups and the relative ease of rotational motions of the side groups. Symmetry of disubstitution of larger atoms or groups for H-atoms on backbone is hypothesized to lower the  $T_g$ , while asymmetry increases it. Tertiary carbon atoms are expected to hinder the motions of the side groups (i.e. the effectiveness of the nominal rotational degrees of freedom) and hence increase  $T_g$  unless these tertiary carbon atoms are separated from backbone by a spacer at proper length.<sup>83</sup> It was reported that branching increases the free volume of the polymer by simply reducing the intermolecular interactions between polymer segments that would arise due to short-range molecular orientation offered by a high content of linear segments without pendant groups.<sup>84</sup> It was observed that the number of shorter side chains grafted to a polymer backbone has a larger effect on the miscibility with CO<sub>2</sub> than longer chains having the same concentration of side chains grafted to the backbone, but with less number. It was argued that this effect is more likely due to the free volume effect, and thus favorable entropy of mixing.<sup>85</sup>

### **3.3.2 Design Strategy for CO<sub>2</sub>-Philic Polymers:**

In the light of the background given above, it was hypothesized that miscibility of a polymer with CO<sub>2</sub> depends on the balance between the entropic and enthalpic contributions of solute-solute, solvent-solvent and solute-solvent interactions. The design strategy was that a CO<sub>2</sub>-philic

polymer should possess low cohesive energy and low glass transition temperature (high flexibility and high free volume), and that Lewis base groups should be included in the polymer in an easily accessible place to promote polymer-CO<sub>2</sub> interactions. It was believed that Lewis acid-Lewis base interactions are important for overwhelming the strong quadrupole-quadrupole interactions between the CO<sub>2</sub> molecules. Thus, one can expect that the miscibility of a polymer in CO<sub>2</sub> can be enhanced by increasing the number of Lewis base groups in the polymer chain. On the other hand, there is a possibility that those Lewis base groups might inflate the cohesive energy density and/or decrease chain flexibility of the polymer. Therefore, the newly designed CO<sub>2</sub>-philic material should maintain a balance between polymer-polymer interactions, polymer-CO<sub>2</sub> interactions, and the entropy of mixing deriving from high chain flexibility, free volume and chain topology.

## 4.0 ACRYLATE COPOLYMERS AS CO<sub>2</sub>-DIRECT THICKENERS

### 4.1 EXPERIMENTAL PROTOCOL

#### 4.1.1 Materials:

3,3,4,4,5,5,6,6,7,7,8,8,9,9,10,10,10,10-heptadecafluorodecyl acrylate (FA, 97%), styrene (St, 99%), 4-bromobenzyl alcohol (99%), 1-naphthalenemethanol (98%), acryloyl chloride, anhydrous dichloromethane (DCM) and triethylamine (Et<sub>3</sub>N) were obtained from Aldrich. 2-phenylethyl acrylate was purchased from Polysciences, Inc.,  $\alpha$ -naphthyl acrylate (NA) from Monomer-Polymer & Dajac Lab. Inc., benzyl acrylate (BEA, 100%) and cyclohexyl acrylate (CHA, 98%) from Scientific Polymer Products, Inc. and phenyl acrylate (PA) from Lancaster, Inc. All monomers were purified via inhibitor remover column prior to use, except acryloyl chloride. Initiator, 2,2'-azobis(isobutyronitrile) (AIBN, 98%, Aldrich) was recrystallized from ethanol. Sulfuric acid (95%) and NaOH pellets were obtained from J. T. Baker. 1,1,2-trichlorotrifluoroethane (TCTFE, 99.8%, Aldrich), methanol (anhydrous, Aldrich), 1,2-dichloroethane (99+%, Aldrich) and acetic anhydride (99+%, Aldrich) were used as received.

## **4.1.2 Synthesis of Copolymers of Styrene with Fluoroacrylate and its Sulfonation:**

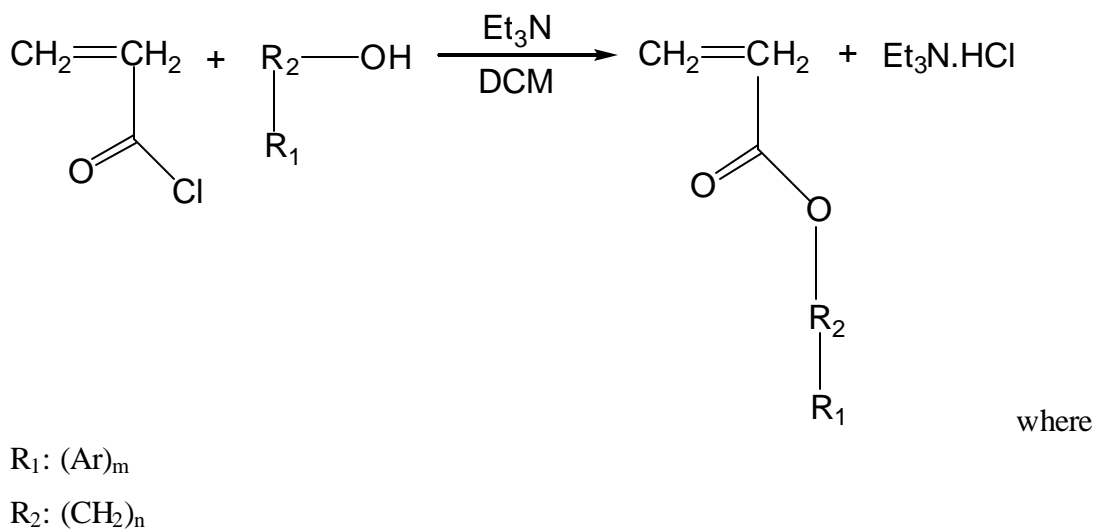
**4.1.2.1 Random Copolymerization of Styrene with Fluoroacrylate:** Copolymerization was carried out by bulk free radical polymerization of fluoroacrylate and styrene in the presence of AIBN. A mixture of AIBN (0.2 mole % of monomers), styrene and fluoroacrylate was placed in an ampule. The mixture was purged with N<sub>2</sub> and then the ampule was flame-sealed. The reaction mixture was kept at 65-70 °C overnight. A white waxy solid resulted after overnight polymerization reaction at 65-70 °C. Polymer was purified by dissolving in TCTFE and precipitating in a large excess of methanol. After vacuum drying overnight, a white foam-like polymer was obtained with 95% yield. General structure of styrene-fluoroacrylate copolymer is given in Table 4.1. (a).

**4.1.2.2 Sulfonation of Styrene-Fluoroacrylate Copolymer:** Sulfonation of phenyl groups was performed using acetyl sulfate as reagent, which was prepared according to the procedure reported in literature.<sup>86,87,88</sup> The copolymer prepared in the previous step was dissolved in TCTFE, and the solution was heated to 48 °C (reflux). After adjustment of its temperature to 48 °C, pre-prepared acetyl sulfate solution was added, and the solution acquired a dark green/brown tint. The reaction was allowed to proceed for 2 hours at reflux and then terminated by the addition of large amount of methanol. To facilitate the complete removal of residual sulfonating agent from the functionalized polymer, the sulfonated polymer was redissolved in TCTFE and reprecipitated in methanol several times. The sample was then dried in a vacuum oven overnight.

**4.1.2.3 Neutralization of Sulfonated Styrene-Fluoroacrylate Copolymer:** To a solution of the sulfonated copolymer in TCTFE, was added 4-5 drops of 1 wt % phenolphthalein (indicator). The solution was titrated by 1.0 N NaOH until the end point indicated by a change from colorless to pink. Resulting functionalized ionomer was precipitated in methanol. The polymer was purified several times by redissolution in TCTFE and reprecipitation in methanol. After drying under vacuum overnight, a slightly brown polymer was obtained. General structure of sulfonated styrene-fluoroacrylate copolymer is given in Table 4.1. (b).

### 4.1.3 Synthesis of Aromatic Acrylate Monomers:

For the synthesis of aromatic acrylates which were not commercially available, the scheme below was followed:



**Scheme 4.1** Reaction route for the synthesis of acrylate monomers.

**4.1.3.1 Synthesis of 4-Bromobenzyl Acrylate:** The glassware was oven-dried overnight prior to use. 14 ml of triethylamine (100.7 mmol) was added to a solution of 4-bromobenzyl alcohol (15 g, 80.2 mmol) in 150 ml dry dichloromethane under argon atmosphere. The mixture was maintained at 0 °C in an ice/water bath and under argon. In the meantime, acryloyl chloride (9.44 g, 104 mmol) dissolved in anhydrous dichloromethane (40 ml) is added in a drop-wise fashion to the mixture of alcohol and Et<sub>3</sub>N in dichloromethane. Upon addition of the acryloyl chloride solution, the reaction was carried out for a further 5 hours in the ice bath and then overnight at room temperature. The Et<sub>3</sub>N.HCl salt was filtered off. The crude product was purified further via extraction three times with 5% NaHCO<sub>3</sub> solution and three times with water. The product was dried over MgSO<sub>4</sub> and concentrated under reduced pressure. 14.5 g monomer was obtained (75 % yield). <sup>1</sup>H NMR (300 MHz, CDCl<sub>3</sub>) δ 7.2-7.5 (m, 5H, Ar), δ 5.9-6.5 (m, 3H, vinyl), δ 5.15 (s, 2H, O-CH<sub>2</sub>-Ar).

**4.1.3.2 Synthesis of Naphthyl Methyl Acrylate:** Synthesis of naphthyl methyl acrylate was performed in a similar manner to 4-bromobenzyl acrylate. 11.3 g (124.5 mmol) acryloyl chloride in 55 ml anhydrous dichloromethane was added in a drop-wise fashion to the solution of triethylamine (16 ml, 114 mmol) and 1-naphthalenemethanol (14.9 g, 94 mmol) in 120 ml anhydrous dichloromethane stirred in an ice bath under argon atmosphere. The crude product was purified in similar manner to that in 4.1.3.1, yielding 18.7 g (94%) of a dark red-brownish oily product. <sup>1</sup>H NMR (300 MHz, CDCl<sub>3</sub>) δ 7.5-8.0 (m, 7H, Ar), δ 6.2-6.5 (m, 3H, vinyl), δ 5.65 (s, 2H, O-CH<sub>2</sub>-Ar).

#### 4.1.4 Synthesis of Copolymers of Aromatic Acrylates with Fluoroacrylate:

The copolymerization of aromatic acrylates with fluoroacrylate was done by bulk free radical polymerization technique similarly to the styrene-fluoroacrylate copolymer. However, the bulk free radical polymerization of aromatic acrylates required special care due to intramolecular and intermolecular H-abstraction (chain transfer) reactions during the course of polymerization. Decrease in the concentration of monomer during polymerization causes an increase in the contribution of intramolecular H-abstraction reactions relative to propagation, and subsequently the rate of intermolecular hydrogen abstraction reaction would increase with increasing polymer concentration.<sup>89,90,91,92</sup> H-abstraction causes branching in the polymer chain via formation of mid-chain radicals. Mid-chain radicals are less reactive than the propagating radicals, so they have a longer life time in comparison with the propagating radicals.<sup>90</sup> During the course of the polymerization, the concentration of mid-chain radical increases as evidenced by a sudden increase in viscosity at some point. On the contrary, concentration of propagating radicals decreases due to high rate of intra- and intermolecular H-abstraction relative to propagation. At the gel state, termination of radicals occurs mostly by mutual combination along with the chain transfer to polymer. Mutual combination of these radicals causes crosslinking of polymer chains. It was observed that there is a “critical conversion” after which polymerization results in insoluble, crosslinked gels (evidenced by insolubility of the copolymers in any organic solvent).

In a typical experiment, an ampule equipped with stir-bar was flashed with Argon. A known amount of aromatic acrylate, fluoroacrylate and AIBN (0.11 wt% of monomers) was added. The ampule was sealed with flame and placed in a bath at  $T=62\pm 1$  °C. Polymerization

was monitored at all times. At the point where the gel effect was observed (monitored by the inability of the magnetic stir-bar to spin), the reaction was stopped by quenching the ampule in liquid N<sub>2</sub>. Higher conversions yielded insoluble gels. Product was purified via dissolution in TCTFE and precipitation into methanol (3 times). General structure of aromatic acrylate-fluoroacrylate copolymers is given in Table 4.1. (c).

#### **4.1.5 Synthesis of Copolymers of Cyclohexyl Acrylate with Fluoroacrylate:**

For the polymerization of cyclohexyl acrylate with fluoroacrylate, the procedure given in Section 4.1.5 was employed. The general structure of the copolymers is given in Table 4.1. (d).

#### **4.1.6 Structural Characterization:**

Chemical characterization of the resulting products was accomplished via 300 MHz <sup>1</sup>H NMR spectroscopy. NMR spectroscopy was carried out by dissolving sample in TCTFE in an 8 mm O.D. inner tube, which was then placed in a 10 mm O.D. outer tube containing deuterated chloroform and tetramethylsilane. Aromatic and acrylate proton peaks were used for calculation of chemical composition since they were well resolved in the spectra. <sup>1</sup>H-NMR spectra of the copolymers are given in Figures A.1-A.6 in Appendix A. Following is the <sup>1</sup>H-NMR peak data for the selective copolymers:

**St-FA Copolymer:**  $\delta$  4.3 (broad, 2H, -CO-O-CH<sub>2</sub>-CH<sub>2</sub>-CF<sub>2</sub>),  $\delta$  7.2 (broad, 5H, Ar). **PHA-FA Copolymer:**  $\delta$  4.3 (broad, 2H, -CO-O-CH<sub>2</sub>-CH<sub>2</sub>-CF<sub>2</sub>),  $\delta$  7.2 (broad, 5H, Ar). **BEA-FA Copolymer:**  $\delta$  4.4 (broad, 2H, -CO-O-CH<sub>2</sub>-CH<sub>2</sub>-CF<sub>2</sub>),  $\delta$  5.05 (broad, 2H, -CO-O-CH<sub>2</sub>-Ar),  $\delta$  7.3 (broad, 5H, Ar). **PEA-FA Copolymer:**  $\delta$  4.3 (broad, 2H, -CO-O-CH<sub>2</sub>-CH<sub>2</sub>-CF<sub>2</sub>),  $\delta$  4.1 (broad, 2H, -CO-O-CH<sub>2</sub>-CH<sub>2</sub>-Ar),  $\delta$  7.2 (broad, 5H, Ar). **NA-FA Copolymer:**  $\delta$  4.4 (broad, 2H, -CO-O-CH<sub>2</sub>-CH<sub>2</sub>-CF<sub>2</sub>),  $\delta$  7.3 (broad, 7H, Ar) **CHA-FA Copolymer:**  $\delta$  4.36 (broad, 2H, -CO-O-CH<sub>2</sub>-CH<sub>2</sub>-CF<sub>2</sub>),  $\delta$  4.8 (broad, H, -CO-O-CH).

**Table 4.1** General Structure of the Fluoroacrylate-Aromatic Acrylate copolymers

Copolymers	General Structure
(a) Styrene-Fluoroacrylate (St-FA)	
(b) Partially sulfonated Styrene-Fluoroacrylate (S.St-St-FA)	
(c) Aromatic acrylate-Fluoroacrylate m=1, n=0 (PHA-FA) n=1 (BEA-FA) n=2 (PEA-FA) m=2, n=0 (NA-FA) n=1 (NMA-FA)	
(d) Cyclohexyl Acrylate-Fluoroacrylate (CHA-FA)	

The degree of sulfonation for the polymer shown in Table 4.1 (c) was determined via sulfur analysis performed by Galbraith Laboratories, Inc. (Knoxville, TN). Sulfur content in the copolymer was reported to be 75 ppm. Sulfonated portion of the polymer was calculated from the mass balance on mole basis as shown in the equation below:

$$(M_x)_x + (M_y)_y + (M_z)_z = \frac{x}{\left(\frac{w_S}{M_S}\right)} \quad (4.1)$$

where

x, y, and z : mole% of each unit in the copolymer;

$M_x$ ,  $M_y$ , and  $M_z$  : the molecular weight of each corresponding unit in the polymer, g/mole;

$w_S$  : the sulfur content in the polymer, g

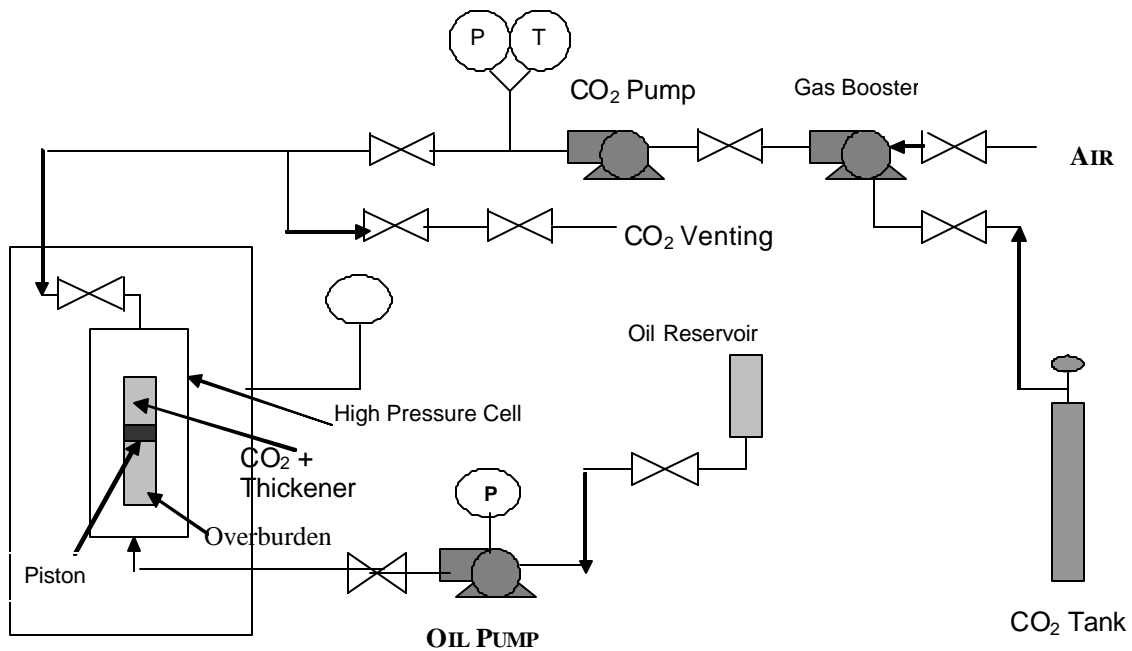
$M_S$  : the molecular weight of sulfur, g/mole.

From  $^1\text{H-NMR}$  spectrum for the starting St-FA copolymer, z was calculated as 0.89 and, (x+y) as 0.11. When numeric values are substituted in the equation, x and y are calculated as 0.001 and 0.109, respectively.

#### 4.1.7 Phase Behavior Measurements:

The phase behavior measurements were performed at 295 K using a high pressure, variable volume windowed cell with a cylindrical sample volume (D.B. Robinson & Assoc.) (Scheme 4.2). Isothermal expansions and compressions of mixtures of specified overall composition were used to determine the two-phase boundary. A known amount of polymer was

introduced to the sample volume, together with stainless steel mixing balls (Scheme 4.3.(a)). High pressure liquid carbon dioxide was then metered via a positive displacement pump into the sample volume. Addition of carbon dioxide was performed isothermally and isobarically by withdrawing the overburden fluid at the same time. The CO<sub>2</sub>-polymer mixture was pressurized and mixed until a transparent single phase resulted. The system was then slowly depressurized by withdrawing the overburden fluid and thus expanding the sample volume. The point at which the transmitted light through sample was visually less than 10 % of that through initial solution was taken as the cloud point pressure of that mixture at that concentration. Measurements were repeated by repressurizing until a single, clear phase was observed and then depressurizing the system again. The average of 3-4 measurements was recorded as the cloud point pressure. Experiments were conducted over a range of compositions, thus the P-x diagram was established; typical variability in our cloud point measurements is less than  $\pm 0.7$  MPa.



**Scheme 4.2** High Pressure, Variable Volume, Windowed Cell (D. B. Robinson Cell)

#### 4.1.8 Solution Relative Viscosity Measurements:

The relative viscosity of CO<sub>2</sub>-polymer solutions was determined using the same high-pressure equipment used for phase behavior experiments (Scheme 4.2). The viscosity of transparent, single-phase thickener-CO<sub>2</sub> solutions was determined by a falling cylinder viscometer. This method relates the viscosity of the fluid to the density difference between the solid and the fluid, terminal velocity of the cylinder, and a viscometer constant which depends on geometry of the system. The governing equation for the system can be expressed as

$$h = k \frac{(\rho_c - \rho_f)}{u_t} \quad (4.2)$$

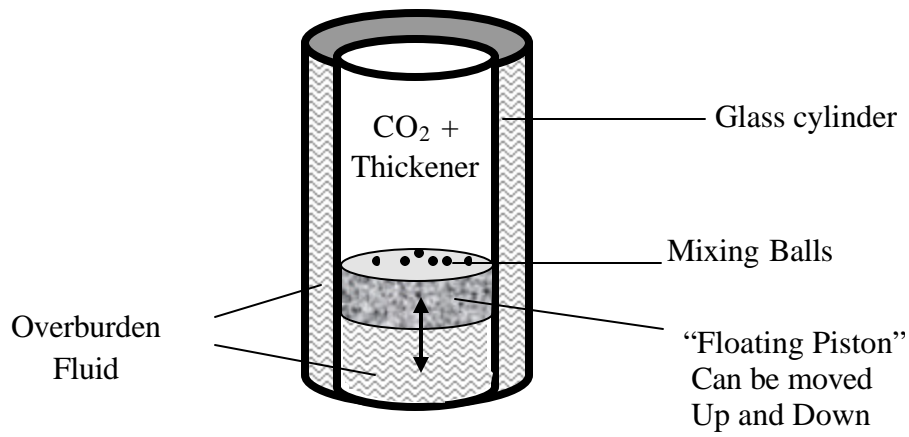
where  $\rho_c$  and  $\rho_f$  are the density of the cylinder and the fluid, respectively,  $u_t$  is terminal velocity of the falling cylinder and  $k$  is the viscometer constant. The viscometer constant is usually determined by calibration against a fluid of known density and viscosity. Although Eq. 4.2 was derived for Newtonian fluids, it can also be used for estimating the viscosity of non-Newtonian fluids provided that the shear rate is low and shear dependence of the viscosity is not considered.<sup>93,94</sup>

Although other viscosity measurements, (e.g. capillary viscometry and flow through porous media) provide more comprehensive and precise assessments of viscosity as a function of shear rate, the falling cylinder viscometer technique is useful for rapid determination of significant viscosity changes in CO<sub>2</sub>-thickener solutions for screening purposes. In the present work, the relative viscosity of the thickened CO<sub>2</sub> solutions (the ratio of viscosity of thickened to that of neat CO<sub>2</sub>) was reported. Assuming that the change in density of the fluid is small upon the addition of thickener, from Eq. 4.2 above, it becomes clear that the ratio of the viscosities is inversely equal to the ratio of terminal velocities. Given the basic relationship (velocity=distance/time), we arrive at:

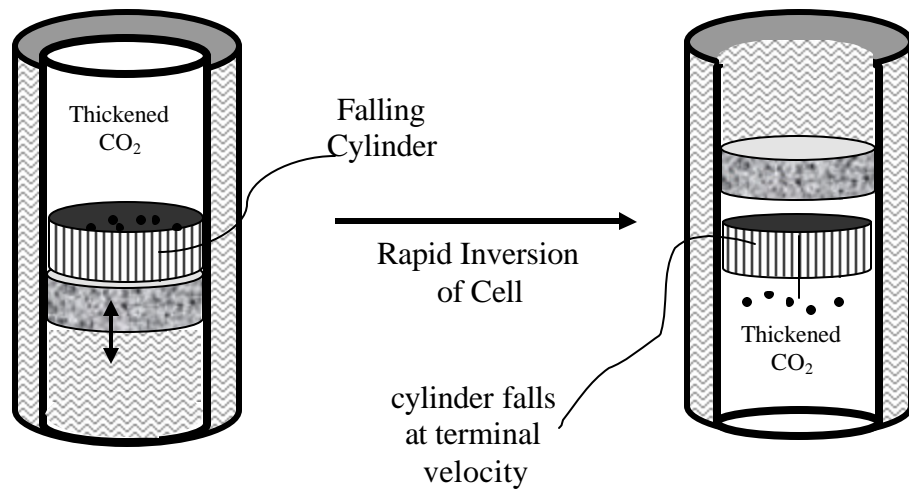
$$\frac{h_{solution}}{h_{CO_2}} = \frac{u_{c,CO_2}}{u_{c,solution}} = \frac{t_{solution}}{t_{CO_2}} \quad (4.3)$$

where  $t_{solution}$  and  $t_{CO_2}$  are fall times of the cylinder across a certain distance in polymer solution and neat CO<sub>2</sub>, respectively. In a typical measurement of fluid viscosity, a finely machined

aluminum cylinder (3.1597 cm in diameter) was placed into the cylindrical sample volume before the polymer sample and the mixing balls were added. Upon equilibration of the system (resulting in a single, transparent phase), the cell was rapidly inverted. It was visually ensured that cylinder falls coaxially through the cell. Measurements taken at different positions of the glass cylinder indicated that the falling cylinder reaches its terminal velocity within the first 1/10 of the length of its fall, even earlier for very viscous fluids. The fall time of the aluminum cylinder was recorded over a fixed distance at constant temperature and pressure Scheme 4.3.(b). Measurement was repeated at least 5 times at each concentration and the average was taken. Experiments were repeated in neat CO<sub>2</sub> as well. The average relative viscosity is calculated from the ratio of fall times, as indicated in Eq. 4.3.



(a) Solubility Measurement



(b) Viscosity Measurement

**Scheme 4.3** Sample volume of the cell used for phase behavior and viscosity measurements.

## 4.2 PHASE BEHAVIOR RESULTS OF COPOLYMERS IN DENSE CO<sub>2</sub>

In previous attempts,<sup>3,4,5,8,9,11,12,19</sup> designing a CO<sub>2</sub>-thickener was hindered by the low solubility of hydrocarbon-based polymers. With the identification of CO<sub>2</sub>-philic moieties (fluoroacrylates), design of a CO<sub>2</sub>-thickener became more tractable. As shown in this research, the solubility of even highly CO<sub>2</sub>-phobic materials can be achieved with the incorporation of sufficient amounts of fluoroacrylate into the polymer. A series of aromatic acrylate-fluoroacrylate copolymers was synthesized and tested for their solubility and viscosity enhancing ability. The change in the series was created by changing either spacer length (number of CH<sub>2</sub> units indicated by “n”) or number of aromatic rings (indicated by “m”), or both in the aromatic acrylate unit in the copolymer. All of the copolymers were found to be miscible with CO<sub>2</sub> at room temperature, 295 K, and increased the solution viscosity to some degree depending upon type and molar composition.

Miscibility behavior of styrene-fluoroacrylate copolymers were earlier evaluated.<sup>26</sup> Figure 4.1 shows experimental miscibility curves for one of the compositions of styrene-fluoroacrylate copolymers and its partially sulfonated analogue. Surprisingly, the location of phase boundary is slightly lower for partially sulfonated styrene than that for its unsulfonated analogue at this particular composition. It was reported earlier that cation- $\pi$  interaction is an important strong non-covalent binding force.<sup>95,96,97</sup> Although a complete, quantitative description of the cation- $\pi$  interaction would involve a number of intermolecular forces, such as charge-quadrupole, charge-dipole, charge-induced dipole, charge transfer, dispersion forces, and in some cases, a hydrophobic component,<sup>95</sup> it was suggested that this interaction is electrostatic in

nature, involving the interaction of the cation with the large, permanent quadrupole moment of benzene. Here, it is surmised that sulfonation at this degree causes “micellization”, decreasing the miscibility pressures for the polymer via exclusion of CO<sub>2</sub>-phobic groups from CO<sub>2</sub> as a result of cation- $\pi$  interactions.

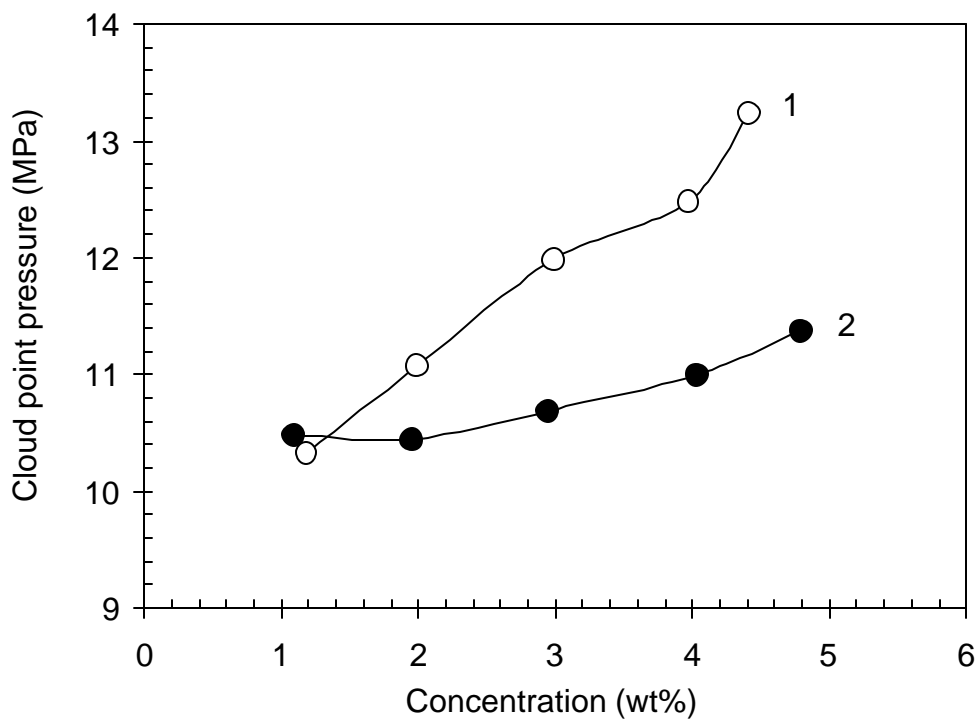


**Figure 4.1** Phase Behavior of Sulfonated and Unsulfonated Styrene-Fluoroacrylate Copolymer in CO<sub>2</sub> at T=295 K (St: Styrene, FA: Fluoroacrylate, S.St: Sulfonated Styrene) 1) 11%St-89%FA, 2) 0.1%S.St-10.9%St-89%FA

The phase behavior of four different types of aromatic acrylate copolymers with fluoroacrylate was also measured. Table 4.2 shows the number of “m” (aromatic rings) and “n” (spacer CH<sub>2</sub>'s) in the acrylate unit.

**Table 4.2** Number of “m” and “n” in the aromatic acrylates used in this study.

	Phenyl Acrylate (PHA)	Benzyl Acrylate (BEA)	Phenyl Ethyl Acrylate (PEA)	Naphthyl Acrylate (NA)	Naphthyl Methyl Acrylate (NMA)
m	1	1	1	2	2
n	0	1	2	0	1

The phase behavior of PHA-FA copolymers is illustrated in Figure 4.2, that of BEA-FA copolymers in Figure 4.3 and that of PEA-FA in Figure 4.4, as a function of concentration at various copolymer compositions. As can be seen in these figures, as the aromatic acrylate content increases in the copolymer, miscibility pressure of the copolymers remains unperturbed. Similarly, miscibility pressures for aromatic acrylate-fluoroacrylate copolymers do not change significantly for the same aromatic acrylate content in the copolymer when the length of spacer unit increases in the aromatic acrylate unit of the copolymer (Figure 4.5). It is believed that, in both cases, the fluoroacrylate unit dominates the miscibility process. In addition, given that both CO<sub>2</sub> and aromatic rings have large, permanent quadrupole moments, there is an additional

possibility that there would be substantial quadrupole-quadrupole interactions between CO<sub>2</sub> and aromatic ring, leading to an increase in solute-solvent interactions or quadrupole-quadrupole interactions between aromatic-aromatic ring, leading to “micellization” and, hence, exclusion of aromatic rings from CO<sub>2</sub> solutions.

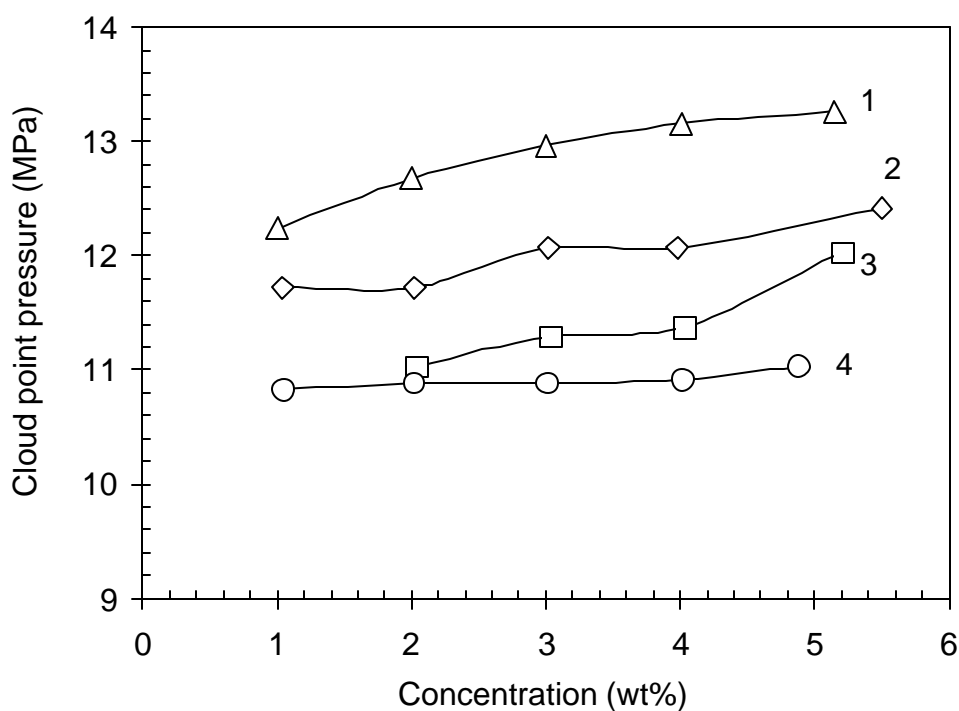


**Figure 4.2** Phase Behavior of PHA-FA Copolymer in CO<sub>2</sub> at T=295 K (PHA: Phenyl Acrylate, n=0, m=1; FA: Fluoroacrylate) 1) 31%PHA-69%FA, 2) 29%PHA-71%FA, 3) 26%PHA-74%FA, 4) 23%PHA-77%FA.

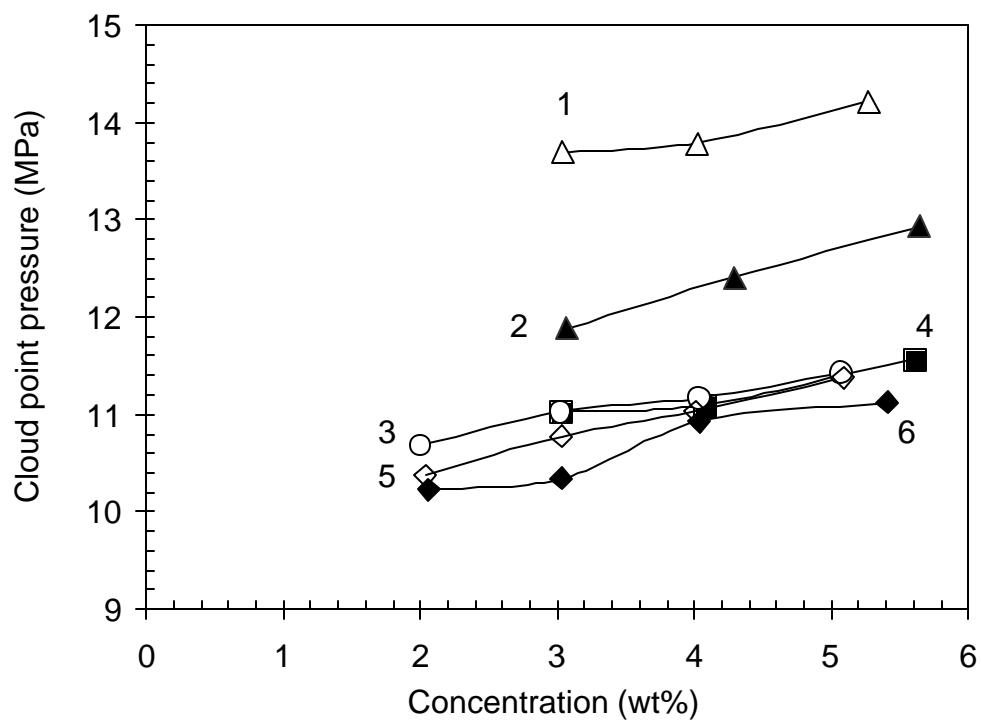


**Figure 4.3** Phase Behavior of BEA-FA Copolymer in CO<sub>2</sub> at T=295 K (BEA: Benzyl Acrylate, n=1, m=1; FA: Fluoroacrylate), 1) 54%BEA-46%FA, 2) 38%BEA-62%FA, 3) 27%BEA-73%FA, 4) 29%BEA-71%FA, 5) 18%BEA-82%FA, 6) 21%BEA-79%FA

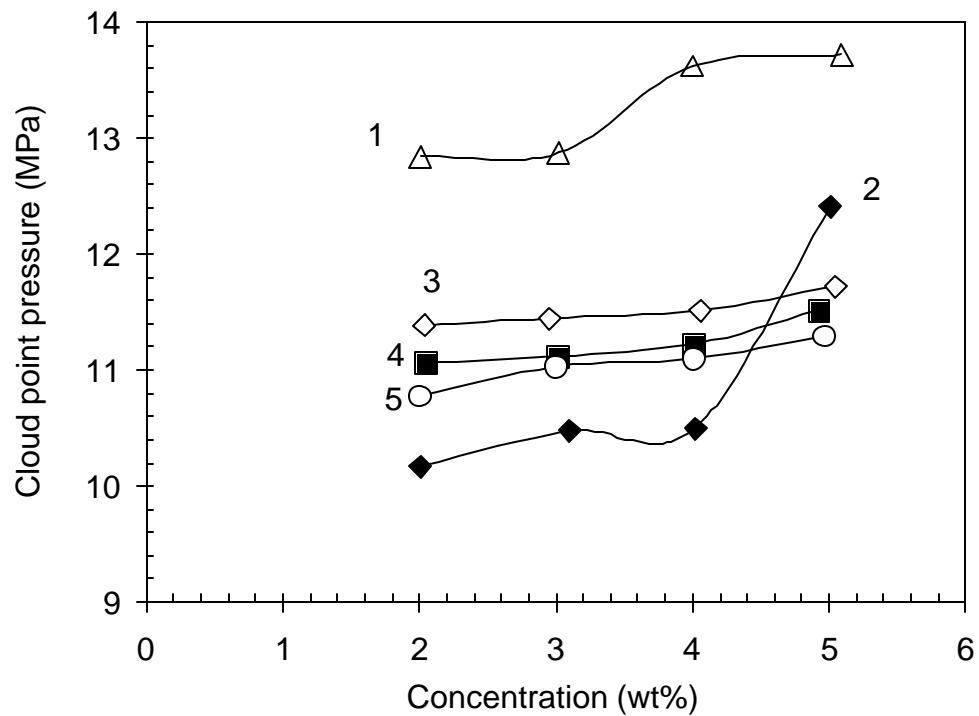


**Figure 4.4** Phase Behavior of PEA-FA Copolymer in CO<sub>2</sub> at T=295 K (PEA: Phenyl ethyl acrylate, n=2, m=1; FA: Fluoroacrylate), 1) 36% PEA-64% FA, 2) 24% PEA-76% FA, 3) 26% PEA-74% FA, 4) 25% PEA-75% FA, 5) 29% PEA-71% FA

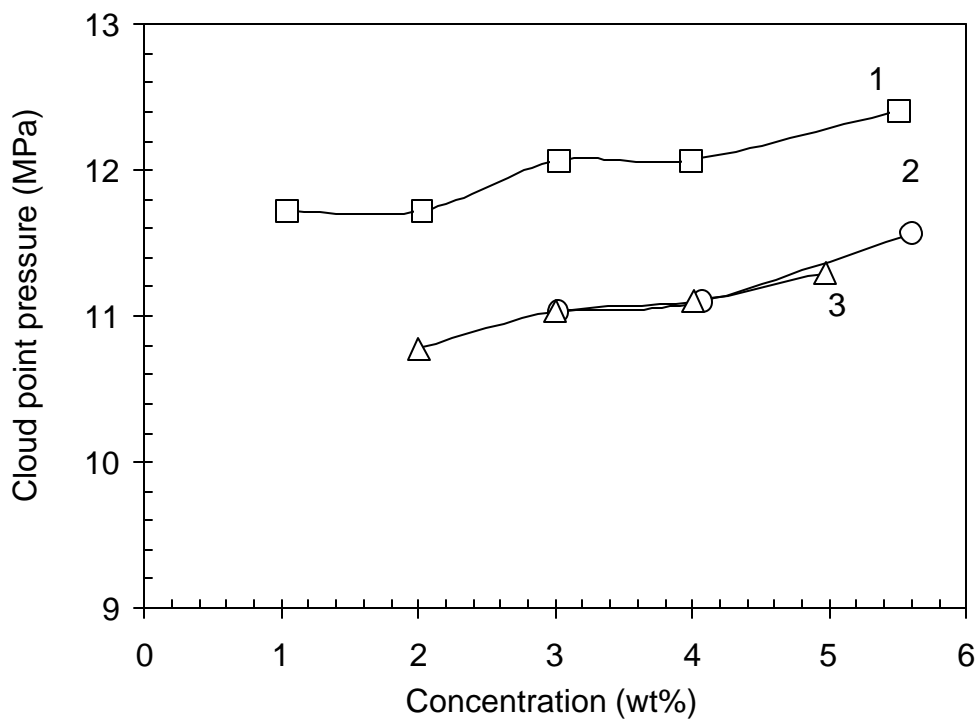


**Figure 4.5** Effect of spacer length on the phase behavior of copolymers in CO<sub>2</sub> at T=295 K (PHA: Phenyl acrylate, n=0, m=1; BEA: Benzyl acrylate, n=1, m=1; PEA: Phenyl ethyl acrylate, n=2, m=1; FA: Fluoroacrylate), 1) 29%PHA-71%FA, 2) 29%BEA-71%FA, 3) 29%PEA-71%FA.

Copolymers of naphthyl acrylate-fluoroacrylate at varying compositions were also synthesized; phase behavior of naphthyl acrylate-fluoroacrylate copolymers is shown in Figure 4.6. Interestingly, the location of phase boundary does not change significantly with the increasing content of naphthyl acrylate in the copolymer. Again, this is a result of the dominance of the fluoroacrylate unit on miscibility pressures.

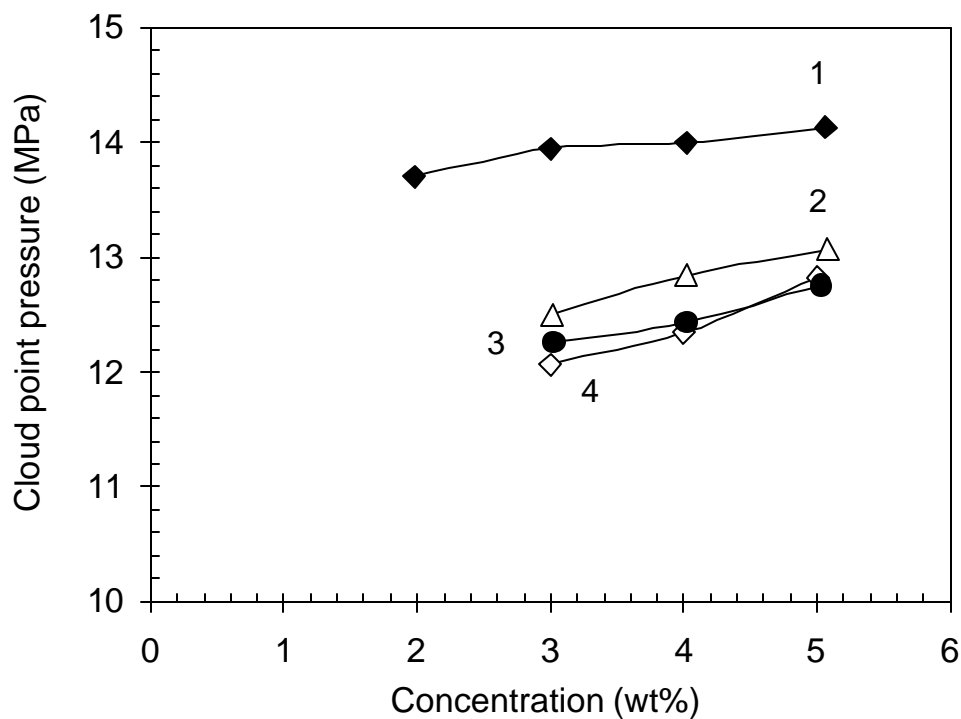


**Figure 4.6** Phase Behavior of NA-FA Copolymer in CO<sub>2</sub> at T=295 K (NA: Naphthyl acrylate, n=0, m=2; FA: Fluoroacrylate), 1) 32%NA-68%FA, 2) 17%NA-83%FA, 3) 22%NA-78%FA, 4) 19%NA-81%FA

The effect of the number of aromatic rings in the acrylate unit on miscibility is illustrated in Figure 4.7. As seen in the figure, despite its bulkiness, the presence of naphthyl unit in the copolymer does not have a serious detrimental effect on miscibility pressures. The miscibility pressure curve of a NA-FA copolymer is located very close to that of a PHA-FA copolymer of the same aromatic acrylate content. As before, it is suggested that the highly CO<sub>2</sub>-philic fluoroacrylate unit is controlling the miscibility of the NA-FA copolymers in CO<sub>2</sub>.

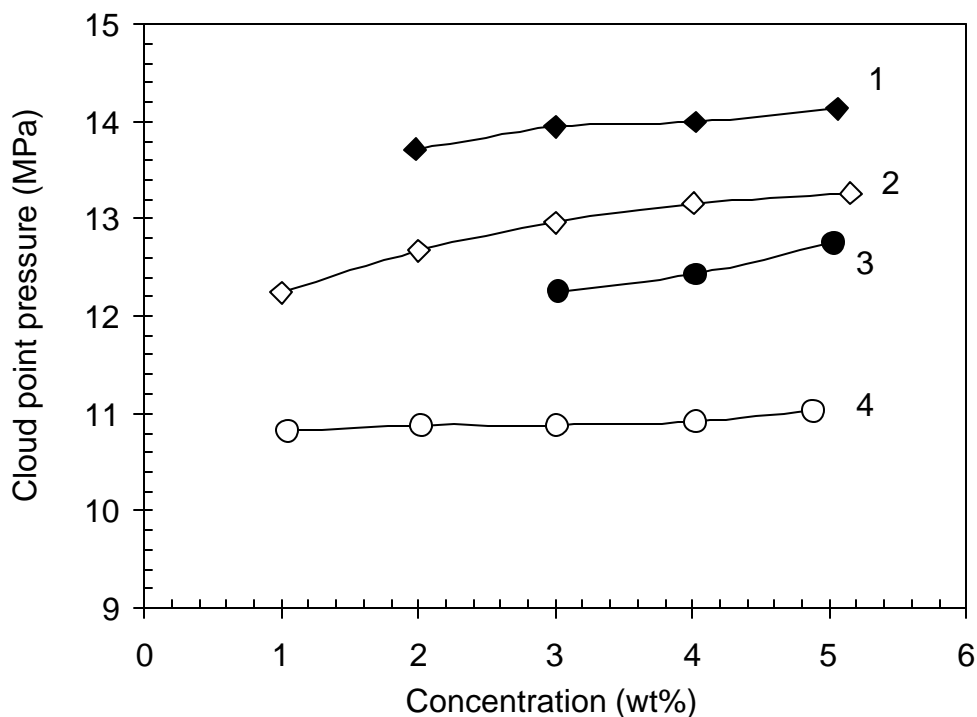


**Figure 4.7** Phase Behavior of NA-FA and PHA-FA Copolymers in CO<sub>2</sub> at T=295 K (NA: Naphthyl acrylate; n=0, m=2; PHA: Phenyl acrylate, n=0, m=1, FA: Fluoroacrylate), 1) 32%NA-68%FA, 2) 31%PHA-69%FA, 3) 22%NA-78%FA, 4) 23%PHA-77%FA

The miscibility pressures of various acrylate copolymers at similar compositions are compared in Figure 4.8, namely PHA-FA, NA-FA, CHA-FA copolymers. Miscibility pressures for the copolymers are again not distinguishable. It was reported earlier that phenyl rings are much more rigid and much more dense than cyclohexyl rings, and thus, having greater stiffness and high cohesive energy.<sup>83</sup> In this case, one would expect that PHA-FA copolymers should be less miscible with CO<sub>2</sub> than CHA-FA copolymer. It seems that favorable quadrupole-quadrupole

interactions between CO<sub>2</sub> and phenyl rings, and those between phenyl and phenyl rings are compensating for this negative effect.

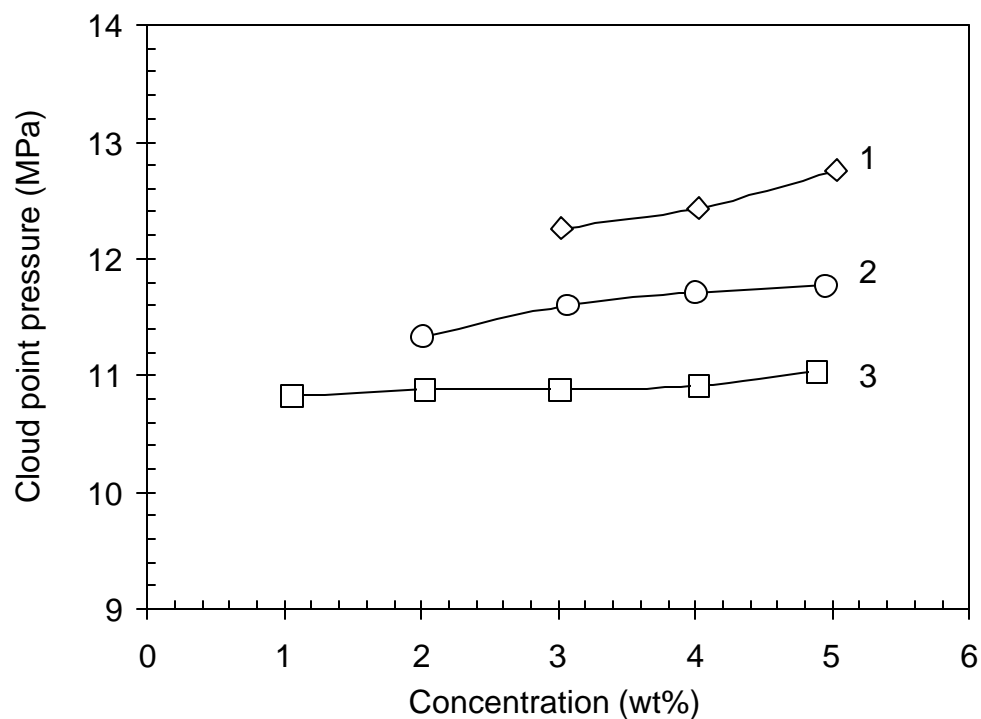


**Figure 4.8** Phase Behavior of NA-FA, CHA-FA and PHA-FA Copolymers in CO<sub>2</sub> at T=295 K (CHA: Cyclohexyl acrylate, NA: Naphthyl acrylate; n=0, m=2; PHA: Phenyl acrylate, n=0, m=1, FA: Fluoroacrylate), 1) 22%NA-88%FA, 2) 22%CHA-78%FA, 3) 23%PHA-77%FA

### 4.3 VISCOSITY BEHAVIOR RESULTS OF COPOLYMERS IN DENSE CO<sub>2</sub>

The power of polymers to influence fluid rheology arises from the high volume of a macromolecule in solution and chain entanglements. Additional influence can be achieved by means of intermolecular associations. These associations should be strong enough to give rise to stable higher order macromolecular architectures, yet not form covalent crosslinks that would hinder the miscibility of polymer chains in the solvent. Stacking of aromatic rings in the copolymer is considered to be the primary force in this work for the intermolecular association needed to raise the viscosity of CO<sub>2</sub>.

As mentioned before, viscosity enhancement ability of styrene-fluoroacrylate copolymers forms the baseline of this particular study. Figure 4.9 shows viscosity enhancement ability of one of the compositions of the styrene-fluoroacrylate copolymers and its partially sulfonated analogue. Not surprisingly, the viscosity enhancement decreases as the concentration of polymer in the solution decreases. The effect on viscosity is more pronounced with sulfonated copolymer solution of CO<sub>2</sub> compared to unsulfonated one, especially at higher wt% of the polymer in solution. This might be explained by additional contribution from the attractive interaction between partially positive charge of Na<sup>+</sup> and  $\pi$ -face of aromatic ring<sup>98</sup> along with stacking of aromatic rings and/or stronger stacking tendency of the rings due to the change in their electronic structure by substitution of electron withdrawing sulfonate salt.

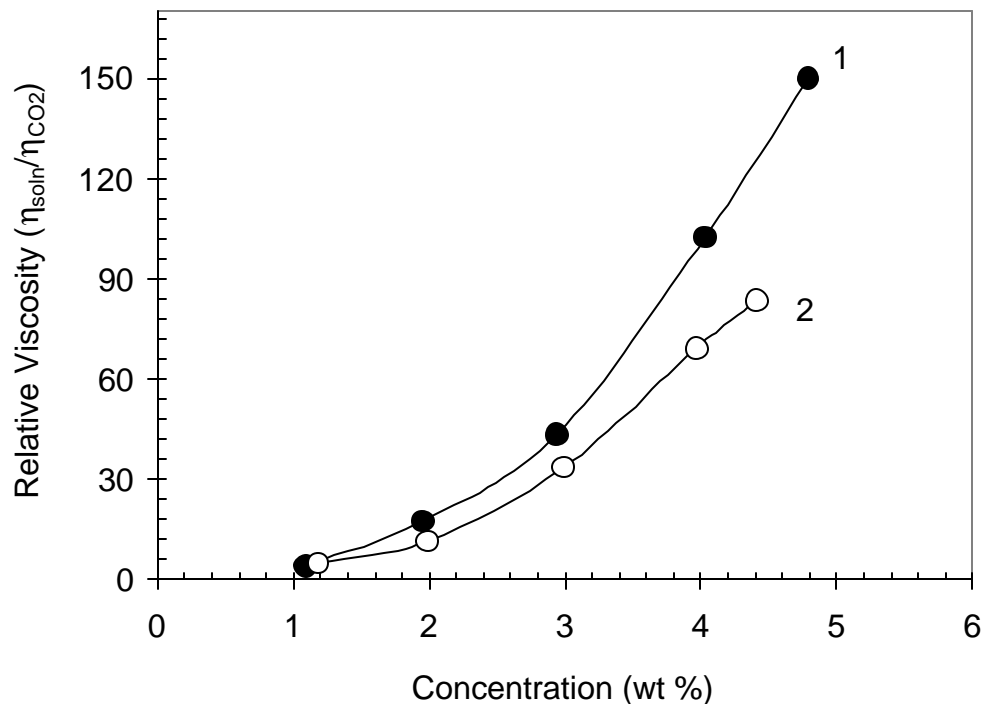


**Figure 4.9** Relative viscosity of Sulfonated and Unsulfonated Styrene-Fluoroacrylate Copolymer Solutions in CO<sub>2</sub> as a function of concentration at T=295 K and P=41.4 MPa (St: Styrene, FA: Fluoroacrylate, S.St: Sulfonated Styrene), 1) 0.1% S.St-10.9%St-89%FA, 2) 11%St-89%FA

Similar to styrene, aromatic acrylates in the copolymers have also the ability to increase the viscosity of neat CO<sub>2</sub>. The degree of increase in viscosity depends on the structure of aromatic acrylate and its content in the copolymer as shown in Figure 4.10, Figure 4.11 and Figure 4.12. In these figures, viscosity increases with the addition of aromatic moiety; but after a certain composition, additional increases in the content of the aromatic acrylate in the copolymer causes viscosity to drop. The same effect was previously observed with styrene-fluoroacrylate

copolymers.<sup>26</sup> The optimum composition for PHA-FA copolymers for maximum viscosity enhancement is 29% PHA. The optimum for BEA-FA and PEA-FA copolymers were not observed in the composition range studied here; but, because a homopolymer of fluoroacrylate does not give rise to considerable increase in the viscosity of CO<sub>2</sub>,<sup>24</sup> it is suggested that optimum for BEA-FA and PEA-FA copolymers falls in the range of 0-18% BEA and 0-24% PEA, respectively.

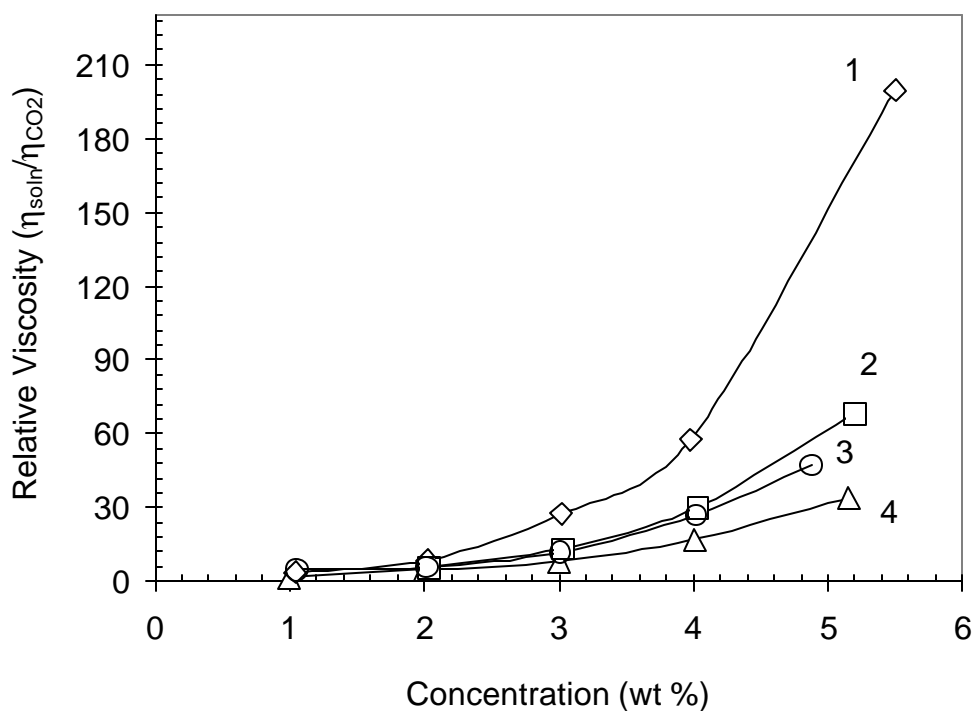


**Figure 4.10** Relative viscosity of x%PHA-y%FA copolymer solutions in CO<sub>2</sub> as a function of concentration at T=295 K at varying copolymer composition, P=41.4 MPa, (PHA: Phenyl Acrylate, n=0, m=1; FA: Fluoroacrylate), 1) 29%PHA-71%FA, 2) 26%PHA-74%FA, 3) 23%PHA-77%FA, 4) 31%PHA-69%FA

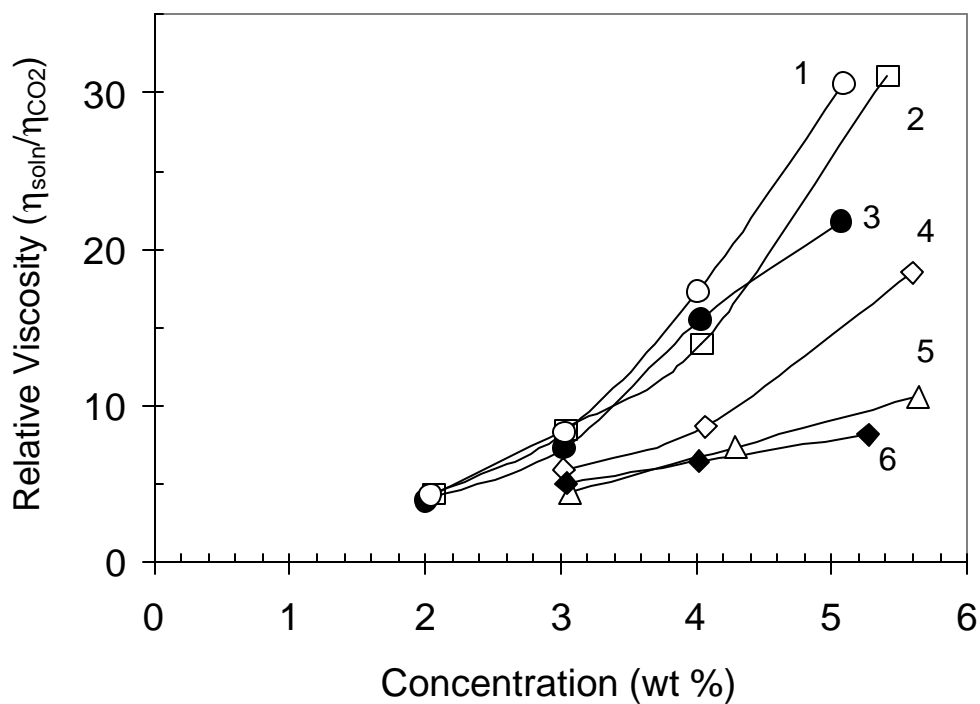


**Figure 4.11** Relative viscosity of x%BEA-y%FA copolymer solutions in CO<sub>2</sub> as a function of concentration at T=295 K at varying copolymer composition, P=41.4 MPa, (BEA: Benzyl Acrylate, n=1, m=1; FA: Fluoroacrylate), 1) 18%BEA-82%FA, 2) 21%BEA-79%FA, 3) 27%BEA-73%FA, 4) 29%BEA-71%FA, 5) 38%BEA-62%FA, 6) 54%BEA-46%FA

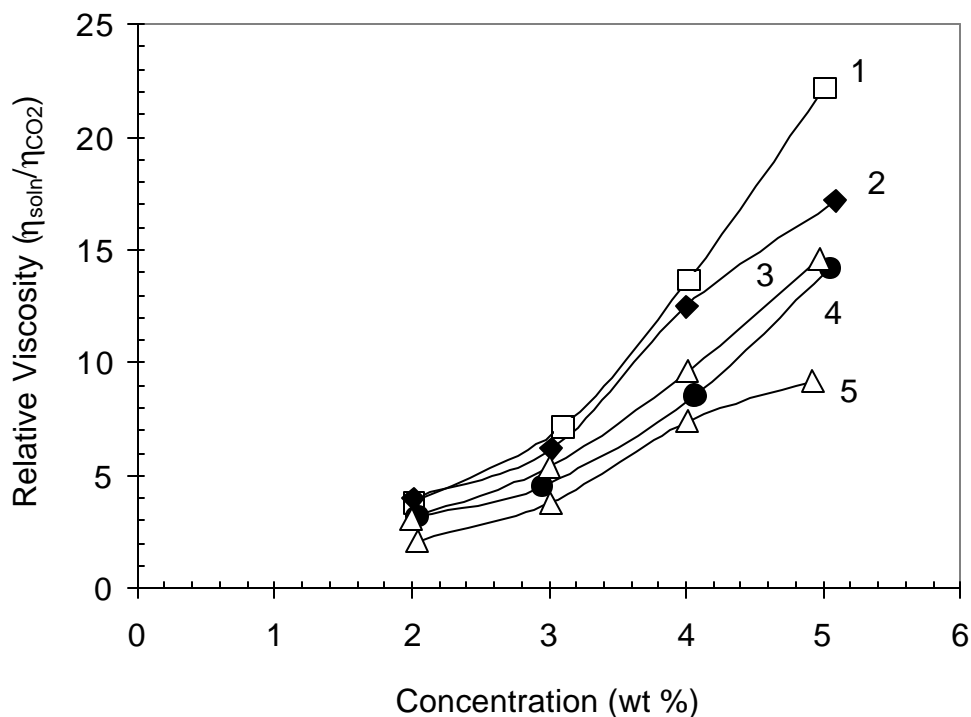


**Figure 4.12** Relative viscosity of x%PEA-y%FA copolymer solutions in CO<sub>2</sub> as a function of concentration at T=295 K at varying copolymer composition, P=41.4 MPa, (PEA: Phenyl ethyl acrylate, n=2, m=1; FA: Fluoroacrylate), 1) 24%PEA-76%FA, 2) 36%PEA-64%FA, 3) 25%PEA-75%FA, 4) 26%PEA-74%FA, 5) 29%PEA-71%FA

Although one would expect that increasing content of aromatic acrylates would increase the number of crosslink points, after an optimum composition, due to the CO<sub>2</sub>-phobic nature of the aromatic acrylates, the hydrodynamic volume of the coils decreases, such that the intrachain attractive interactions dominate. Then, interaction becomes mostly intramolecular rather than intermolecular, resulting in lower viscosity enhancement.

Although, initially, it was hypothesized that by increasing the length of the spacer unit (number of  $n$ ), the aromatic rings could relax to achieve the optimum stacking position resulting in higher viscosity, it was experimentally observed that increasing spacer length has a reverse effect on viscosity with the copolymers possessing only a single aromatic ring (Figure 4.13). It is surmised that the difference between anticipated and the actual behavior results from the change in electronic nature of the aromatic ring. It is suggested that, by changing electron density of the ring with substituents, one can alter the magnitude of the interactions between closely aligned aromatic rings.<sup>59</sup> One way to determine the effect of substituent on electron density of the ring is to look at the Hammett Sigma constant ( $\sigma$ ), which is a measure of the effect of a given *m*- or *p*-substituent on the acidity of benzoic acid (in other words, it represents the e-withdrawing or e-donating power of a substituent). The more positive  $\sigma$  is, the more e-withdrawing is the substituent, similarly, the more negative  $\sigma$  is, the more e-releasing is the substituent. For example, the Hammett Sigma constant ( $\sigma$ ) is given as -0.15 and +0.31 for  $-\text{CH}(\text{CH}_3)_2$  and  $-\text{OCOR}$ , respectively.<sup>99,100</sup> The  $-\text{CH}(\text{CH}_3)_2$  group, as in styrene, increases the electronic density of the ring, on the other hand, the  $-\text{OCOR}$  group, as in phenyl acrylate, decreases electron density. However, data are not available for benzyl acrylate and phenyl ethyl acrylate. It is possible that both the spacer unit ( $\sigma=-0.17$  for  $\text{CH}_3$  and  $\sigma=-0.15$  for  $\text{C}_2\text{H}_5$ ) and the  $-\text{OCO}$  group might have combining effect on the electron density of the ring in the benzyl acrylate and phenyl ethyl acrylate. Therefore, it is not easy to arrive at a solid conclusion on the effect of electronic structure on the strength of interactions. In order to assess the effect of change of the electron density of the ring on association of aromatic rings, it was attempted to synthesize 4-bromobenzyl acrylate-FA copolymer, in which an e-withdrawing bromine at the *para* position will compensate for the effect of e-donating power of  $\text{CH}_2$  (the value of  $\sigma$  is +0.23 for  $-\text{Br}$  and -

0.17 for CH<sub>3</sub>). However, the attempts to synthesize the copolymer resulted in failure because the “critical conversion” was reached before obtaining enough polymer to evaluate due to H-abstraction (chain transfer reactions) as explained in section 4.1.5.

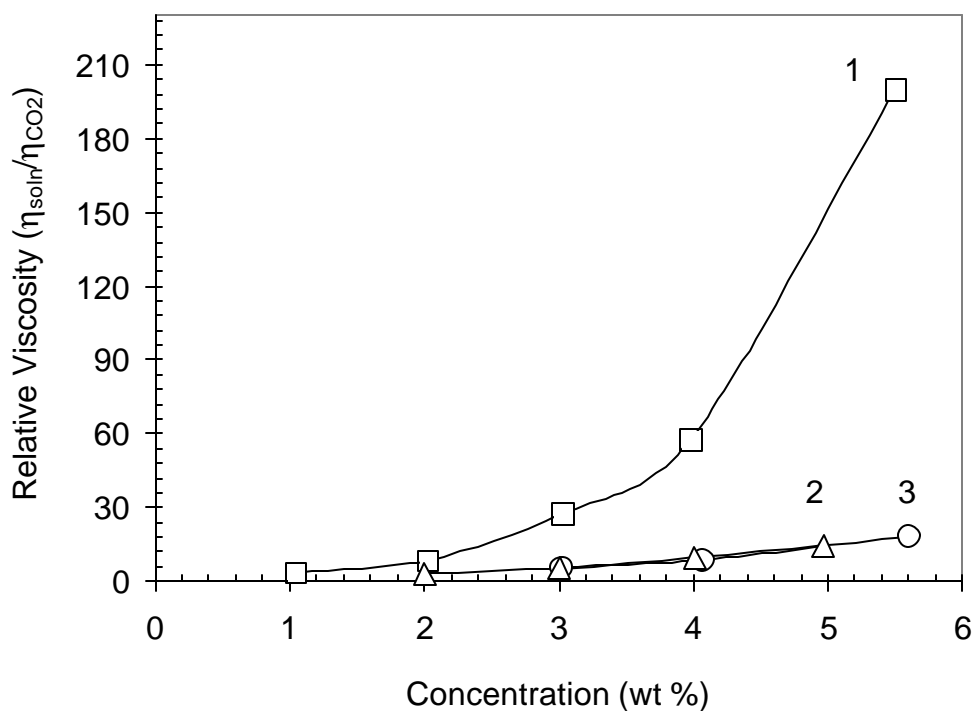


**Figure 4.13** Effect of spacer length on CO<sub>2</sub>-viscosity enhancement of copolymer solutions as a function of concentration at T=295 K and P= 41.4 MPa, (BEA: Benzyl Acrylate, n=1, m=1; PHA: Phenyl acrylate, n=0, m=1; PEA: Phenyl ethyl acrylate, n=2, m=1; FA: Fluoroacrylate), 1) 29%PHA-71%FA, 2) 29%PEA-71%FA, 3) 29%BEA-71%FA

The hydrodynamic volume of the polymer chain in CO<sub>2</sub> solution is an important parameter determining viscosity enhancement. Increased hydrodynamic volume is an indication of swelling of polymer chains in the solution. When highly swollen, it is much easier for the polymer chains to acquire intermolecular interactions rather than intramolecular. A number of studies have investigated the change in polymer conformation as a function of solvent density in supercritical fluids.<sup>101,102</sup> Those works indicated that the polymer chains expand as the density of supercritical fluid increases, screening attractive intrachain forces. In other words, solvent quality of CO<sub>2</sub> improves with pressure. This outcome was also reflected in our results, as higher viscosity enhancement at higher system pressures (Figure 4.14). This result suggests that associations between aromatic rings are more likely intermolecular rather than intramolecular due to the chain expansion induced by pressure (higher hydrodynamic volume). The same effect of pressure was also observed with BEA-FA and PEA-FA copolymers.

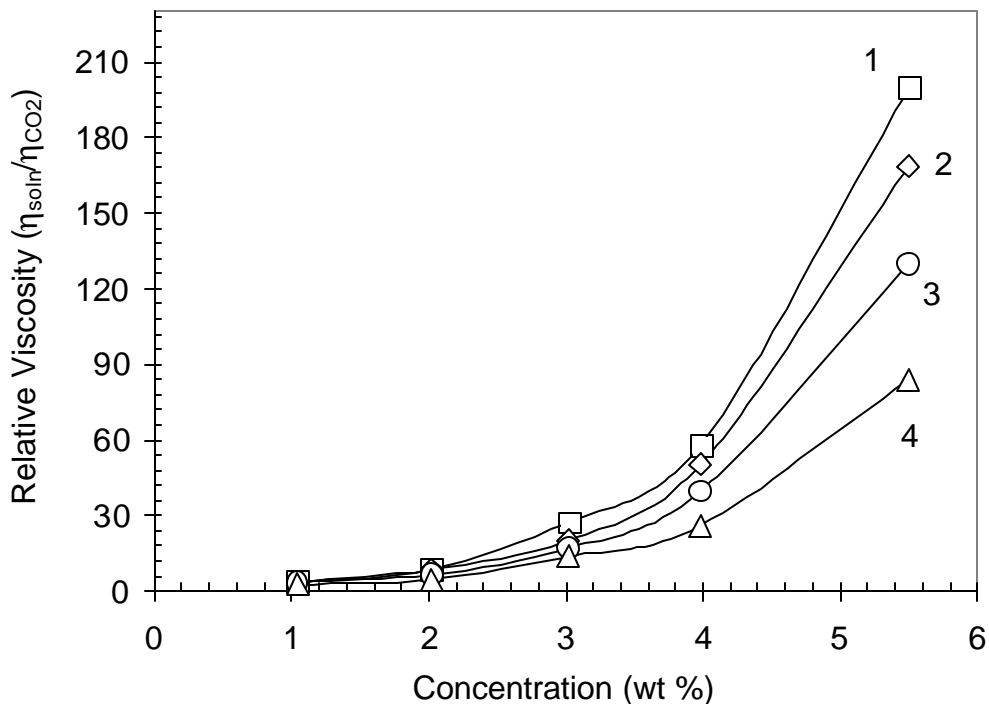


**Figure 4.14** The effect of pressure on relative viscosity of 29%PHA-71%FA copolymer solutions in CO<sub>2</sub> as a function of concentration at T=295 K (PHA: Phenyl Acrylate, n=0, m=1; FA: Fluoroacrylate), 1) P=41.4 MPa, 2) P=34.5 MPa, 3) P=27.6 MPa, 4) P=20.7 MPa.

Success in designing effective CO<sub>2</sub> thickeners in the present work was arisen from discovering suitable polymer groups that have the ability to associate in CO<sub>2</sub> to form stable supramolecular structures. One can question whether the association of the aromatic rings is the key governing viscosity enhancement of CO<sub>2</sub>. In order to investigate this, the copolymer of fluoroacrylate with a cycloaliphatic acrylate, namely cyclohexyl acrylate, was synthesized. Cyclohexyl acrylate is analogous to phenyl acrylate in structure, where the aromatic ring is replaced with an unsaturated, cyclic ring. Results showed that presence of aromatic rings plays

the key role in viscosity enhancement. Figure 4.15 compares the viscosity enhancement ability of CHA-FA and PHA-FA copolymers at similar compositions, and Figure 4.16 does so at their optimum composition.

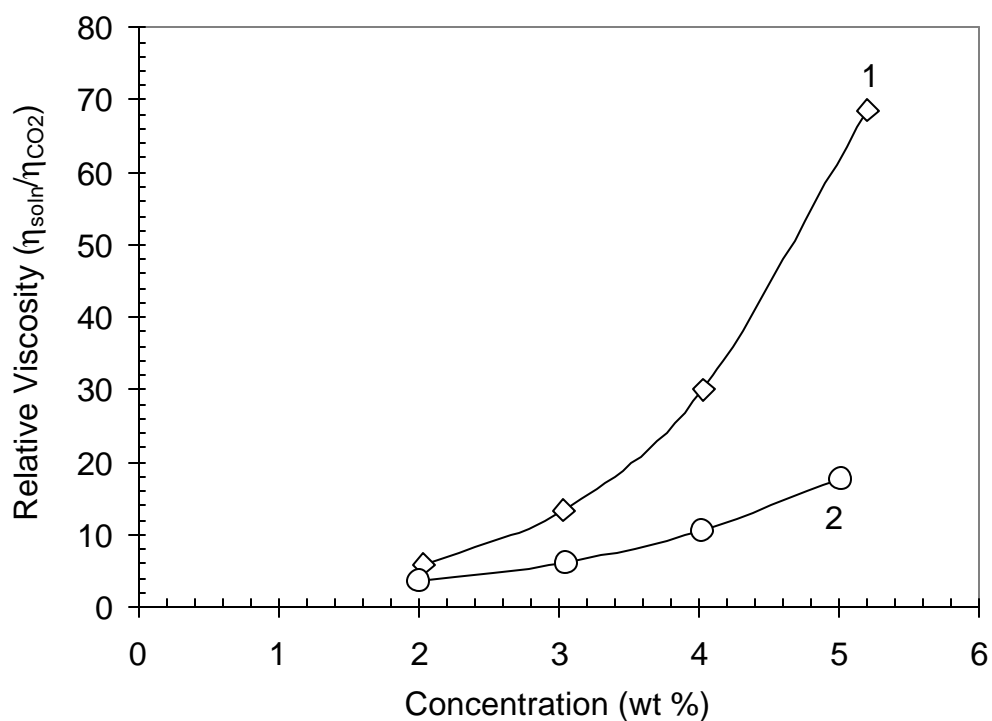


**Figure 4.15** Comparison of aromatic and non-aromatic rings on CO<sub>2</sub>-viscosity enhancement *at similar compositions* at T=295 K and P=41.4 MPa as a function of concentration (PHA: Phenyl Acrylate; CHA: Cyclohexyl Acrylate; FA: Fluoroacrylate), 1) 26%PHA-74%FA, 2) 27%CHA-73%FA.

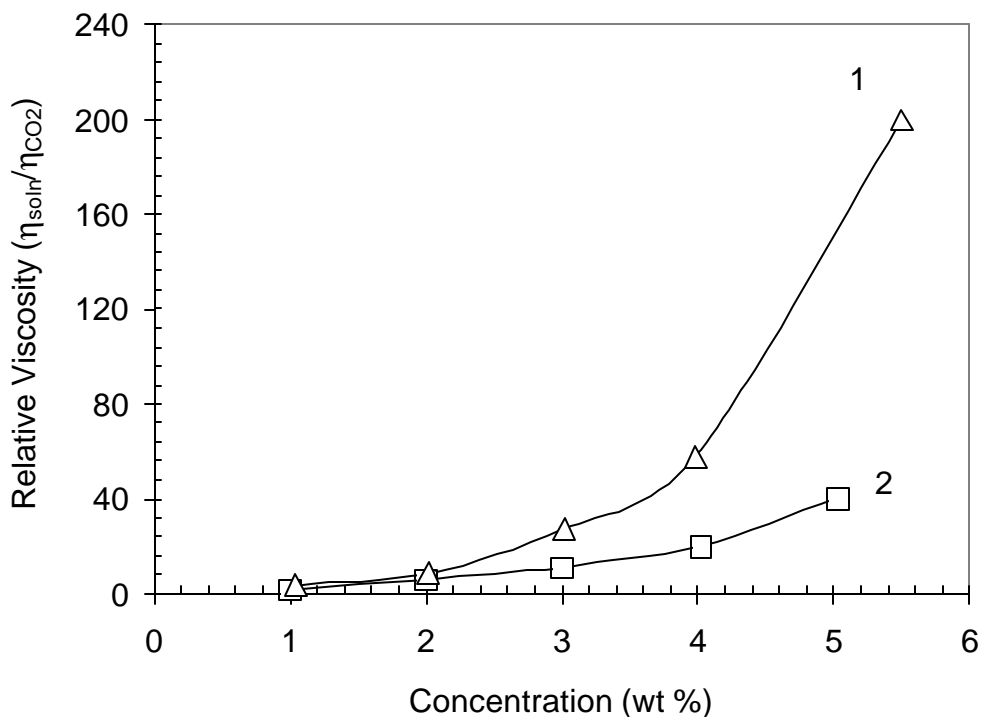


**Figure 4.16** Comparison of aromatic and non-aromatic rings on CO<sub>2</sub>-viscosity enhancement *at their optimum composition* at T=295 K and P=41.4 MPa as a function of concentration (PHA: Phenyl Acrylate; CHA: Cyclohexyl Acrylate; FA: Fluoroacrylate), 1) 29%PHA-71%FA, 2) 16%CHA-84%FA.

In the present study, it was initially hypothesized that by increasing the surface area of aromatic structure, one might get stronger association between rings, and thus higher viscosity enhancement. Figure 4.17 compares the effect of size of the aromatic functional group on viscosity enhancement at similar compositions, and Figure 4.18 does so at the optimum compositions. For the same composition of acrylate unit in the copolymer, results showed that single aromatic ring (referring to PHA-FA copolymer) produces a better viscosity enhancement

than two aromatic rings (referring to NA-FA copolymer) in the acrylate unit (Figure 4.17). However, at their optimum composition, single and double ring in the aromatic acrylate unit show similar effect on viscosity enhancement at low concentrations; but, at higher concentrations, there is a considerable difference between viscosity enhancement of PHA-FA and NA-FA copolymers (Figure 4.18). There is a possibility that association between the bulky naphthyl rings is made difficult due to obstruction from long polymer backbone.

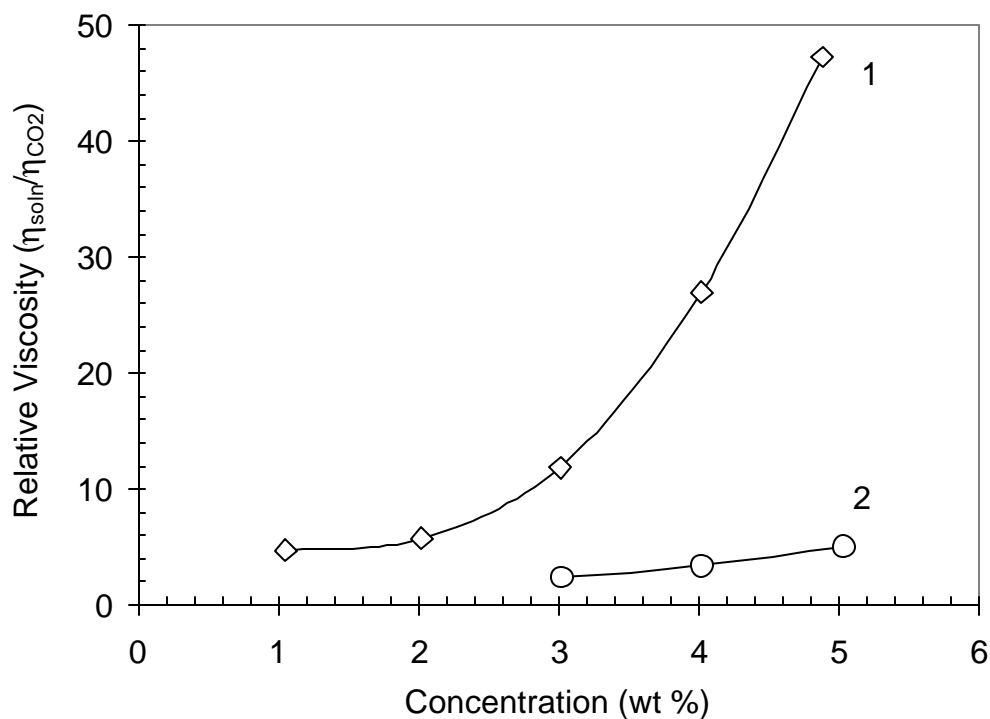


**Figure 4.17** Comparison of effect of size of aromatic rings on viscosity enhancement ability of CO<sub>2</sub> at similar compositions at T=295 K and P=41.4 MPa as a function of concentration (PHA: Phenyl acrylate; NA: Naphthyl acrylate; FA: Fluoroacrylate), 1) 23%PHA-77%FA, 2) 22%NA-78%FA.

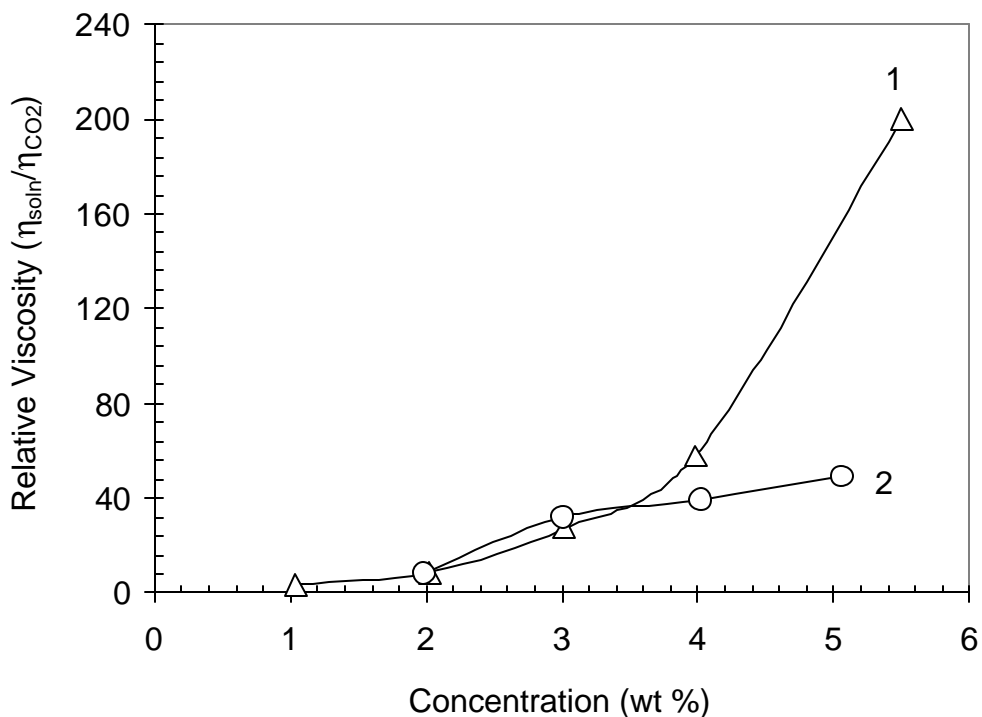


**Figure 4.18** Comparison of effect of size of aromatic rings on viscosity enhancement ability of  $\text{CO}_2$  at their optimum compositions at  $T=295\text{ K}$  and  $P=41.4\text{ MPa}$  as a function of concentration (PHA: Phenyl acrylate; NA: Naphthyl acrylate; FA: Fluoroacrylate), 1) 29%PHA-71%FA, 2) 32%NA-68%FA.

In an effort to understand the need for a spacer for favorable associations of rings in naphthyl acrylate, it was attempted to synthesize naphthyl methyl acrylate-fluoroacrylate copolymer (NMA-FA,  $m=2$ ,  $n=1$ ) so that naphthyl rings can relax to an optimum geometry to achieve the strongest interactions via spacer. Unfortunately, enough copolymer yield could not be obtained before the “critical conversion” was reached due to the chain transfer reactions.

Therefore, at present, why relative viscosity diminishes with increasing size of the aromatic group cannot be explained.

In general, one might argue that the differences in relative viscosities might be a result of the differences in molecular weights. Unfortunately, it is not possible to measure the molecular weight of the polymers studied due to insolubility of the polymers in traditional GPC solvents. Intrinsic viscosity is the most useful of the various viscosity expressions because it can be related to molecular weight by the Mark-Houwink equation:

$$[\eta] = K \cdot M^a \quad (4.4)$$

where  $[\eta]$  and  $M$  are the intrinsic viscosity and the molecular weight of the chain, respectively.  $K$  and  $a$  are the constants for a given polymer-solvent-temperature system. The exponent  $a$  increases with the solvent power of the medium. Intrinsic viscosity is related to relative viscosity ( $\eta_{\text{rel}}$ ), which is the viscosity of a polymer solution ( $\eta$ ) divided by the viscosity of the pure solvent ( $\eta_0$ ), in the dilute regime as follows:

$$\eta_{\text{rel}} = \frac{\eta}{\eta_0} = 1 + [\eta] \cdot c \quad (4.5)$$

where  $c$  is the concentration. As one can see, if molecular weight of a polymer is doubled, intrinsic viscosity changes as

$$[\eta]_{2M} = [\eta]_M \cdot 2^a \quad (4.6)$$

where  $[\eta]_M$  and  $[\eta]_{2M}$  are the intrinsic viscosities when molecular weights are  $M$  and  $2M$ , respectively. After substituting this equation in Eq, 4.5 and taking the ratio of relative viscosities:

$$\frac{\eta_{\text{rel},2M}}{\eta_{\text{rel},M}} = \frac{1/[\eta]_M + 2^a \cdot c}{1/[\eta]_M + c} \quad (4.7)$$

For randomly coiled polymers, the exponent  $a$  varies from 0.5 (theta solvent) to 0.8 (good solvent). As can be seen, when the molecular weight is doubled, the increase in relative viscosity is always less than 2. However, observed differences in relative viscosities in this work are much larger than 2. This suggests that the structural effects play a more significant role than molecular weights in viscosity increase of CO<sub>2</sub> solution. Moreover, it was previously observed that the homopolymer of fluoroacrylate does not induce any significant increase in the viscosity of a CO<sub>2</sub> solution due to lack of associating groups.<sup>26</sup>

The relative viscosity enhancement of NA-FA copolymer with varying content of naphthyl acrylate is illustrated in Figure 4.19. The results showed that the increasing content of the naphthyl unit in the copolymer is desirable to obtain better enhancement in viscosity. As explained before, with the increase in the naphthyl unit content, the number of interaction points increases, leading to better viscosity enhancement.

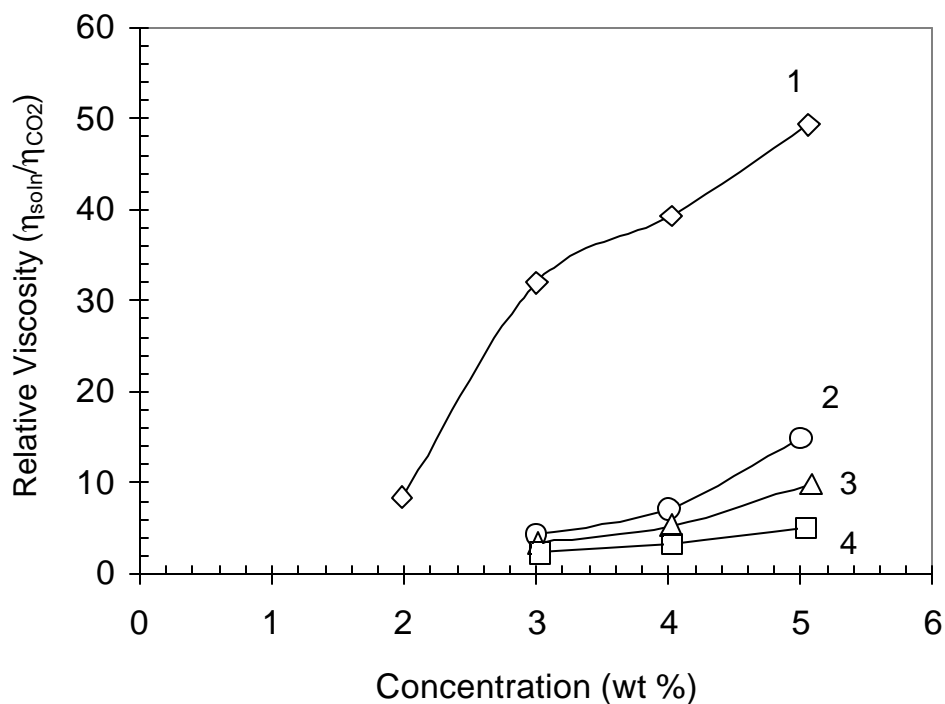


**Figure 4.19** Relative viscosity of x%NA-y%FA copolymer solutions in CO<sub>2</sub> as a function of concentration at T=295 K at varying copolymer composition, and P=41.4 MPa, (NA: Naphthyl Acrylate, n=0, m=2; FA: Fluoroacrylate), 1) 32%NA-68%FA, 2) 19%NA-81%FA, 3) 17%NA-83%FA, 4) 22%NA-78%FA

As mentioned before, with increasing pressure, CO<sub>2</sub> becomes a better solvent for the polymer, causing the polymer coil to swell to higher degree (larger hydrodynamic volume). Consequently, intermolecular interactions between the rings become more likely than intramolecular interactions, leading to formation of a large structures, which can increase the viscosity to higher extents. That is, at larger hydrodynamic volume, higher viscosity enhancement is observed, as one can see in NA-FA copolymers (Figure 4.20).

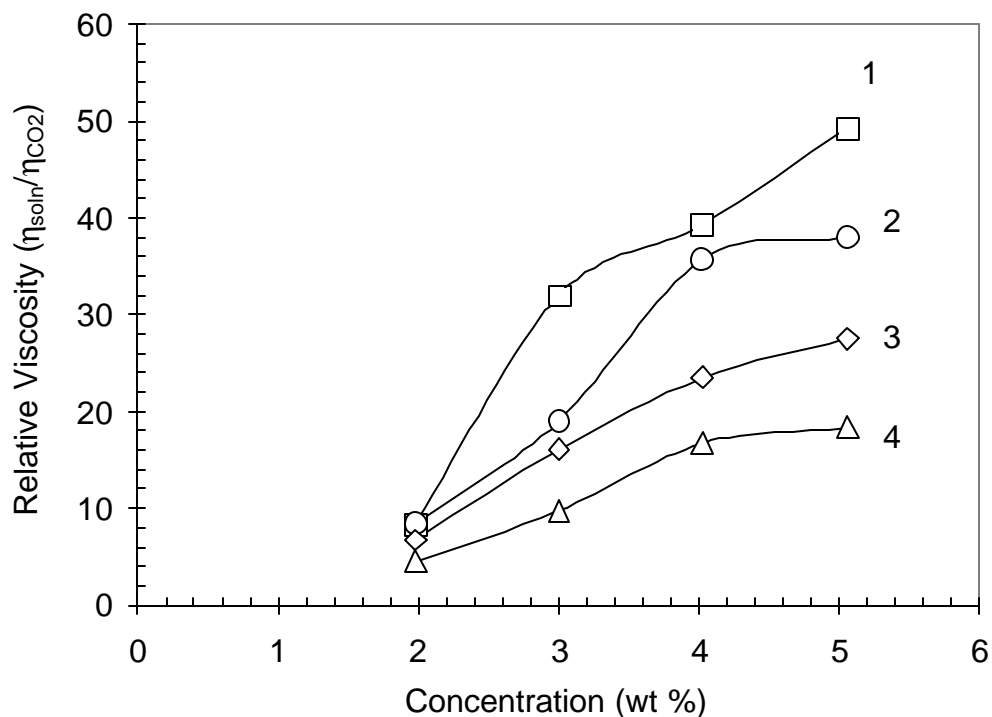


**Figure 4.20** The effect of pressure on relative viscosity of 32%NA-68%FA copolymer solutions in CO<sub>2</sub> as a function of concentration at T=295 K (NA: Naphthyl Acrylate, n=0, m=2; FA: Fluoroacrylate), 1) 41.4 MPa, 2) 34.5 MPa, 3) 27.6 MPa, 4) 20.7 MPa.

#### 4.4 CONCLUSIONS

The effect of the structure of copolymers of aromatic acrylate-fluoroacrylate on the viscosity enhancement of CO<sub>2</sub> was investigated. For this purpose, a series of aromatic acrylate-fluoroacrylate copolymers were synthesized. The change in the series was produced by systematically changing either spacer length (between the ring and carbonyl unit), or the number of aromatic rings, or both in the aromatic acrylate unit of the copolymer. In general, these

copolymers were all found to be miscible with CO<sub>2</sub> at 295 K and induce an increase in the viscosity to some degree, depending upon the type and content of aromatic acrylate unit in the copolymer. It was shown that stacking of aromatic rings is the key factor in viscosity enhancement.

Location of miscibility pressure curves of the copolymers was found not to be strongly affected by the type and/or content of the aromatic acrylate unit. This was attributed to the dominance of the highly CO<sub>2</sub>-philic fluoroacrylate unit in the copolymer on miscibility.

It was also observed that the increasing the length of the spacer unit has a negative effect on viscosity, such that the maximum viscosity was observed in the case of the PHA-FA copolymer. Results, especially in the case of PHA-FA copolymers, showed that viscosity of the solution increases with the increasing content of the aromatic acrylate unit in the copolymer, but a point is reached beyond which additional increase causes the relative viscosity to drop. Existence of such an optimum composition suggests that, beyond an optimum, the aromatic rings associate through intramolecular rather than intermolecular interactions, resulting in a decrease in viscosity enhancement. It is surmised that the decreasing affinity of CO<sub>2</sub> for the copolymer with increasing content of aromatic acrylate unit in the copolymer (i.e. decreasing hydrodynamic volume) is simply the cause for this effect.

Increase in viscosity was found to be dependent on the pressure of the solution; higher viscosities were measured at higher pressures. This is again simply due to CO<sub>2</sub> becoming a

weaker solvent for the polymer at lower pressures, resulting in a switch in the type of association from intermolecular to intramolecular.

At present, it is difficult to comment about the size of aromatic ring on viscosity enhancement. Naphthyl rings do have an ability to induce a raise in viscosity of neat CO<sub>2</sub> to some extent.

Being aware of the high cost of the fluoroacrylates and their insolubility in crude oil, the current study was extended to investigation of inexpensive, non-fluorous, CO<sub>2</sub>-philic polymers to improve the viability of the EOR process. Therefore, the following chapters focus on the design and synthesis of polymers composed of inexpensive building blocks.

## **5.0 EFFECT OF GRAFTED LEWIS BASE GROUPS ON THE PHASE BEHAVIOR OF MODEL POLY (DIMETHYL SILOXANES) IN CO<sub>2</sub>**

### **5.1 INTRODUCTION**

This particular study has aimed to evaluate the impact of various Lewis bases on the miscibility of polymers in CO<sub>2</sub>. Methylhydrosiloxane-dimethylsiloxane copolymers (with a total of 25 repeat units and a varying number of methylhydro units for grafting reaction) were chosen as model backbones because of their low glass transition temperature and relatively low cohesive energy density. By placing a series of side chains containing various Lewis bases and varying the amounts of those side chains onto constant chain-length silicone backbones, the effect of each chain and the extent of substitution on phase behavior in CO<sub>2</sub> were examined independently.

## 5.2 EXPERIMENTAL PROTOCOL

### 5.2.1 Materials:

Copolymers of methylhydrosiloxane-dimethylsiloxane (Table 5.1) and platinum-(vinyl tetramethyldisiloxane) complex in xylene (low color) were purchased from Gelest (Tullytown, PA). Anhydrous toluene, allyl ethyl ether, allyl acetate, allyl methyl carbonate, methyl-3-butenolate, 5-hexen-2-one were obtained from Aldrich. N,N-Dimethyl allylamine was purchased from Fisher Scientific. All materials were used without additional purification. Ultra-high purity argon was purchased from Praxair.

**Table 5.1** Methylhydrosiloxane-dimethylsiloxane copolymers<sup>(a)</sup> used in this study

Entry	Mole % MeHSiO	Mole % Me <sub>2</sub> SiO	z # of Si-H
1	3.5	96.5	1
2	6.5	93.5	2
3	16.5	83.5	5
4	27.5	72.5	11
5	100	0	25

<sup>(a)</sup> Total chain length of the copolymers is 25 repeat units

### 5.2.2 Synthesis of Lewis Base Grafted Siloxane Polymers:

Grafted copolymers were synthesized via a hydrosilylation reaction between an allyl compound and a methylhydrosiloxane-dimethylsiloxane copolymer,<sup>103</sup> as shown in Scheme 5.1. Glassware was oven-dried overnight and purged with ultra-high purity argon before use. In a typical experiment, 10 g (27.5 mmol Si-H) of 16.5 mole% methylhydro containing copolymer and 3.3 g (33.0 mmol) allyl acetate were charged to a 250 ml three-neck, round-bottomed flask, equipped with a magnetic stir-bar, a condenser, and an argon feed. 60 ml of anhydrous toluene and 100 mg of platinum-vinyl tetramethyldisiloxane complex in xylene (low color) were added to the reaction mixture. The solution was stirred for 3 – 4 hours at room temperature under an argon atmosphere, then heated to 45 °C and stirred overnight. During heating the color of the solution turned a slight brownish-yellow. The reaction was monitored using FT-IR, where the disappearance of the Si-H band at 2157 cm<sup>-1</sup> was used to establish the point at which the hydrosilylation reaction had gone to completion (Figure B.1 in Appendix B.). 0.3 g of decolorizing carbon was then added to the hot solution, and the mixture was stirred at 65 °C for 1–2 hours. The solution was then filtered while hot. Upon evaporation of the solvent under reduced pressure, a slightly yellow copolymer was isolated. Completion of the reaction was also verified using <sup>1</sup>H-NMR (300 MHz Bruker) by following the disappearance of the peak at 4.7 ppm (corresponding to Si-H), (Figure B.2-Figure B.5 in Appendix B).

### 5.2.3 Structural Characterization:

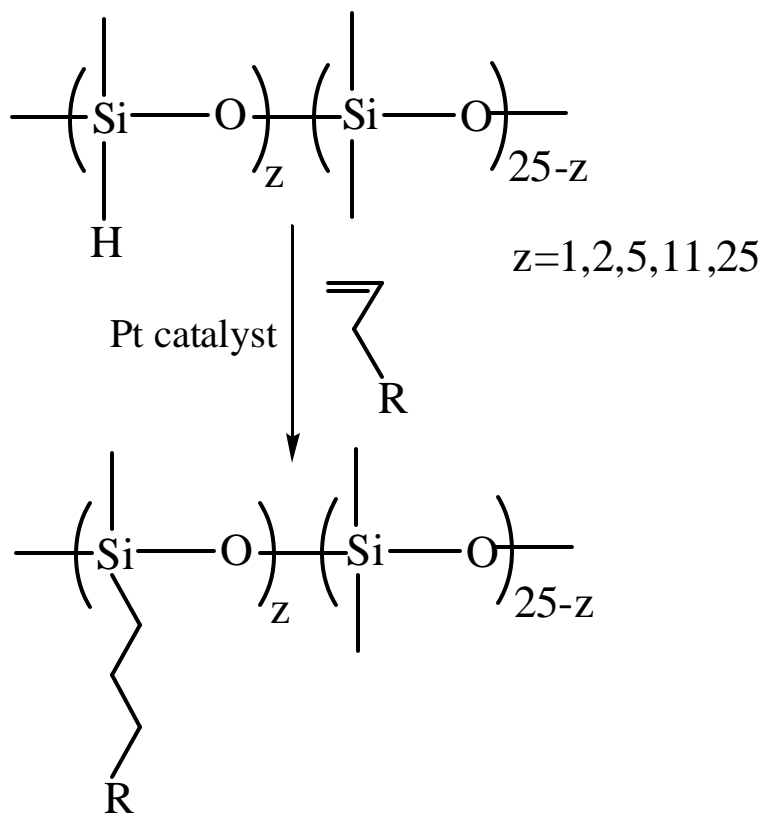
Infrared spectra were obtained on a Madison Instruments Inc. Research Series FT-IR spectrometer, and the samples were prepared as a thin film between two NaCl windows. Disappearance of the Si-H stretching at  $2157\text{ cm}^{-1}$  was indication of completion of the hydrosilylation reaction. Grafted siloxane copolymers were characterized using  $^1\text{H-NMR}$  (Bruker DMS 300) where the samples were dissolved in d-chloroform. All chemical shifts were referenced to tetramethylsilane (TMS) at zero ppm. Disappearance of the peak at 4.7 ppm (corresponding to Si-H) was also indication of the completion of hydrosilylation reaction. Complete removal of starting allyl material was verified by the disappearance of the allyl double peaks typically located between 5 and 6 ppm.

Figure B.1 in Appendix B shows the FT-IR spectra of ( $z=5$ ) propyl acetate-functional siloxane copolymer before and after hydrosilylation reaction, as an example.  $^1\text{H-NMR}$  spectra of ( $z=5$ )-functional siloxane copolymers are presented in Figures B.2-B.5 in Appendix B. Following is the  $^1\text{H-NMR}$  peak data for the grafted siloxane copolymers: **Methylhydrosiloxane:**  $\delta$  0.1 (broad, 3H, Si- $\text{CH}_3$ ),  $\delta$  4.7 (s, 1H, Si-**H**), **Propyl acetate:**  $\delta$  0.54 (broad, 2H, Si- $\text{CH}_2\text{-CH}_2$ ),  $\delta$  1.58 (broad, 2H, Si- $\text{CH}_2\text{-CH}_2$ ),  $\delta$  2.06 (s, 3H, O-CO- $\text{CH}_3$ ),  $\delta$  4.03 (t, 2H,  $\text{CH}_2\text{-CH}_2\text{-O-CO-CH}_3$ ). **Methyl butyrate:**  $\delta$  0.58 (t, 2H, Si- $\text{CH}_3$ ),  $\delta$  1.73 (broad, 2H, Si- $\text{CH}_2\text{-CH}_2$ ),  $\delta$  2.37 (t, 2H,  $\text{CH}_2\text{-CO-O-CH}_3$ ),  $\delta$  3.7 (s, 3H, CO-O- $\text{CH}_3$ ). **Propyl methyl carbonate:**  $\delta$  0.48 (broad, 2H, Si- $\text{CH}_2$ ),  $\delta$  1.66 (broad, 2H, Si- $\text{CH}_2\text{-CH}_2$ ),  $\delta$  3.71 (s, 3H, -O-CO-O- $\text{CH}_3$ ),  $\delta$  4.04 (t, 2H, - $\text{CH}_2\text{-O-CO-O}$ ). **Propyl dimethylamine:**  $\delta$  0.54 (broad, 2H, Si- $\text{CH}_2$ ),  $\delta$  1.01 (broad, 2H,  $\text{CH}_2\text{-N}(\text{CH}_3)_2$ ),  $\delta$  1.54 (broad, 2H, Si- $\text{CH}_2\text{-CH}_2$ ),  $\delta$  2.2 (d, 6H,  $\text{CH}_2\text{-N}(\text{CH}_3)_2$ ). **Butyl methyl ketone:**<sup>124</sup>  $\delta$  0.52 (t,

2H, Si-CH<sub>2</sub>-CH<sub>2</sub>),  $\delta$  1.36 (broad, 2H, Si-CH<sub>2</sub>-CH<sub>2</sub>-CH<sub>2</sub>),  $\delta$  1.61 (2H, Si-CH<sub>2</sub>-CH<sub>2</sub>-CH<sub>2</sub>),  $\delta$  2.14 (s, 3H, -CH<sub>2</sub>-CO-CH<sub>3</sub>),  $\delta$  2.42 (t, 2H, -CH<sub>2</sub>-CO-CH<sub>3</sub>). **Propyl ethyl ether:** <sup>124</sup> $\delta$  0.63 (broad, 2H, Si-CH<sub>2</sub>-CH<sub>2</sub>),  $\delta$  1.31 (t, 3H, -O-CH<sub>2</sub>-CH<sub>3</sub>),  $\delta$  1.75 (2H, Si-CH<sub>2</sub>-CH<sub>2</sub>-CH<sub>2</sub>),  $\delta$  3.49 (2H, -O-CH<sub>2</sub>-CH<sub>3</sub>),  $\delta$  359 (2H, Si-CH<sub>2</sub>-CH<sub>2</sub>-CH<sub>2</sub>-O-)

#### 5.2.4 Phase Behavior Measurements:

Phase behavior measurements of the siloxane copolymers were performed in the same manner as described in section 4.1.8.



	Propyl acetate (PA)	Methyl butyrate (MB)	Butyl <sup>(a)</sup> methyl ketone (BMK)	Propyl methyl carbonate (PMC)	Propyl <sup>(a)</sup> ethyl ether (PEE)	Propyl dimethyl amine (PDA)
R G r o u p						

**Scheme 5.1** Synthetic route for preparation of grafted silicone polymers and structures of functional groups. <sup>(a)</sup> Ref. 124

### 5.3 PHASE BEHAVIOR RESULTS OF LEWIS BASE GRAFTED SILOXANE POLYMERS

Poly(siloxanes) are probably the most CO<sub>2</sub>-philic polymers known other than fluoroacrylates. Although it has been suggested that there is a favorable specific interaction between the oxygens of CO<sub>2</sub> and Si atoms,<sup>104</sup> their solubility in CO<sub>2</sub> is mostly attributed to their low glass transition temperature (and thus high chain flexibility) and relatively low cohesive energy density.<sup>44</sup> High chain flexibility can be attributable to the longer bond length of silicone atoms compared to carbon atoms to their neighbors, and the much lower force constants for bond stretching, bending and torsional motions for Si-C versus C-C bonds.<sup>105,106,107,108</sup>

Previous studies show that CO<sub>2</sub> can act as both a Lewis acid and a Lewis base<sup>29,32,109,110</sup> However, the Lewis acidity of CO<sub>2</sub> has occupied most of the attention where the solubility of polymers in CO<sub>2</sub> is concerned. Therefore, efforts typically focus on incorporation of Lewis bases into a polymer chain to enhance the solubility in CO<sub>2</sub> via Lewis acid-base complex formation. For example, Fink et al. generated silicone polymers with propyl acetate and with hexyl groups in the side chain. They found that the propyl acetate functionalized polymer is miscible with CO<sub>2</sub> at significantly lower pressures than the hexyl functionalized polymer, attributing this result to specific interactions between the side chain carbonyl and CO<sub>2</sub>.<sup>103</sup> Similarly, in a recent study, Shen et al. investigated the CO<sub>2</sub> solubility of various oligomers and polymers that contain the carbonyl group. Among poly(vinyl formate), poly(methyl acrylate), poly(vinyl acetate) and poly(lactide), poly(vinyl acetate) was found to exhibit the lowest miscibility pressures in CO<sub>2</sub>.<sup>56</sup>

One aim of this work was to clarify the effect of the carbonyl group structure on phase behavior of CO<sub>2</sub>-polymer solutions for future design of CO<sub>2</sub>-philes. Due to the low glass transition temperature and relatively low cohesive energy density, methylhydrosiloxane-dimethylsiloxane copolymers were chosen as model polymers, and carbonyl containing groups were incorporated into the polymers by a hydrosilation reaction with an allylic precursor. The silicone copolymers all have a total of 25 repeat units, in which the number of methylhydro units available for hydrosilylation varies from one to twenty five. By placing the carbonyl containing side chains on a constant length backbone, the effect of backbone chain length on the phase behavior was eliminated, and thus the effects of each side chain and the degree of substitution were ascertained independently. Similar investigations were performed with two additional Lewis base functionalities, ether and tertiary amine.

Figure 5.1 illustrates the phase behavior of two poly(siloxanes) with isomeric pendant units, namely propyl acetate (PA) and methyl butyrate (MB) (Scheme 5.2). Although these side chains are isomers, Figure 5.1 shows that the miscibility pressures are higher for the MB-functional polymer than that for PA-functional analog.

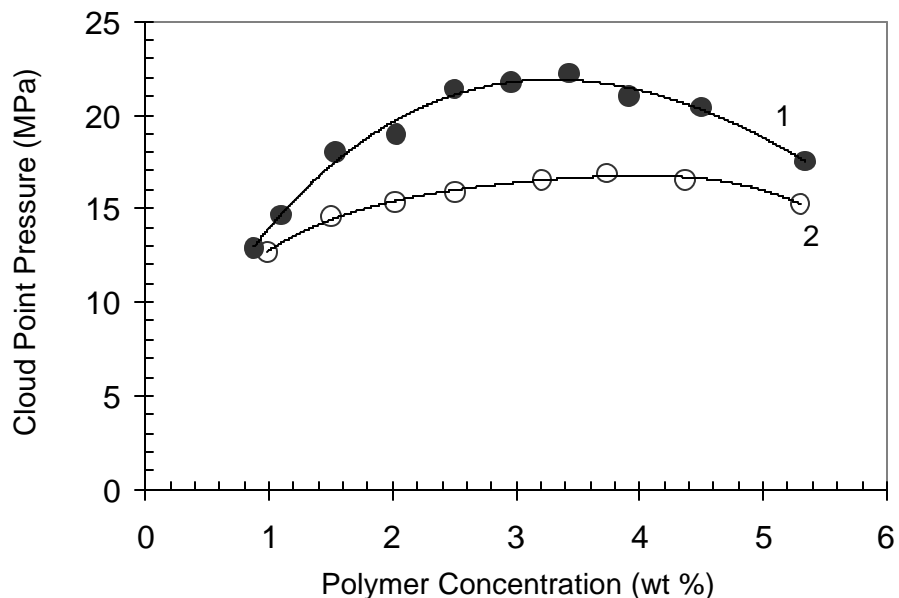


**Figure 5.1** Phase behavior of functionalized ( $z=5$ ) siloxane copolymers, 1) methyl butyrate (MB), 2) propyl acetate (PA), at 295 K.

Similarly, McHugh et al. reported that the miscibility pressures for poly(vinyl acetate) are much lower than those for poly(methyl acrylate), despite a much higher molecular weight for poly(vinyl acetate) in their study.<sup>55</sup> These authors stated that the ether oxygen in poly(vinyl acetate) acts as a spacer between the main chain and carbonyl group, providing the necessary free volume to allow CO<sub>2</sub> to interact with each carbonyl oxygen. Here, however, accessibility to the carbonyl group was not an issue, since each carbonyl moiety is separated from the backbone by a propyl chain. Using ab initio calculations, Wallen et al. suggested that a weaker, but cooperative C-H...O hydrogen bond between the hydrogen of the acetate methyl group and oxygen of the CO<sub>2</sub>, along with the stronger Lewis acid-Lewis base interaction of the carbonyl

oxygen and the carbon of CO<sub>2</sub>, is responsible for the enhanced solubility of acetate functional compounds in CO<sub>2</sub>. However, it was observed that the keto-functional analog (BMK, Scheme 5.2) is miscible at significantly higher pressures than PA-functional analog (Figure 5.2). Despite both the separation of the carbonyl functionality from the backbone by a butyl chain and the presence of protons attached to the  $\alpha$ -carbons for cooperative interactions with CO<sub>2</sub> in BMK side chain, the cloud point curve for BMK-functional polymer is located at higher pressures than that for the PA-functional analog. Hence, neither McHugh's nor Wallen's rationale for the enhanced miscibility of acetate structures seems operative here.

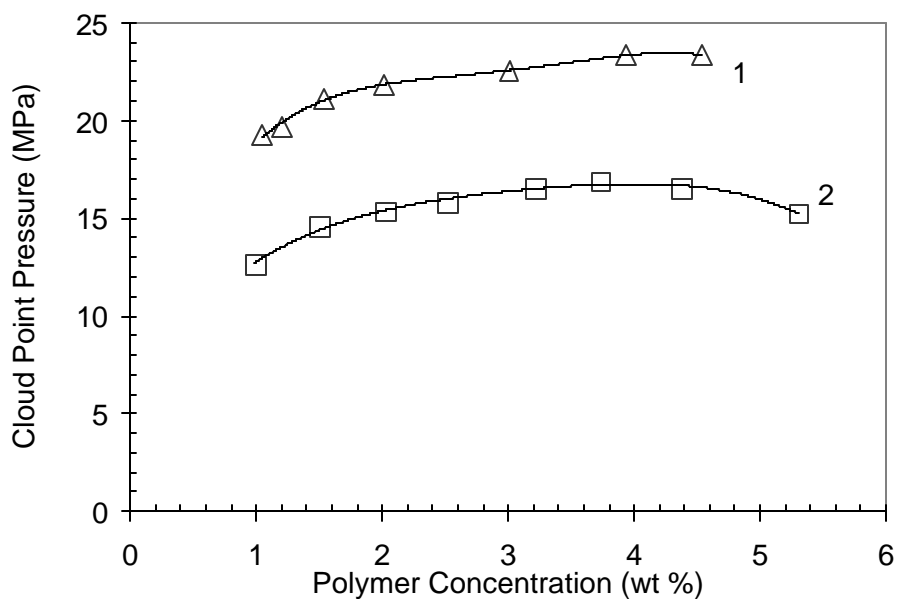


**Figure 5.2** Phase behavior of functionalized ( $z=5$ ) siloxane copolymers 1) butyl methyl ketone (BMK), 2) propyl acetate (PA), at 295 K.

Previous studies have shown that CO<sub>2</sub> can interact with the carbonyl oxygen at various positions, but not all the interacting positions are favorable from the energetic point of view.<sup>48,49</sup> Nelson and Borkman evaluated the possible configurations between CO<sub>2</sub> and five simple carbonyl containing compounds, namely formaldehyde, acetic acid, acetaldehyde, acetone and methyl acetate.<sup>48</sup> Ab initio calculations indicated that C<sub>s</sub> symmetry was preferred over C<sub>2v</sub>? (Figure 5.3). The angle,  $\alpha$ , in C<sub>s</sub> symmetry was found to be dependent on the type of model compounds. For example, for methyl acetate in C<sub>s</sub> symmetry, the binding to the carbonyl group could be from either the methyl side or ester side. Calculations show that the binding energy is higher if the attack is from methyl side, and the angle is 130.42° in that case, otherwise 159.21°. Wallen et al. predicted similar results in their ab initio calculations,<sup>49</sup> and they stated that in C<sub>s</sub> symmetry, repulsive interactions between the lone pairs of the carbonyl oxygen and the oxygen atoms of CO<sub>2</sub> are minimized. Recent ab initio calculations suggest no differences in the strength of interaction between CO<sub>2</sub> and the PA, MB or BMK functional silicones,<sup>111</sup> yet the differences in the miscibility pressures are apparent. It may be that the observed differences in phase behavior are due more to entropic considerations than strength of interaction. The energy barrier to the rotation of the C-O bond and C-C bond was reported as 1.1 and 3.0 kcal/mole, respectively,<sup>112</sup> and hence rotation of the carbonyl group will be easier in the PA-functional material than in either of the other two. This may allow for easier access to the Lewis base groups by CO<sub>2</sub> in the case of the PA-functional material, or simply more flexibility (and hence higher entropy of mixing). However, there is an additional possibility that the carbonyl group is not the key feature where specific interactions with CO<sub>2</sub> are concerned. Aforementioned ab initio calculations suggest that CO<sub>2</sub> will interact as favorably (or perhaps more favorably) with the ether oxygen as with carbonyl; the calculations are consistent where the BMK versus PA

functional behavior is concerned, but would not explain the differences between PA and MB functional analogs.



**Figure 5.3** CO<sub>2</sub>-carbonyl interactions having a) C<sub>2v</sub> b) C<sub>s</sub> symmetry

Interestingly, the cloud point curve for the PMC-functionalized polymer is located at higher pressures than that for the PA-functionalized one (Figure 5.4). However, one should consider that the side chain in PMC is one atom longer. Apparently, the unfavorable entropic effect of the increased chain length more than negates the effect that an additional oxygen might have on specific binding of CO<sub>2</sub>. As seen in Figure 5.4, whereas there are substantial differences in miscibility pressures at some concentrations in the P-x diagram, the curves become coincident at lower and high concentrations. This latter feature is required, as all of the P-x diagrams must intersect the y-axis at CO<sub>2</sub>'s vapor pressure, and also must pass through the vapor pressures of the siloxane polymers (which are all essentially zero) at the 100% polymer axis.

As one can see, the shape of the cloud point curve changes as one alters the nature of the pendant group. In general, when a change in structure prompts a drop in cloud point pressures, it also tends to render the cloud point curve “flatter”, less sensitive to concentration. This can be explained phenomenologically by examining the definition for changes in Gibbs free energy at constant temperature, namely:

$$dG = VdP + S\mu_i dn_i \quad (5.1)$$

As the polymer is added to the solution, the chemical potential is changed and the free energy perturbed; changes to the pressure balance this perturbation in the free energy. As such, if one examines two cloud point curves where one is relatively flat while the other is steep, this could be due to (a) substantial differences in the compressibility of the two mixtures, or (b) substantial differences in the sensitivity of the chemical potential to changes in polymer concentration. If (a) were true, then one would expect that the mixture associated with the “flatter” curve would have a significantly higher compressibility than that associated with the steep curve; a smaller pressure change is then required for the case of the flat curve to counteract the free energy perturbation caused by adding polymer to the mixture. However, all of the mixtures in this study are relatively dilute in polymer, and hence one would not expect to see dramatic differences in compressibility. One therefore expect that option (b) is more likely; “flat” cloud point curves represent cases where the chemical potential is relatively insensitive to polymer concentration. Indeed, this suggests that mixing is favorable, and hence a relatively flat cloud point curve may simply be one of the more obvious signs of a “CO<sub>2</sub>-philic” material.

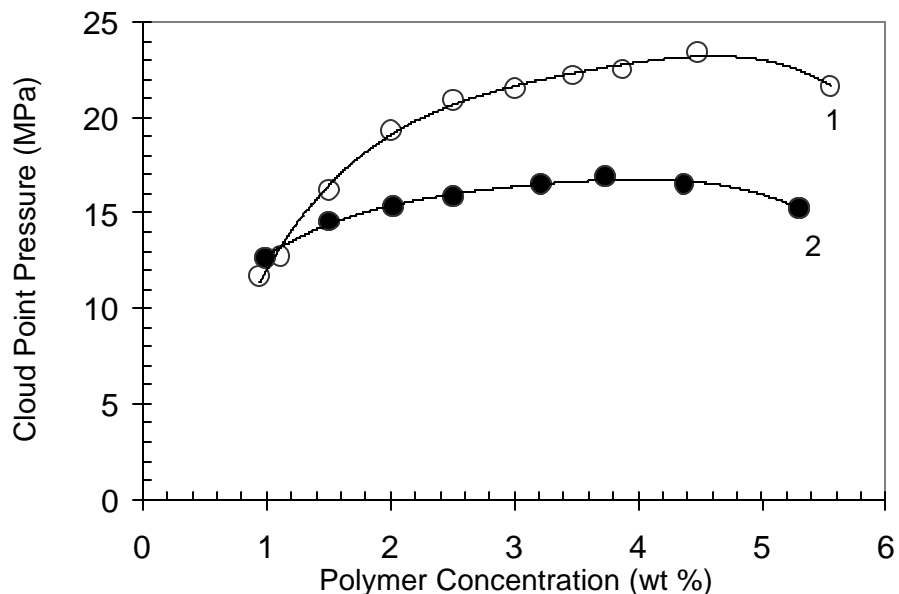


**Figure 5.4** Phase behaviors of functionalized ( $z=5$ ) siloxane copolymers, 1) propyl methyl carbonate (PMc), 2) propyl acetate (PA) at 295 K.

Figure 5.5 compares the miscibility pressures of two methylhydro-dimethylsiloxane copolymers ( $z=1$  and  $2$ ) versus poly(dimethylsiloxane) at the same chain length. The figure reveals that poly(dimethylsiloxane) ( $z=0$ ) is miscible at slightly higher pressures than a one Si-H functional siloxane copolymer ( $z=1$ ), but at slightly lower pressures than a two Si-H functional siloxane copolymer ( $z=2$ ). Typically, it was found that miscibility of the polymer requires higher pressures when the number of Si-H groups in the chain increases; why a one Si-H functional siloxane copolymer ( $z=1$ ) is miscible slightly at lower pressures than fully methylated siloxane polymer (Polydimethylsiloxane,  $z=0$ ) still remains as an unanswered question.

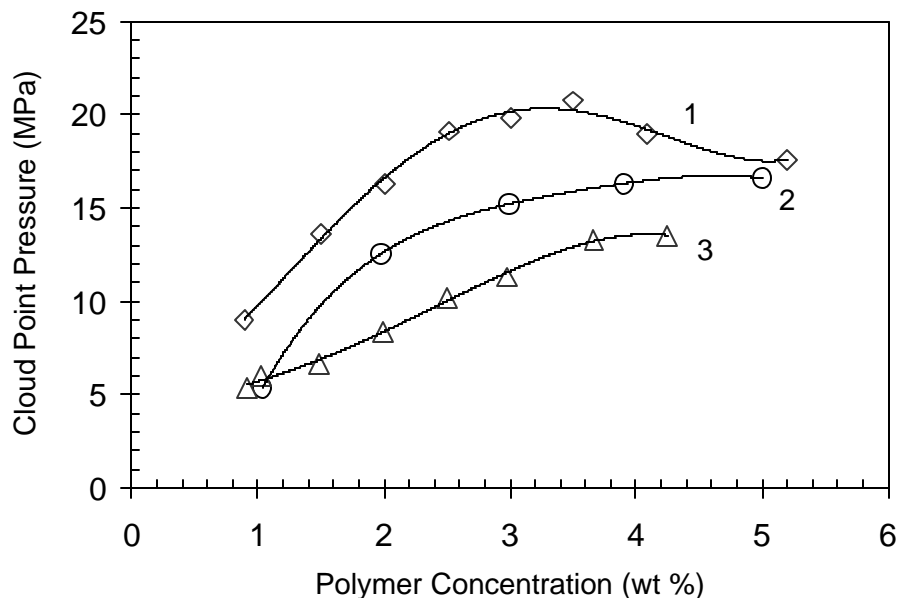


**Figure 5.5** Comparison of phase behaviors of hydromethyl-dimethyl siloxane copolymers at varying functionality with a total of 25 repeat units, at 295 K, 1)  $z=2$ , 2)  $z=0$ , 3)  $z=1$ .

Each carbonyl containing functional group in this study has a higher cohesive energy density than an  $\text{Si}(\text{CH}_3)_2$  unit. While it is known that  $\text{CO}_2$  exhibits favorable interactions with carbonyl groups, the carbonyl-containing polymer can only dissolve in  $\text{CO}_2$  if favorable cross-interactions between polymer and  $\text{CO}_2$ , plus the entropy of mixing, outweigh the sum of the  $\text{CO}_2$  and polymer self-interactions. The experimental results showed that this balance is best achieved at different degrees of substitution for different side chain functional groups, as seen in Figure 5.6-Figure 5.8. For the propyl acetate functional polymers, miscibility pressures of the ( $z=5$ ) polymer are lower than those of the ( $z=1$ ) and ( $z=2$ ) analogs (Figure 5.6). Increasing the number of side chains increases the number of carbonyl- $\text{CO}_2$  contacts per chain; however, with eleven

side chains the increase in cohesive energy density of the polymer dominates over cross interactions, disfavoring dissolution of polymer in CO<sub>2</sub>. Although PA and MB are similar in their chemical structure, it seems that self-interactions always outweigh cross-interactions for MB-functional materials (Figure 5.7), with each additional MB side chain the polymer becomes less CO<sub>2</sub>-philic and the cloud point curves moves progressively to higher pressures. Because the interaction of CO<sub>2</sub> with the MB carbonyl is apparently not as favorable as with the PA carbonyl (perhaps because of the rotational barrier as explained above), self-interactions govern the dissolution process. Therefore, there was no obvious optimum number of side chains observed with MB-functional siloxane copolymers.

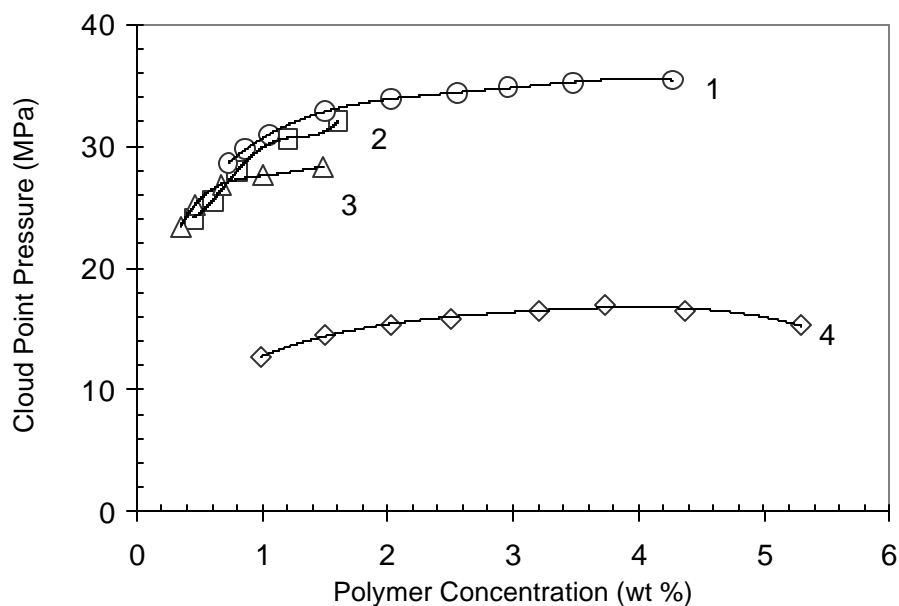


**Figure 5.6** Phase behavior of propyl acetate (PA)-functionalized siloxane copolymers at different degree of substitution 1)  $z=11$ , 2)  $z=1$ , 3)  $z=2$ , 4)  $z=5$ , at 295 K.

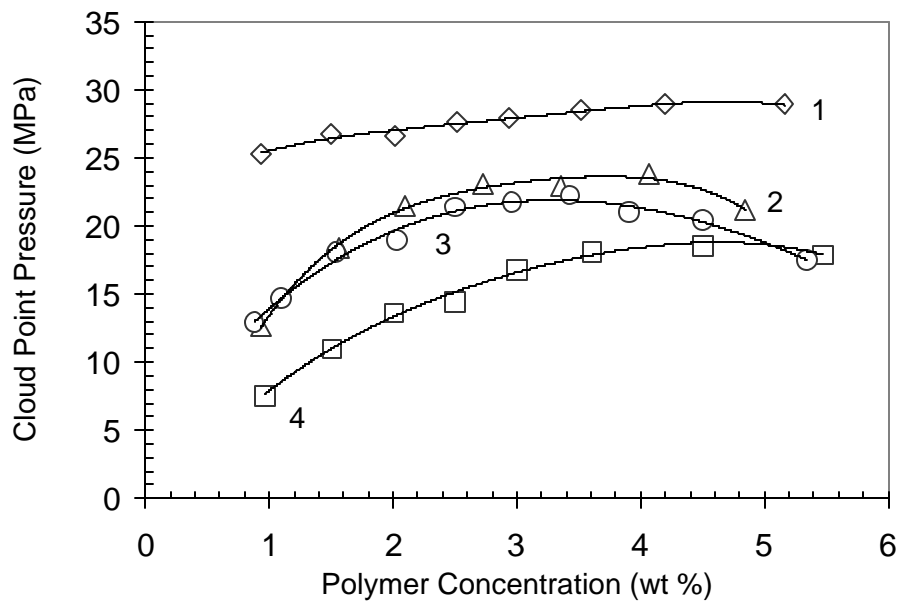


**Figure 5.7** Phase behaviors of methyl butyrate (MB)-functionalized siloxane copolymers at different degree of substitution 1)  $z=11$ , 2)  $z=2$ , 3)  $z=5$ , 4)  $z=1$ , at 295 K.

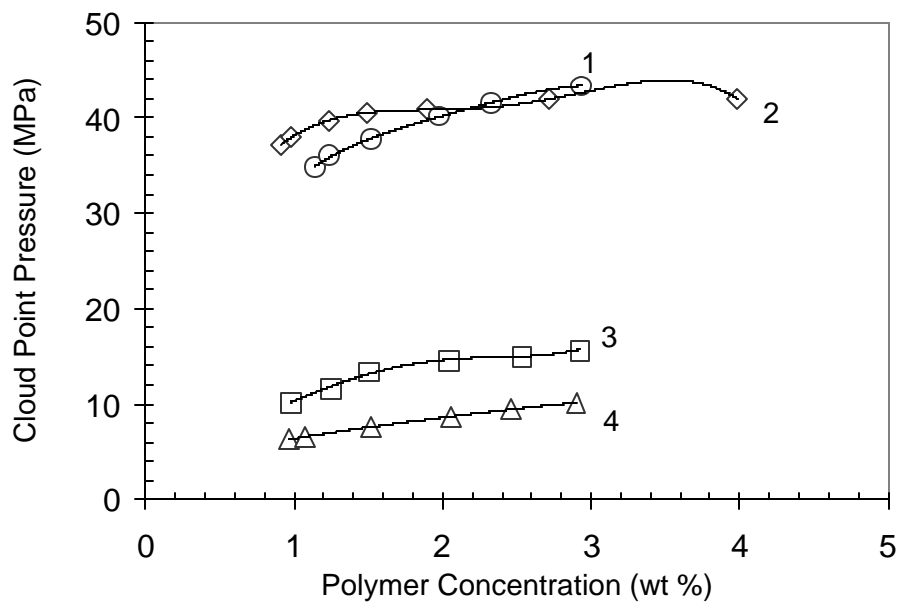


**Figure 5.8** Phase behavior of propyl ethyl ether-functionalized siloxane copolymers at different degree of substitution 1)  $z=11$ , 2)  $z=5$ , 3)  $z=1$ , 4)  $z=2$ , at 295 K.

Although there are apparently no literature spectroscopic measurements of ether-CO<sub>2</sub> interactions at high pressure, Drohmann et al. concluded that the ether oxygen behaves as a weak base towards CO<sub>2</sub><sup>113</sup> because they found that poly(propylene oxide) is miscible with CO<sub>2</sub> at approximately the same or just slightly higher pressures than poly(butadiene) despite the fact that the latter possesses lower T<sub>g</sub> and cohesive energy density. Indeed, the electron donor capacity of ethers is slightly larger than that of carbonyls.<sup>114</sup> Specific interactions between carbonyl groups and CO<sub>2</sub> have received significant attention in the literature, from both experimental and theoretical perspective. Ether-CO<sub>2</sub> interactions, by contrast, have received less attention, perhaps because of the perception that such interactions are too weak to make much of an impact on the thermodynamics of mixing. Ab initio calculations strongly suggest that ether will interact at least as favorably with CO<sub>2</sub> as carbonyls,<sup>111</sup> and because they add less to the cohesive energy density of a material, they could prove to be far more important than carbonyls in the design of CO<sub>2</sub>-philic materials, if judiciously employed. Indeed, aforementioned ab initio calculations also suggest that CO<sub>2</sub> interacts with the ether oxygen in ester groups with the same interaction energy as with the carbonyl.

Cloud point curves of PEE-functionalized polymers with varying number of side chains are shown in Figure 5.8. The cloud point curve shifts to slightly lower pressures as the number of ether side chains increases from one to two, yet the cloud point pressure curve moves to higher pressures when the number of side chains increases to five and eleven. Because the ether segment is flexible, it enhances the flexibility of the resulting polymer and hence entropy of mixing. As mentioned above, ethers add the less to the cohesive energy density of resulting polymer compared to other groups employed in this study.<sup>115</sup> In addition, ab initio calculations

show that specific interactions between ethers and CO<sub>2</sub> should be relatively favorable.<sup>111</sup> Naturally, as one adds additional ether-functional side chains to the silicone, one also increases molecular weight and adds a number of methylene groups; these additions will detract from the CO<sub>2</sub>-philicity of the material, leading to the observed optimum in miscibility pressures in Figure 5.8.

Figure 5.9 compares the phase behavior of ( $z=2$ ) PA-, BMK- and PEE-functional silicone polymers in CO<sub>2</sub>. It is noteworthy that, according to the Van Krevelen group contribution theory,<sup>115</sup> the ether produces the lowest contribution to the cohesive energy of the three functional groups. The cohesive energy density of the groups decreases in the order of acetate, ketone, ether, and the polymers' miscibility pressures are located in the order of their cohesive energy. Even if these functional groups add to the cohesive energy density of the polymer, favorable cross-interactions with CO<sub>2</sub> could compensate, promoting the formation of single phase solution.

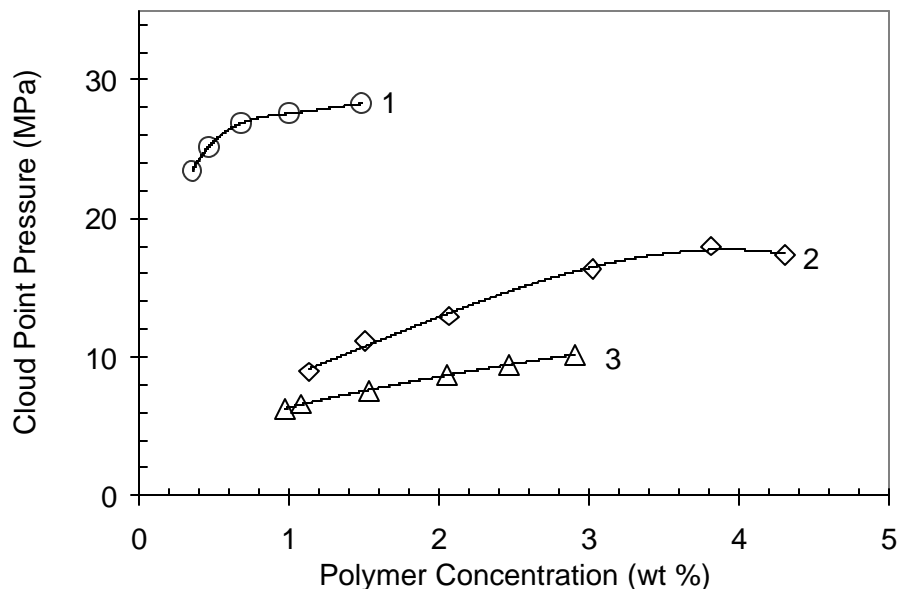


**Figure 5.9** Phase behaviors of ( $z=2$ ) functional siloxane copolymers with 1) Propyl acetate (PA), 2) Butyl methyl ketone (BMK), 3) Propyl ethyl ether (PEE) at 295 K.

The phase behavior of polymers with degree of substitution five ( $z=5$ ) is shown in Figure 5.10. This time, cloud point pressure curves of the polymers do not appear in the order of their cohesive energy density. The ( $z=5$ ) PA-substituted polymer is miscible at lower pressures than the PEE-substituted analog. This indicates that despite its addition to cohesive energy density, the acetate-functionalized chain is more  $\text{CO}_2$ -philic due to favorable Lewis acid-base interactions. From Figure 5.9 and Figure 5.10, it can be concluded that, although it seems that solubility of a polymer can be enhanced by increasing the number of cross-interactions with  $\text{CO}_2$ , the solubility of the polymer in fact depends on whether self- or cross-interaction are

dominant. Miscibility pressures may rise or fall with the addition of each side chain (Figure 5.7), or may exhibit an optimum, as seen in Figure 5.6 and Figure 5.8.

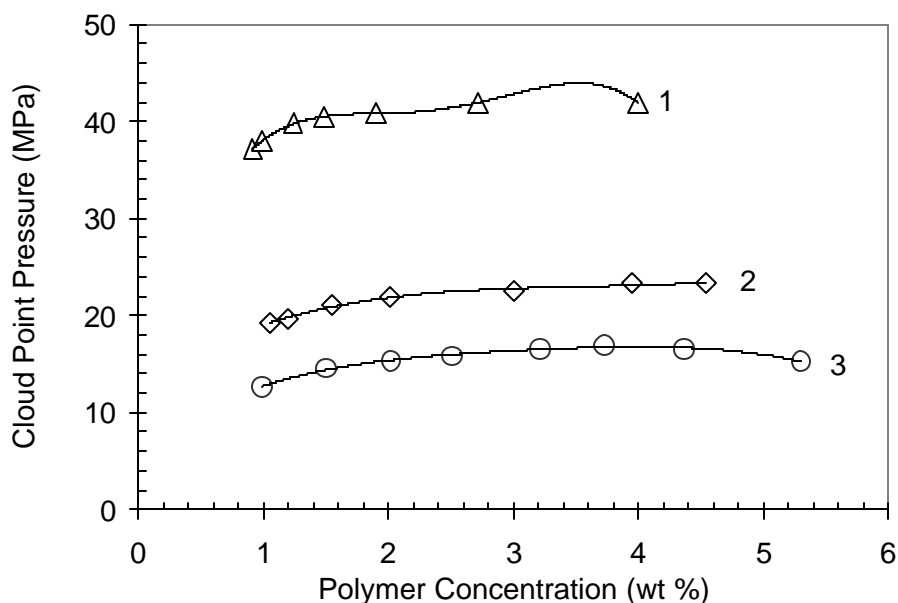


**Figure 5.10** Phase behaviors of ( $z=5$ ) functional siloxane copolymers with 1) Propyl ethyl ether (PEE), 2) Butyl methyl ketone (BMK), 3) Propyl acetate (PA), at 295 K.

The effect of tertiary amine substitution on  $\text{CO}_2$ -solubility was also investigated. A tertiary amine is a much stronger Lewis base than either a carbonyl or ether.<sup>114</sup> Figure 5.11 compares the phase behavior of a PDA-functionalized polymer with a PA-functionalized analog at their optimum number of side chains. According to group contribution model by Fedor,<sup>115</sup> a tertiary amine contributes less to the cohesive energy of the polymer than the acetate. However,

it is noteworthy that the ( $z=5$ ) PDA-substituted polymer exhibits miscibility pressures beyond the limit of our instrument ( $\sim 45$  MPa) at room temperature. Meredith et al. suggested that the steric repulsion of ethyl groups is responsible for the unfavorable mixing of triethylamine (TEA) with  $\text{CO}_2$ .<sup>82</sup> They arrived at this conclusion because they found that pyridine can interact with  $\text{CO}_2$  much more strongly when compared to TEA. A very different picture emerges from a recent paper, in which ab initio quantum mechanical method was used to compute the zero temperature binding energy between  $\text{CO}_2$  and trimethylamine.<sup>111</sup> The authors suggested that the binding energy between nitrogen atom and  $\text{CO}_2$  is considerably larger than that between  $\text{CO}_2$  and carbonyl oxygen. Therefore, at present, it is very difficult to arrive at a solid conclusion on the poor miscibility of tertiary amine functional silicone polymers.

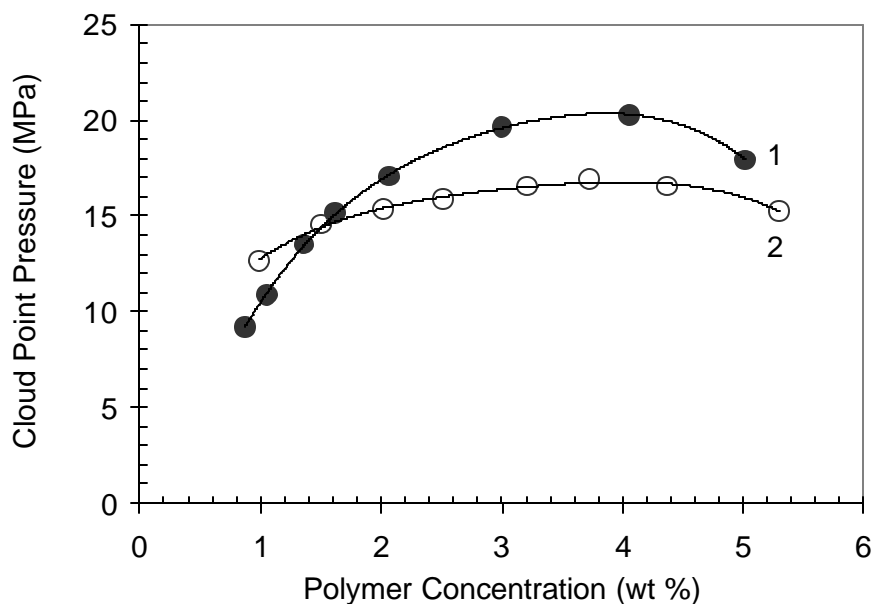


**Figure 5.11** Comparison of phase behaviors of 1) ( $z=1$ ) propyl dimethyl amine-functional (PDA), 2) ( $z=5$ ) propyl acetate (PA)-functional siloxane copolymers at 295 K.

## 5.4 CONCLUSIONS

The impact of various Lewis bases on miscibility of siloxane polymers in CO<sub>2</sub> was investigated. A series of side-chain functional silicones were synthesized containing various Lewis bases in the side chain, and their phase behavior compared in CO<sub>2</sub> at 295K. As Lewis bases, carbonyl groups with adjacent oxygen at either side, both sides and neither side relative to the polymer backbone as well as tertiary alkyl amine and dialkyl ether were incorporated on constant chain length siloxane copolymers with varying degrees of functionalization. One might expect that miscibility of siloxane copolymers in CO<sub>2</sub> could be enhanced through Lewis acid-Lewis base interactions by increasing the number of Lewis base groups in the side chain. However, results showed that maximum miscibility (low miscibility pressures) of a polymer in CO<sub>2</sub> is obtained in fact only when the cross-interactions outweigh the self-interactions. Results also suggest that the oxygen placed in the side chain, but between polymer backbone and carbonyl moiety (referring to propyl acetate side chain), allows for free rotation to the carbonyl group to acquire the optimum position for the interaction with CO<sub>2</sub>, eliminating the hindrance resulting from the long polymer backbone.

In general, the location of the phase boundary in CO<sub>2</sub> is governed by a balance between forces working to increase miscibility pressures, such as increased cohesive energy density of the polymer or factors suppressing the entropy of mixing, and those working to lower miscibility pressures, such as enhanced specific interactions with CO<sub>2</sub> and increased free volume or chain flexibility. In some cases, these counteracting forces produced an optimum in the number of side chains that one should add to a silicone to minimize miscibility pressures.

Despite the fact that tertiary alkyl amine is the strongest Lewis basic group of those examined, tert-alkyl amine functional silicone polymers were found to be poorly miscible with CO<sub>2</sub>. At present time, there is no clear consensus in the literature at theoretical level on the interaction of tert-amine with CO<sub>2</sub>. But, in general, subtle structural changes can generate large changes in phase behavior when CO<sub>2</sub> is employed as the solvent.

## **6.0 EVALUATION OF PHASE BEHAVIOR OF NITROGEN CONTAINING POLYMERS IN CO<sub>2</sub>**

### **6.1 INTRODUCTION**

It was reported that polyethyleneimines exhibit surface tensions as low as those of siloxanes and relatively low glass transition temperatures.<sup>127</sup> Moreover, previous ab initio calculations suggest that interactions between tert-amine and CO<sub>2</sub> are stronger than those between the other Lewis base groups and CO<sub>2</sub>.<sup>111</sup> This particular study has aimed to evaluate the polyethyleneimines as a potential backbone chain and also the effect of nitrogen as a Lewis base on the miscibility of the polymers with CO<sub>2</sub>.

## 6.2 EXPERIMENTAL PROTOCOL

### 6.2.1 Materials:

Linear Poly(ethyleneimine) hydrochloric salt ( $M_w \approx 2,000$ ) was a gift from Polymer Chemistry Innovations, Inc. Poly(2-ethyl-2-oxazoline) with molecular weight of 5,000 (50 repeat units) was purchased from Scientific Polymer Products, Inc. N,N-dimethylacrylamide, 2,2,6,6-Tetramethyl-1-piperidinyloxy (TEMPO, 99%), anhydrous toluene, AIBN, anhydrous 1 M  $BH_3 \cdot THF$  complex, methyl acrylate, formaldehyde (37% solution), and formic acid (96%) were obtained from Aldrich. N,N-dimethylacrylamide was purified by distillation under reduced pressure, and AIBN was purified by crystallization from ethanol prior to use. Poly(4-vinyl pyridine) ( $M_n=3,000$ , PDI=1.50), Poly(2-vinyl pyridine) ( $M_n=3,000$ , PDI=1.12), and poly(N-vinyl imidazole) ( $M_n=9,500$ , PDI=3.00) were purchased from Polymer Source, Inc. (All materials were used as received).

### 6.2.2 Polymerization of N,N-dimethylacrylamide :

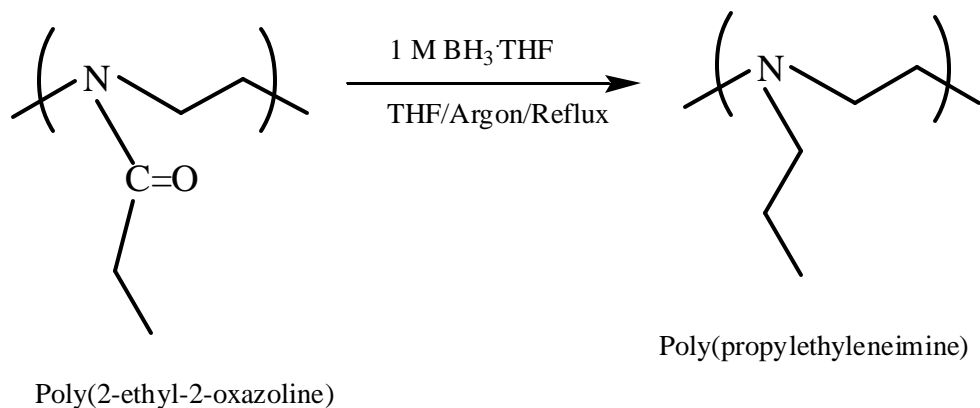
N,N-dimethyl acrylamide was polymerized following a procedure given by Li and Brittain.<sup>116</sup> 0.50 g (3.04 mmol) AIBN and 0.47 g (3.01 mmol) TEMPO, such that  $[AIBN]/[TEMPO]=1$ , were charged into a 250 ml round-bottomed, three-neck flask equipped with a condenser and argon feed. 25.0 g (0.25 mol) N,N-dimethyl acrylamide and 100 ml anhydrous toluene were then added to the flask. The flask was then placed in an oil bath at 98 °C. Initially, the solution

exhibited the orange color of TEMPO, but the color disappeared in less than 30 minutes. After 14 hours of polymerization, the product was precipitated into hexane. The polymer was re-dissolved in toluene and re-precipitated into hexane twice, followed by vacuum drying overnight. White, hygroscopic, polymer powder was recovered at 99% yield. Molecular weight of poly(N,N-dimethylacrylamide) was determined via GPC using toluene as eluent ( $M_n=1,298$ ,  $M_w=1,672$ ,  $PI=1.29$ ).  $^1H$  NMR (300 MHz,  $C_6D_6$ ):  $\delta$  2.7-2.9 (broad, 1H,  $-CH-CO-N-(CH_3)_2$ ),  $\delta$  2.9-3.0 (broad, 6H,  $-N-(CH_3)_2$ ),  $\delta$  1.5-1.9 (broad, 2H,  $-CH_2-CH-CO$ ). For spectrum, see Figure C.1 in Appendix C.

### 6.2.3 Synthesis of Poly(propylethyleneimine):

Poly(propylethyleneimine) were synthesized via the reduction of poly(2-ethyl-2-oxazoline) by borane (Scheme 6.1). The glassware was oven-dried overnight and purged with ultra-high purity argon before use. 9.4 g of polymer was charged into a 500-ml three-neck, round-bottomed flask. The system was equipped with a magnetic stir-bar, a condenser, addition funnel and an argon feed. 25 ml of anhydrous tetrahydrofuran were added to completely dissolve the polymer. After dissolution, 430 ml 1 M  $BH_3 \cdot THF$  complex (4.2 equivalent) were added to the flask drop-wise over 180 min. The solution temperature was raised to reflux, and the solution was stirred for 4 days. After cooling, the excess borane was eliminated by dropwise addition of methanol until hydrogen gas ceased evolving. The THF/methanol mixture was evaporated under reduced pressure, and the sample was dissolved in 144 ml methanol. To the solution, HCl aqueous solution (6 N, 48 ml, 3 times excess) was added and the solution heated to 65 °C and stirred for 40 hours. Upon cooling the green solution, NaOH aqueous solution (6 N, 50 ml) was added to

neutralize the mixture. Methanol was removed on rotary evaporator under reduced pressure, and water by azeotropic distillation with toluene. The salt was removed by filtration after re-dissolving the polymer in methanol. In case some salt remained dissolved in the residual water after azeotropic distillation with toluene, methanol was removed, and polymer was dissolved in an non-aprotic solvent, chloroform. The solution was dried over  $\text{MgSO}_4$ . Upon removal of chloroform, a viscous, brown polymer was obtained (47% yield). Disappearance of the peak at  $1647\text{ cm}^{-1}$  (corresponding to  $\text{C}=\text{O}$  stretching in poly(2-ethyl-2-oxazoline) in Figure C.2 in Appendix C) in Figure C.3 in Appendix C was a sign of complete reduction of the amide.  $^1\text{H}$  NMR (300 MHz,  $\text{CDCl}_3$ )  $\delta$  0.90 (broad, 3H,  $-\text{N}-\text{CH}_2-\text{CH}_2-\text{CH}_3$ ),  $\delta$  1.5 (broad, 4H,  $-\text{N}-\text{CH}_2-\text{CH}_2-\text{CH}_3$ ),  $\delta$  2.3-2.5 (broad, 4H,  $\text{N}-\text{CH}_2$ ). (Figure C.5 in Appendix C).



**Scheme 6.1** Synthetic route for preparation of poly(propylethyleneimine)

#### 6.2.4 Preparation of Poly(propylmethacrylate ethyleneimines):

Prior to Michael addition reaction,<sup>117,118,119</sup> poly(ethyleneimine) hydrochloric salt was neutralized with aqueous NaOH solution. 11.0 g poly(ethyleneimine) hydrochloric salt was allowed to dissolve in 60 ml water, then 5 g NaOH dissolved in 20 ml water was added slowly to the polymer solution until the pH of the solution was 8.0-8.5 by pH paper. The solution was stirred overnight. Upon precipitation of the polymer into acetone (twice), a yellowish viscous, oily polymer precipitated at the bottom of the flask. In case some salt remained dissolved in the residual water, polymer was dissolved in methanol and dried over K<sub>2</sub>CO<sub>3</sub>. Upon filtration, excess methanol was removed on rotary evaporator if necessary. The solution (~75 ml) was transferred to a 250-ml 3-neck, round bottom flask equipped with a condenser, and 18.5 g (0.22 mol) of methyl acrylate was then added. Initially, solution was opaque and yellow in appearance, but after 72 hours of stirring, the color turned to orange. After filtration, the solution was concentrated under vacuum to remove unreacted methyl acrylate and methanol. A very viscous, red-brownish polymer was obtained (92% yield). <sup>1</sup>H NMR (300 MHz, CDCl<sub>3</sub>) δ 1.5 (broad, 2H, -N-CH<sub>2</sub>-CH<sub>2</sub>), δ 2.3-2.5 (broad, 4H, -N-CH<sub>2</sub>), δ 2.5-2.9 (broad, 2H, N-CH<sub>2</sub>-CH<sub>2</sub>-CO), δ 3.7 (s, 3H, CO-O-CH<sub>3</sub>). (Figure C.6 in Appendix C).

#### 6.2.5 Phase Behavior Measurements:

Phase behavior measurements were done in the same way described in section 4.1.8.

### 6.3 PHASE BEHAVIOR RESULTS OF NITROGEN CONTAINING POLYMERS

Interactions between CO<sub>2</sub> and many polymers are known to be relatively weak. In the late 1990s, O'Neill et al. therefore suggested that a CO<sub>2</sub>-philic material should exhibit weak self interactions.<sup>68</sup> In fact, many of the known CO<sub>2</sub>-philic materials (fluoroacrylates, silicones, fluoroether) exhibit a low cohesive energy density (weak solute-solute interaction). Polyethyleneimines were examined because they exhibit weak self interactions and a relatively low glass transition temperature.<sup>127</sup> Polyethyleneimines' surface tension, and thus cohesive energy density (CED), is comparable to that of silicones, but higher than that of fluorinated polymers. For example, poly(hexanoyliminoethylene) and polydimethylsiloxane have surface tension values of 23 and 21 mN/m at 20 °C, respectively.<sup>127</sup> Glass transition temperatures for these polymers are given as 283 K and 150 K, respectively.<sup>127</sup>

In light of O'Neill's premise, the CO<sub>2</sub>-philicity of a series of poly(ethyleneimines) (Table 6.1) were evaluated. Poly(ethylene imines) are also of interest because recent *ab initio* calculations suggest that interactions between nitrogen in a trialkyl amine and CO<sub>2</sub> are much stronger than the interactions between carbonyl and CO<sub>2</sub>.<sup>111</sup> Indeed, the electron-donating capacity of nitrogen was earlier reported to be higher than that of carbonyl.<sup>114</sup>

Contrary to expectations, none of the side chain functional ethyleneimine-based polymers (PPEI, PEO, PPMAEI) was miscible with CO<sub>2</sub> up to 1 wt % and pressures up to 45 MPa. Given substituted siloxane polymer results in chapter 5, it is surmised that an optimum number of side chains are needed to maximize miscibility. None of the 100 % substituted siloxane polymers was

miscible with CO<sub>2</sub> below the pressure limit of 45 MPa. It is likely that such an optimal degree of functionalization also exists for the ethyleneimine polymers. On the other hand, one might expect that ethyleneimine polymers would exhibit superior miscibility in CO<sub>2</sub> since, on the basis of ab initio calculations, the nitrogen in the polymer backbone can have favorable interactions with CO<sub>2</sub> and thus overcome forces acting against miscibility (e.g. high cohesive energy density, high T<sub>g</sub>). In mid 1990s, an opposing idea emerged from a study by Meredith et al.<sup>82</sup> Based on their ab initio calculations; the authors stated that interactions between CO<sub>2</sub> and nitrogen in triethylamine (TEA) are not favorable because the ethyl groups are repelled by the oxygen of CO<sub>2</sub>, causing higher energy configuration of TEA. If the latter is the case, these results are not surprising, but consistent with the results obtained with propyl-dimethylamine (PDMA) functional siloxane polymers in chapter 5. However, there is an additional possibility that the large number of methylene groups in the polymers works against the CO<sub>2</sub>-philicity of the polymer, leading to immiscibility of the polymer with CO<sub>2</sub>. One or the other or both effects might be operative here.

In order to elucidate the existence of an optimal point, analogous polymers to siloxane polymers were synthesized. For example, an attempt was made to generate fully methylated ethyleneimine polymer (PMEI) to compare its miscibility behavior directly to that of poly(dimethylsiloxane). However, the efforts to synthesize PMEI resulted in failure, giving partially reduced polymer. The resulting polymer was not tested in CO<sub>2</sub> for miscibility because the remaining amine groups can react with CO<sub>2</sub>. An attempt was made to cap the remaining N-H groups in the partially reduced polymer with methyl acrylate (via Michael addition) to obtain a copolymer of PMEI/PPMAEI; but, reaction did not take place on the partially methylated

ethyleneimine polymer. Therefore, at this point, it is not possible to comment on the miscibility behavior of ethyleneimine copolymers.

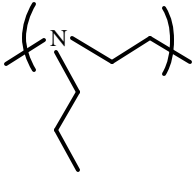
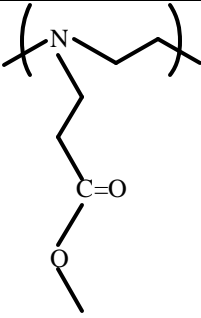
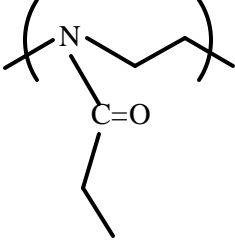
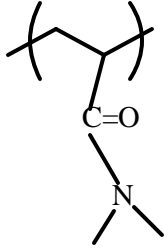
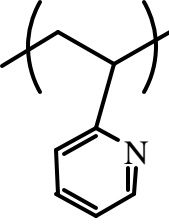
In an attempt to understand if placing of nitrogen in the side chain as a Lewis base would make any difference to the CO<sub>2</sub>-philicity of a material, poly(N,N-dimethylacrylamide) (PDMA) was prepared according to a procedure given in the literature. PDMA was obtained with a molecular weight of 1298 (13 repeat units). Unfortunately, PDMA was not miscible with CO<sub>2</sub> at pressures of 45 MPa and concentrations of 0.7 wt %. The polymer was swollen to some degree by CO<sub>2</sub> possibly due to carbonyl-CO<sub>2</sub> interactions. Increased temperature (80 °C) did not produce a single phase solution. The immiscibility of PDMA with CO<sub>2</sub> was attributed to the very high cohesive energy density of the polymer (surface tension: ~52 mN/m at 20 °C) and very high T<sub>g</sub> (362 K).<sup>127</sup> Here again, Lewis acid-base interactions of CO<sub>2</sub> with neither carbonyl nor nitrogen were effective in achieving miscibility. One would expect favorable interactions between carbonyl and CO<sub>2</sub> towards miscibility even if interaction of nitrogen with CO<sub>2</sub> has not been proved to promote miscibility as of yet. Besides, one would expect that the nitrogen atom as an electron donor strengthens the carbonyl group as a potential Lewis base and thereby increases carbonyl CO<sub>2</sub>-philicity. However, it is possible that the amine group can create steric barrier for carbonyl-CO<sub>2</sub> interactions as well as a rotational barrier (rotational energy barrier for C-N bond is 18 kcal/mole).<sup>112</sup>

Contrary to the interactions between trialkyl amine and CO<sub>2</sub>, Meredith and coworkers suggested that interactions between pyridine and CO<sub>2</sub> are energetically favorable because the nitrogen in pyridine is not sterically hindered for possible interactions with CO<sub>2</sub>. In light of

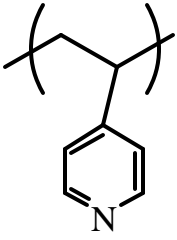
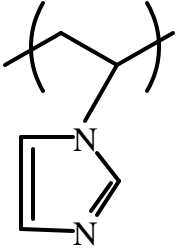
above premise, phase behavior of poly(2-vinyl pyridine) (P2VP), poly(4-vinyl pyridine) (P4VP) and poly(N-vinyl imidazole) (PVIZ) was tested. None of the three samples was found to be miscible with CO<sub>2</sub> at pressures up to 55 MPa and at concentration down to 0.7 wt%. Elevated temperature (70 °C) did not result in a single phase solution. Surface tensions of P2VP and P4VP were earlier reported as 45 and 71.5 mN/m at 20 °C, respectively.<sup>120</sup> On the basis of these data, the experimental observations suggest that the self interactions between the polymer chains are dominating over the cross interactions between CO<sub>2</sub> and nitrogen, resulting in immiscibility of the polymers with CO<sub>2</sub>.

In summary, it is believed that poly(ethyleneimines) would show similar miscibility behavior with CO<sub>2</sub> to that of siloxane polymers, provided that the polymers contain the optimal fraction of Lewis base groups in the chain, just as in siloxane polymers. Results at this particular stage suggest that low cohesive energy density and low glass transition temperature are not the only factors playing roles in the miscibility of the polymer with CO<sub>2</sub>, but cross interactions (e.g. Lewis acid-Lewis base) are also important to impart miscibility, provided that they are favorable and inclusion of functional groups for a possible interaction does not inflate the other two features (i.e. cohesive energy density and glass transition temperature). The chemistry for functionalization should be chosen judiciously to avoid having undesirable groups (e.g. extra methylene groups) in the polymer structure. Finally, the results obtained with the vinyl pyridine (and perhaps imidazole) polymers indicate one more time the importance of dominance of self interactions over cross interactions suppressing miscibility.

**Table 6.1** Structure of Polymers Possessing Nitrogen

Name of the polymer	Structure
Poly(propylethyleneimine) (PPEI)	
Poly(propylmethylacrylate - ethyleneimine) (PPMAEI)	
Poly(2-ethyl-2-oxazoline) (PEO)	
Poly(N,N-dimethylacrylamide) (PDMA)	
Poly(2-vinyl pyridine) (P2VP)	

**Table 6.1** (cont'd)

<p>Poly(4-vinyl pyridine) (P4VP)</p>	 <p>The diagram shows a polymer backbone consisting of a carbon-carbon chain with two bonds extending from each carbon, enclosed in large parentheses. One of the backbone carbons is also bonded to a side chain consisting of a methylene group (-CH<sub>2</sub>-) attached to the 4-position of a pyridine ring. The pyridine ring is a six-membered aromatic ring with one nitrogen atom at the bottom position.</p>
<p>Poly(N-vinyl imidazole) (PVIZ)</p>	 <p>The diagram shows a polymer backbone consisting of a carbon-carbon chain with two bonds extending from each carbon, enclosed in large parentheses. One of the backbone carbons is also bonded to a side chain consisting of a methylene group (-CH<sub>2</sub>-) attached to the 2-position of an imidazole ring. The imidazole ring is a five-membered aromatic ring with two nitrogen atoms at the top and bottom positions.</p>

## **7.0 EFFECT OF BACKBONE TYPE AND ETHER OXYGEN ON PHASE BEHAVIOR OF POLYMERS IN CO<sub>2</sub>**

### **7.1 INTRODUCTION**

Recent ab initio calculations suggest that interaction of ether oxygen with CO<sub>2</sub> is as strong as that of a carbonyl with CO<sub>2</sub>.<sup>111</sup> Moreover, when considered that ether oxygen contributes little the cohesive energy density of the polymers (on the basis of group contribution theory),<sup>115</sup> and presence of the oxygen in the chain increases the chain flexibility, the ether oxygen can be more effective than the carbonyl oxygen in attaining miscibility of the polymers with CO<sub>2</sub>. This particular study has aimed to assess the effect of ether oxygen as a Lewis base and importance of its placement (backbone versus side chain) on miscibility of the polymers with CO<sub>2</sub>.

## 7.2 EXPERIMENTAL PROTOCOL

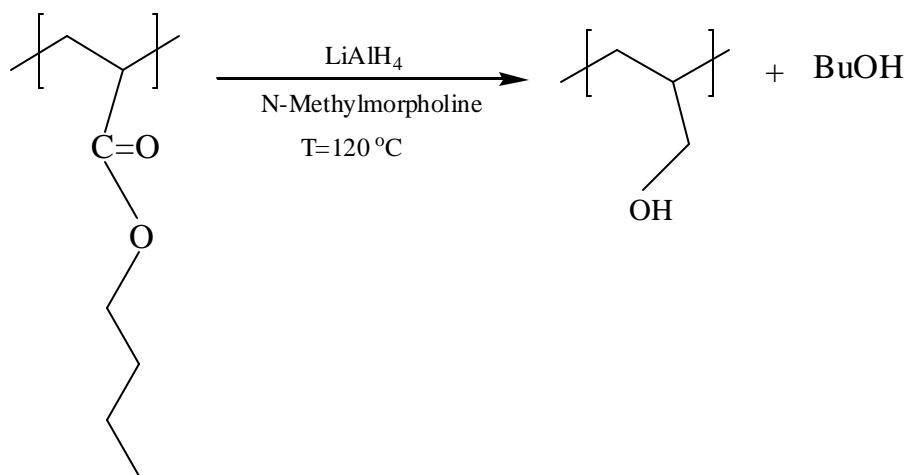
### 7.2.1 Materials:

Poly(*n*-butyl acrylate) with nominal molecular weight of 10,000 (78 repeat units) was purchased from Polysciences, Inc. Poly(propylene glycol) with average molecular weight of 3,500, *N*-methylmorpholine, lithium aluminum hydride (95 %), sodium hydride (60% in mineral oil), chloromethyl methyl ether (95%), methyl iodine (99.5%), anhydrous THF, and anhydrous DMF were obtained from Aldrich. Poly(epichlorohydrin) (85%, nominal molecular weight of 2,400, 25 repeat units) was a gift from 3M. Sodium methanesulfinate (95% tech) and sodium potassium tartrate were purchased from Fisher Scientific. Poly(vinyl methyl ether) with  $M_n=3,850$  and  $PDI=1.05$  was purchased from Polymer Source Inc. All materials were used as received.

### 7.2.2 Synthesis of Poly(allyl alcohol) via Reduction:

As adapted from existing literature,<sup>121</sup> poly(allyl alcohol) was synthesized via reduction of poly(*n*-butyl acrylate) using  $LiAlH_4$  (Scheme 7.1). In a typical experiment, to a 500-ml, three-neck, round-bottomed flask equipped with a stir-bar, a condenser, addition funnel and argon inlet was charged 6.6 g (0.165 mol) of  $LiAlH_4$ . 150 ml *N*-methyl-morpholine was added and the suspension was heated in an oil bath to 120 °C. A solution of 18.5 g (0.145 mol) of poly(*n*-butyl acrylate) in 150 ml *N*-methyl-morpholine was added dropwise over 120 min. The mixture was stirred overnight. While the solution was still hot, 45 g (0.16 mol) of sodium potassium tartrate

in 140 ml water was added dropwise to decompose the excess hydride. Caution was taken during addition due to rapid hydrogen gas formation. After the addition, the solution was stirred for an additional hour and then allowed to cool to room temperature. The solution was filtered. The salt was washed with additional N-methyl-morpholine. Filtrate was concentrated on a rotary evaporator. The residue was dissolved in a methanol/water (9:1) mixture and precipitated in acetone. The dissolution/precipitation procedure was repeated three times. The polymer was dried in the presence of toluene azeotropically. A very tough, white polymer was obtained (7.3 g, 87 % yield).  $^1\text{H NMR}$  (300 MHz, d-DMSO):  $\delta$  1.2-1.5 (broad, 3H,  $\text{CH}_2\text{-CH}$ ),  $\delta$  3.4 (broad, 2H,  $\text{CH}_2\text{-OH}$ ),  $\delta$  4.3 (broad, 1H,  $\text{-OH}$ ).  $^1\text{H NMR}$  (300 MHz,  $\text{D}_2\text{O}$ ):  $\delta$  1.2-1.5 (broad, 3H,  $\text{CH}_2\text{-CH}$ ),  $\delta$  3.4 (broad, 2H,  $\text{CH}_2\text{-OH}$ ),  $\delta$  4.7 (broad, 1H,  $\text{-OH}$ ), shifting of the peak at 4.3 ppm in d-DMSO to 4.7 ppm in  $\text{D}_2\text{O}$  is due to proton exchange between  $\text{-OH}$  and  $\text{D}_2\text{O}$  (Figure D.1 in Appendix D).



**Scheme 7.1** Synthetic route for preparation of poly(allyl alcohol)

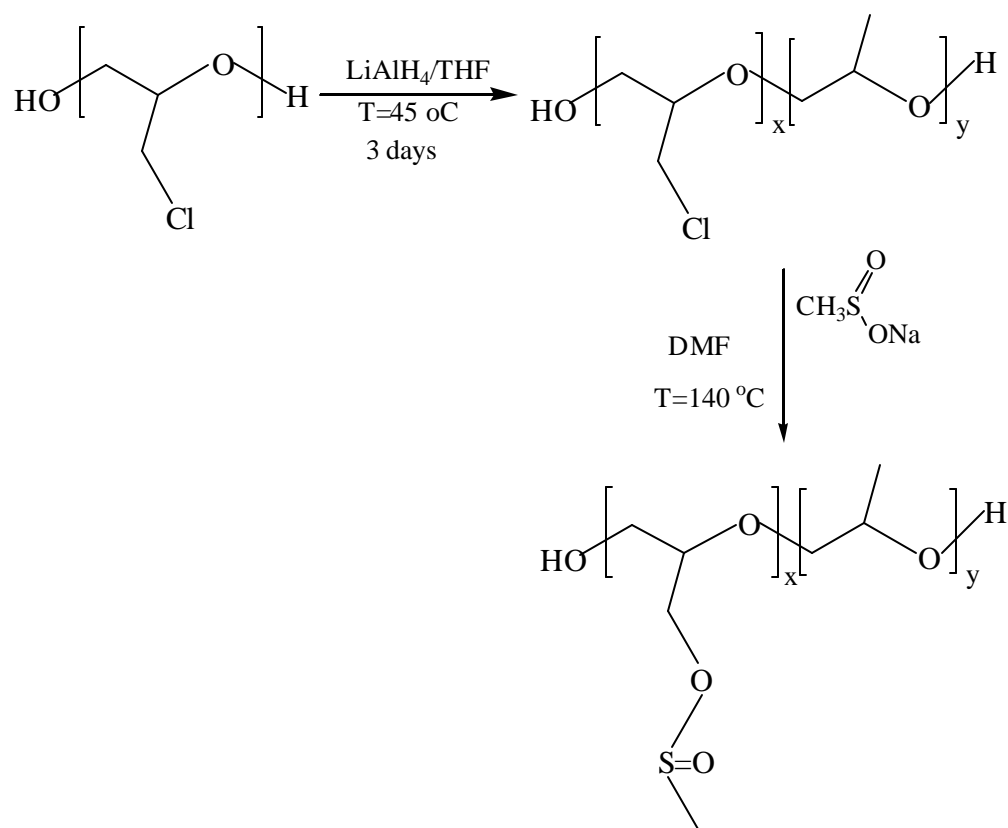
### 7.2.3 Synthesis of Poly(allyl acetate):

Previous results showed that the acetylation of poly(allyl alcohol) with acetyl chloride in the presence of triethylamine gave insoluble product.<sup>122</sup> Therefore, poly(allyl acetate) was synthesized via acetylation of poly(allyl alcohol) with acetic anhydride according to an earlier procedure.<sup>123</sup> In a typical experiment, a mixture of 6.5 g (0.112 mol) of poly(allyl alcohol) and 90 ml (0.95 mol) of acetic anhydride in 170 ml pyridine was stirred at room temperature for 2 days, and then an additional 12 hours at 110 °C. During stirring, the solution acquired a transparent yellow color. After reaction, the product was precipitated in water. After re-dissolution/re-precipitation in pyridine/water system, the crude product was dissolved in benzene and dried over MgSO<sub>4</sub>. Upon removal of benzene on rotary evaporator, a sticky, brown wax resulted (9.1 g, 82% yield). <sup>1</sup>H NMR (300 MHz, C<sub>6</sub>D<sub>6</sub>): δ 1.5 (broad, 3H, -CH<sub>2</sub>-CH-CH<sub>2</sub>-O-CO), δ 2.0 (s, 3H, -O-CO-CH<sub>3</sub>), δ 4.2 (broad, 2H, -CH<sub>2</sub>-O-CO-CH<sub>3</sub>). Spectrum is given in Figure D.2 in Appendix D.

### 7.2.4 Synthesis of Partially Sulfinat-functionalized Poly(propylene glycol):

For the synthesis of partially sulfinat-functionalized poly(propylene glycol), poly(epichlorohydrin) was chosen as a starting material. Poly(epichlorohydrin) was first, partially reduced using lithium aluminum hydride (LiAlH<sub>4</sub>) by a co-worker, Stephen Michalik<sup>124</sup> (Scheme 7.2). The remaining chloride groups, in the second step, were reacted with sodium methane sulfinat in DMF. Grafting was done on 56 % reduced poly(epichlorohydrin) (x=0.44

and  $y=0.56$ ). Here, 5.2 g (25.3 mmol  $\text{CH}_2\text{-Cl}$ ) of reduced polymer was charged to a 250 ml, three-neck, round-bottomed flask. 60 ml DMF was added to the flask, which was equipped with stir-bar and a condenser. After the dissolution of the polymer, 5.7 g (53 mmol) sodium methanesulfinate was added to the solution. The reaction was carried out at 140 °C for 2 days. Water was not a useful nonsolvent for the resulting polymer, and thus most of the DMF was removed azeotropically with water and polymer then dissolved in dichloromethane. NaCl was removed by filtration. The polymer was dried over  $\text{MgSO}_4$  and concentrated under vacuum. Further purifications were done by dissolving the polymer in THF and precipitating into ether (3 times). The polymer was rendered free of any solvent on a rotary evaporator under reduced pressure, yielding a brown, very viscous material.  $^1\text{H}$  NMR (300 MHz,  $\text{CDCl}_3$ ):  $\delta$  1.15 (broad, 3H,  $-\text{CH}_2\text{-CH}(\text{CH}_3)\text{-O}$ ),  $\delta$  3.0 (s, 3H,  $\text{CH}_3\text{-SO-O-}$ ),  $\delta$  3.2-3.7 (broad, 2H,  $-\text{CH}_2\text{-O-SO-}$ ),  $\delta$  4.1 (broad, 1H,  $-\text{OH}$ ).



**Scheme 7.2.** Synthetic route for preparation of partially sulfonate-functionalized poly(propylene glycol)

### 7.2.5 Synthesis of Poly(propylene oxide)-dimethyl ether:

Dimethoxy end-capped poly(propylene oxide) was synthesized via reaction of the hydroxyl end groups in Poly(propylene glycol) with methyl iodine. As adapted from existing literature,<sup>125</sup> the glassware was oven-dried overnight before use. 1.1 g (0.76 mmol) of sodium hydride (60 % in

mineral oil) was charged to a 250 ml, three-neck, round bottomed flask equipped with a stir-bar, a condenser, addition funnel and argon feed, and 60 ml of anhydrous THF was then added. The suspension was then heated to 45 °C. A solution containing 9.4 g of poly(propylene glycol) (Mw=3,500, 5.4 mmol end groups) and 12.4 g (87.3 mmol) of methyl iodine dissolved in 60 ml anhydrous THF was added dropwise over 75 min. Note that a large excess of methyl iodine was used in the experiment to ensure complete reaction, since methyl iodine is very volatile. The solution was stirred at 45 °C for 19 hours under argon atmosphere. Upon cooling, 30 ml of water was added dropwise to hydrolyze the excess sodium hydride. THF was removed under reduced pressure and water was removed by azeotropic distillation with toluene. The sample was dissolved in THF and insoluble NaI salt from the reaction was filtered out. The mineral oil accompanying the NaH is soluble in ether, THF, hexane and pentane, and hence the sample was precipitated into ether. The dissolution/precipitation procedure was repeated 5 times to remove the mineral oil. The sample was concentrated under vacuum, then dissolved in toluene and dried over MgSO<sub>4</sub>. Upon concentration, a pale-yellow, viscous polymer was obtained (70% yield). The peaks at 3480 s<sup>-1</sup> in FT-IR and 3.92 ppm in <sup>1</sup>H-NMR (Bruker 300 MHz, CDCl<sub>3</sub>) correspond to –OH end groups in the Poly(propylene glycol) (Figure D.3 and D.5 in Appendix D). Absence of these peaks in the modified polymer is a sign that effectively all of the –OH groups in the poly(propylene glycol) were capped by the –CH<sub>3</sub>, producing poly(propylene oxide) dimethyl ether (see Figure D.4 and D.6 in Appendix D).

### **7.2.6 Phase Behavior Measurements:**

Phase behavior measurements were performed at 295 K following the procedure given in section 4.1.8.

## **7.3 PHASE BEHAVIOR RESULTS OF THE POLYMERS IN CO<sub>2</sub>**

As mentioned in the initial design strategy for CO<sub>2</sub>-philic polymers, it is hypothesized that a CO<sub>2</sub>-philic polymer should possess a relatively low glass transition temperature (high flexibility and free volume), a relatively low cohesive energy density and also a number of Lewis base groups to create sites for specific interactions with CO<sub>2</sub>. It is known that poly(propylene oxide) exhibits very low glass transition temperature (190-220 K). It has also been shown that the acetate group can interact favorably with CO<sub>2</sub>. In the light of these facts, and knowing that side chains provide the necessary high free volume, a series of polymers composed of a polyether backbone and acetate side chains at varying content (0%-100%) was synthesized in our laboratory and tested for their miscibility with CO<sub>2</sub>.<sup>124</sup> Poly(epichlorohydrin) (PECH) with approximately 25 repeat units was chosen as a starting material and side chain-functionalization was performed on this polymer. Thus, the effect of chain length on the phase behavior of the polymers was eliminated. Results in the aforementioned study showed that cloud point curve of the acetate functional polymers shifted to lower pressures when degree of acetylation was increased from 12% to 22%, but beyond this point (22 % acetylation), further increase in the number of acetate side chains caused the cloud point pressures to increase. This result was

attributed to existence of a balance between cohesive energy density and number of cross interactions. In the abovementioned study, it was suggested that miscibility pressures needed to achieve a single phase of the polymer in CO<sub>2</sub> decrease due to favorable Lewis acid-Lewis base interactions and the increase in the cohesive energy can be compensated through favorable Lewis acid-Lewis base interactions; but beyond a certain degree of functionalization, solute-solute (self) interactions dominate so that cross interactions can not overcome these self interactions, leading one to observe higher miscibility pressures. Surprisingly, poly(propylene oxide) (fully reduced PECH, having no acetate functionalization) was found to be miscible with CO<sub>2</sub> at much lower pressures than all the acetate-functionalized PPO's (for structures, see Figure 7.1), suggesting that optimal degree of functionalization is 0% acetate.

Recent ab initio calculations suggested that ether oxygen can be as effective as the carbonyl as a Lewis base to interact with CO<sub>2</sub>.<sup>111</sup> In addition, the contribution of the ether oxygen to the cohesive energy density of a material is much less as compared to the acetate group.<sup>115</sup> Methyl ether-functionalized PPO's were therefore synthesized and their phase behaviors in CO<sub>2</sub> were evaluated in the abovementioned study<sup>124</sup> (for structure, see Figure 7.1). Unexpectedly, none of the ether-functionalized PPO's was found to be miscible with CO<sub>2</sub> at pressures up to approximately 50 MPa.<sup>124</sup> Their immiscibility was attributed to unfavorable Lewis acid-Lewis base interactions due to close proximity of backbone and side chain oxygens and thus repulsion between oxygens of carbon dioxide and ether oxygen of one when CO<sub>2</sub> attempts to interact with the other (Figure 7.2).

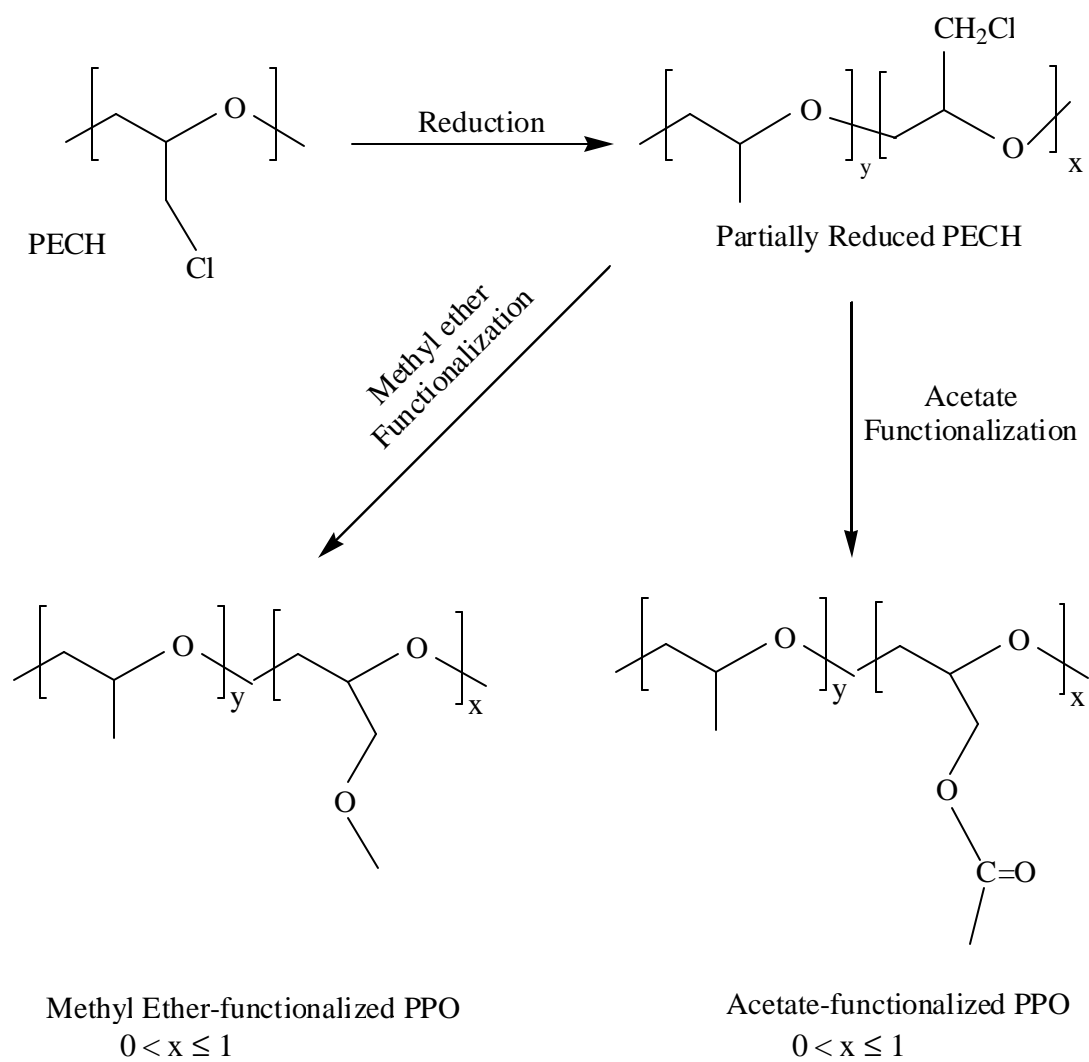


**Figure 7.1** Schematic for reduced and functionalized poly(epichlorohydrin) (PECH)

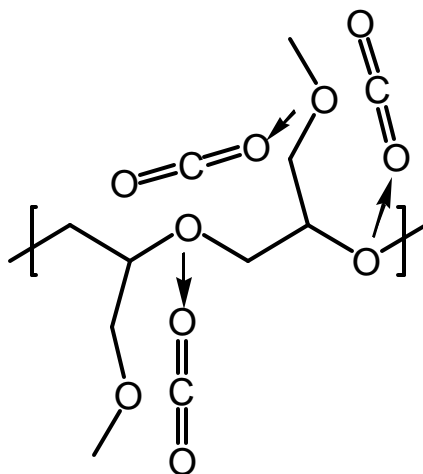


**Figure 7.2** Schematic for hypothesized steric hindrance in ether-functionalized PPO's (repulsive effects indicated by arrows)

Having seen the results above, one might question whether the backbone is problematic or not. As one can imagine, omission of the oxygen from the backbone chain in the acetate-functionalized PPO results in poly(allyl acetate), as shown in Figure 7.3. Poly(allyl acetate) was synthesized via modification of poly(allyl alcohol), which was itself obtained via reduction of poly(*n*-butyl acrylate). Surprisingly, poly(allyl acetate) is not miscible with CO<sub>2</sub> at pressures up to 60 MPa and concentrations down to 0.8 wt%. Poly(allyl acetate) and poly(vinyl acetate) are very similar in structure, with the only difference a CH<sub>2</sub> unit situated between acetate and backbone in the former. However, PVAc with molecular weight of 7,700 (89 repeat units) is miscible with CO<sub>2</sub> at pressures of ca. 43 MPa at concentrations ranging from 5 to 1 wt%.<sup>56</sup> At this point, it is not easy to arrive a solid conclusion on why poly(vinyl acetate) exhibits superior miscibility than the poly(allyl acetate) and the acetate-substituted PPO's. It is surmised that

superior miscibility of poly(vinyl acetate) results from not only enthalpic but also entropic factors. There is a possibility that the oxygen in close proximity to the backbone in poly(vinyl acetate) provides free motion for the side chain, lessening restrictions reflected in the side chains resulting from long backbone chain, and the carbonyl-CO<sub>2</sub> interactions are therefore more favored. On the other hand, the carbonyl-CO<sub>2</sub> interactions in poly(allyl acetate) may not be as favorable as in poly(vinyl acetate) due to lack of oxygen. However, there is also possibility that unfavorable interaction between CO<sub>2</sub> and extra methylene group in the poly(allyl acetate) can reduce the CO<sub>2</sub>-philicity of the polymer.

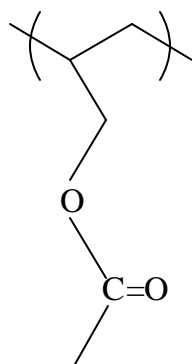


**Figure 7.3** Structure of poly(allyl acetate)

Simulations by Wallen et al. showed that the binding energy between CO<sub>2</sub> and the sulfonyl group is much higher than that between CO<sub>2</sub> and the carbonyl group.<sup>49</sup> It was also reported earlier that the sulfonyl group in dimethyl sulfoxide is more electron-rich than the carbonyl group.<sup>114</sup> However, the effect of the sulfonyl group as a Lewis base on miscibility of

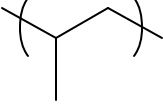
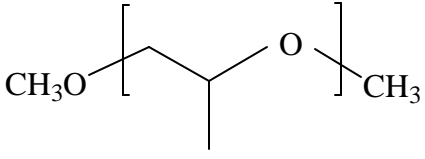
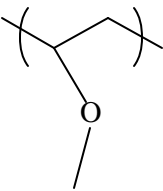
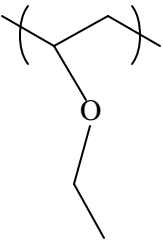
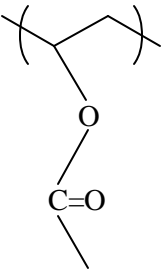
polymers with CO<sub>2</sub> has not been investigated in the literature. Herein, sulfonyl group was substituted onto a polyether backbone to give sulfinate-functionalized poly(propylene glycol) (Scheme 7.2). However, the polymer was found to be immiscible with CO<sub>2</sub> at concentrations higher than 0.7 wt % and pressures lower than 60 MPa. It is believed that similar arguments made for acetate-functional polyether apply for sulfinate-functionalized poly(propylene glycol) as well. Moreover, sulfinate-functionalized poly(propylene glycol) exhibits even poorer miscibility with CO<sub>2</sub> than the acetate-functionalized analogue. One can attribute this to higher contributions of the sulfonyl group to cohesive energy density of the polymer, which leads one to believe that degree of functionalization should be always lower than that of the acetate-functional polyether to attain similar miscibility. Here, to expect any steric hindrance for CO<sub>2</sub>-sulfonyl interactions would be unrealistic since it is analogous to CO<sub>2</sub>-carbonyl interactions, though Wallen et al. found the optimized geometry for sulfonyl-CO<sub>2</sub> interactions somewhat different than that for carbonyl-CO<sub>2</sub> interactions.<sup>49</sup> However, the main goal here remains as to place sulfinate group onto a hydrocarbon backbone (not a polyether).

Despite the availability of a handful of both experimental and theoretical studies on carbonyl-CO<sub>2</sub> interactions, ether oxygen-CO<sub>2</sub> interactions have not received much attention. Only one experimental study in the literature suggests existence of Lewis acid-Lewis base interactions between ether oxygen and CO<sub>2</sub>, promoting miscibility.<sup>113</sup> A recent ab initio calculation also suggested that ether oxygen-CO<sub>2</sub> interactions are as favorable as carbonyl-CO<sub>2</sub> interactions.<sup>111</sup> Moreover, the ether oxygen has contributes relatively less to the cohesive energy density of a polymer.<sup>115</sup> Therefore, it is anticipated that ether oxygens could be far more

important than carbonyl groups in the design of CO<sub>2</sub>-philic polymers, if they are wisely incorporated in a polymer structure.

The structure of polymers studied to assess the effect of oxygen on phase behavior is shown in Table 7.1. Figure 7.4 shows the phase behavior of poly(propylene) with a molecular weight of 425 (PP-425)<sup>124</sup> and poly(propylene glycol)-monomethylether (Mw=1,000)<sup>113</sup> in CO<sub>2</sub>. Poly(propylene glycol)-monomethylether is miscible with CO<sub>2</sub> at much lower pressures than PP-425, despite the higher molecular weight and possession of one –OH end group of the former. This result suggests that the ether oxygens in the poly(propylene glycol)-monomethylether is responsible for the superior miscibility of poly(propylene glycol)-monomethylether compared to that of PP-425. It is likely that, due to presence of oxygen in the poly(propylene glycol)-monomethylether, the polymer chain exhibits greater inherent chain flexibility, which leads to an increase in entropy of mixing, and that the ether oxygen in poly(propylene glycol)-monomethylether exhibits favorable Lewis acid-Lewis base interactions with CO<sub>2</sub>, yielding much lower cloud point pressures.

**Table 7.1** Surface tension and glass transition temperature of the polymers used to assess the effect of oxygen on phase behavior.<sup>126,127,128</sup>

Polymer	Structure	Surface Tension (mN/m @ 20 °C)	Tg (°C)
Poly(propylene) (PP)		31	-10
Poly(propylene oxide)-dimethylether (PPO-DME)		31	-75
Poly(vinyl methyl ether) (PVME)		29	-31
Poly(vinyl ethyl ether) (PVVE)		36	-60
Poly(vinyl acetate) (PVAc)		36	30

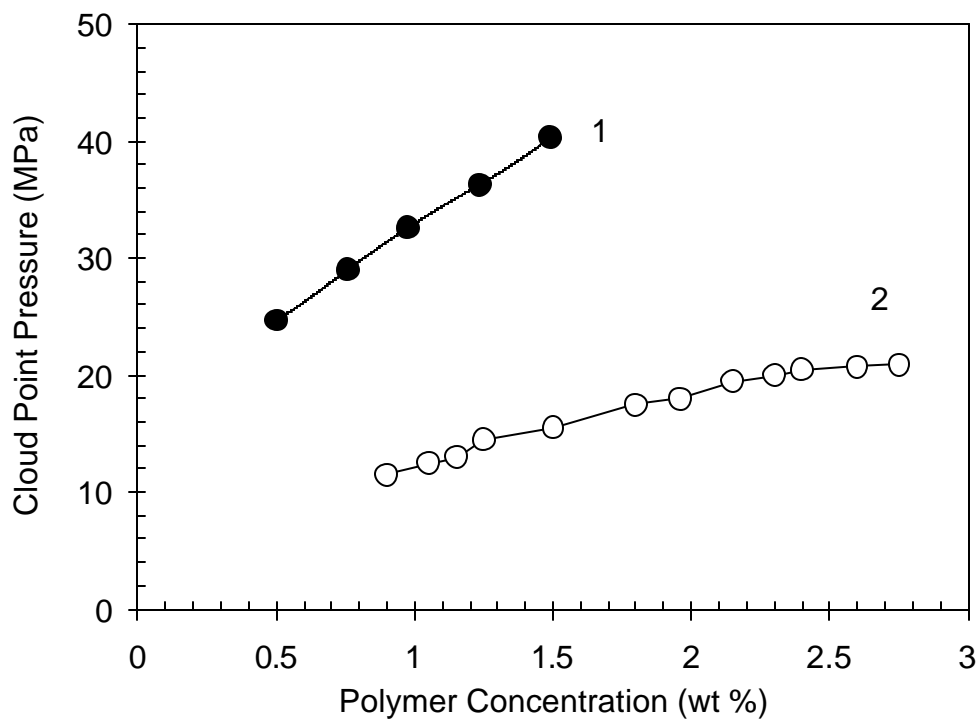


**Figure 7.4** Phase behavior of 1) PP-425,<sup>124</sup> 2) Poly(propylene glycol)-monomethylether, Mw=1000, at 295 K.

Phase behavior of two isomeric polymers, namely poly(vinyl methyl ether) (PVME) and poly(propylene oxide)-dimethylether (PPO-DME), was tested to assess the effect of oxygen placement on the phase behavior (Figure 7.5). The polymers have similar molecular weights. The only difference between the two polymers is the placement of oxygen in the side chain in the former and in the backbone in the latter (Table 7.1). As seen from the figure, placement of oxygen in the side chain has a positive effect on miscibility pressures, although miscibility curves show the same trend. As the polymer concentration in the solution increases, the pressure

required to achieve a single phase steeply increases for both polymers. Note that PVME has a slightly lower cohesive energy density, but higher  $T_g$  than PPO-DME (Table 7.1). Figure 7.5 suggests that the weak self interactions of PVME result in lower miscibility pressures of PVME with  $\text{CO}_2$  relative to PPO-DME and it is surmised that the ether oxygen in PVME is more accessible to  $\text{CO}_2$  than that in PPO-DME (side chain versus backbone chain) for Lewis acid-base interactions, compensating for disfavoring effect of entropy of mixing resulting from chain stiffness of PVME.

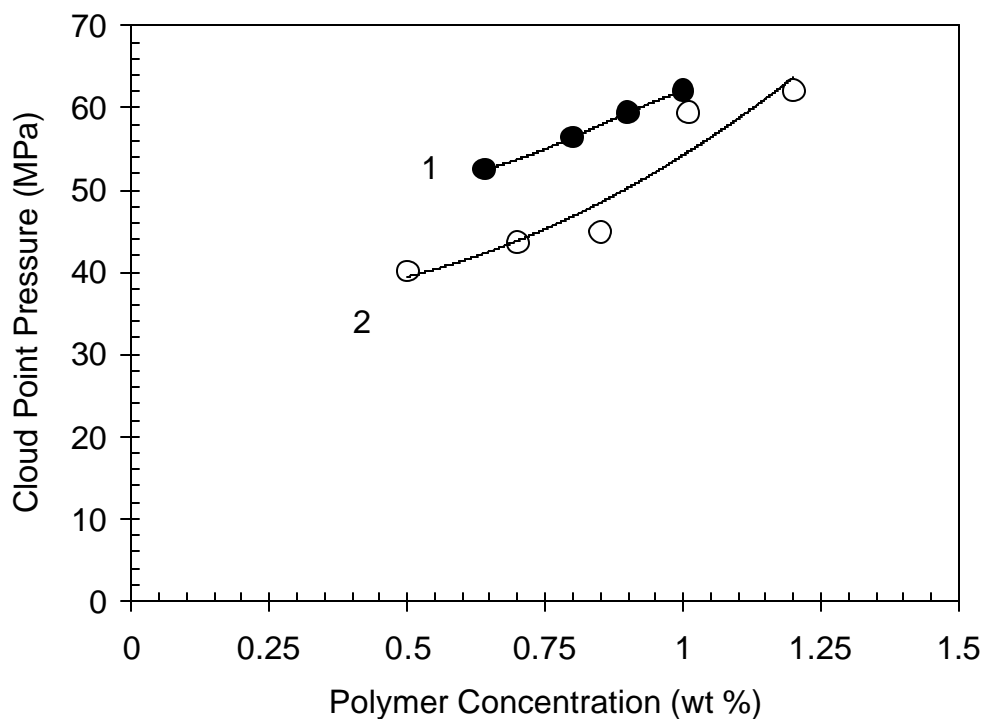


**Figure 7.5** Effect of location of oxygen (backbone versus side chain) in the polymer on phase behavior: 1) PPO-DME 3500, 2) PVME -3850 at 295 K.

It is hypothesized that increasing polymer free volume plays a positive role in determining the location of phase boundary via enhanced entropy of mixing.<sup>129</sup> Figure 7.6 compares phase behavior of PVME-3850 and PVEE-3800. PVEE differs from PVME by an extra  $-\text{CH}_2$  unit in the side chain. Despite the relatively higher surface tension and thus the higher cohesive energy density, miscibility of PVEE with  $\text{CO}_2$  is more favorable than PVME. It has been suggested that as the side chain length increases, the polymer gains more free volume. Therefore, it is surmised that miscibility of PVEE is more likely entropically driven. It is also possible that the ether oxygen can be more accessible by  $\text{CO}_2$  for Lewis acid-Lewis base interactions due to increasing free volume. Miscibility pressure curve drastically increases with increasing PVME concentration, exceeding the pressure limit of our equipment at concentrations higher than 1.2 wt%. On the contrary, the miscibility pressure curve of PVEE increases gradually as the polymer concentration increases in the solution. This suggests that the negative effect of relatively strong self interactions of PVEE on phase behavior are offset by enhanced entropy of mixing and perhaps relatively more favored Lewis acid-base interactions (relative to PVME) due to increased free volume. Gradual increase of miscibility curve with increasing PVEE concentration suggests that PVEE can be considered a potential  $\text{CO}_2$ -philic material.

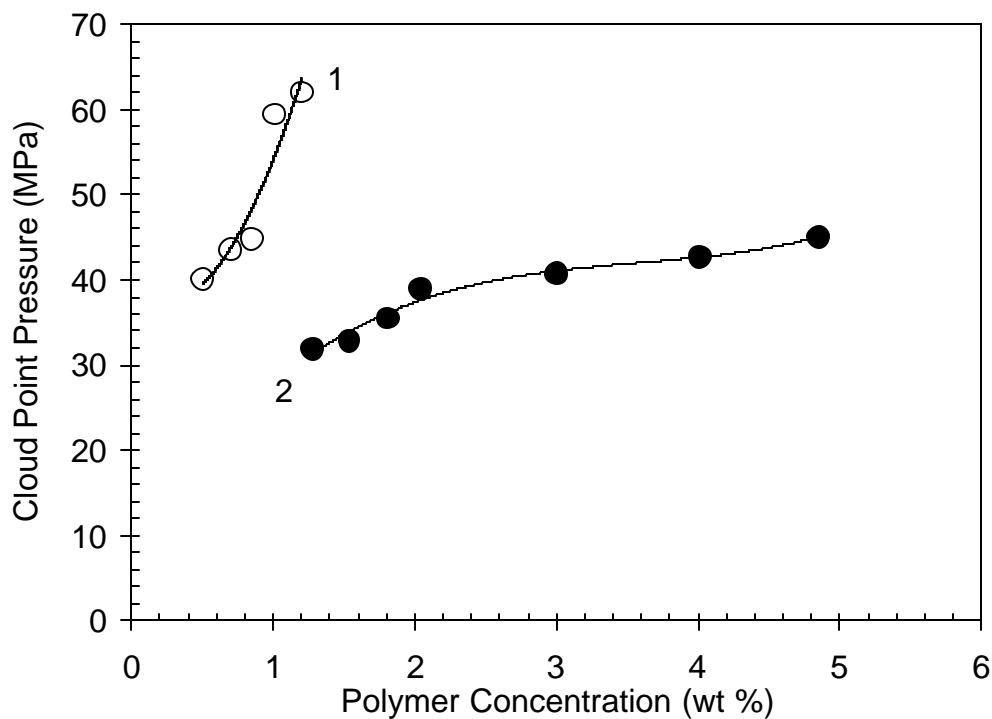


**Figure 7.6** Effect of length of side chain on phase behavior in vinyl ether polymers, 1) PVME 3850, 2) PVVE-3800,<sup>124</sup> at 295 K

The role of the placement of the ether oxygen in the side chain is more distinct when the miscibility behavior of PVVE is compared with that of PPO-DME (Figure 7.7). PVVE exhibits both a higher surface tension (thus the cohesive energy density) and a lower glass transition temperature. Therefore, comparing just the surface tension and glass transition temperature of the polymers, one might expect greater miscibility of PPO-DME than PVVE. However, the experimental results show the opposite (Figure 7.7). This is a clear indication that ether oxygen is more accessible to CO<sub>2</sub> in the side chain than in the backbone and favorable ether oxygen-CO<sub>2</sub>

interactions of PVVEE can negate the effect from strong self interactions and decreased entropy of mixing (due to high Tg).

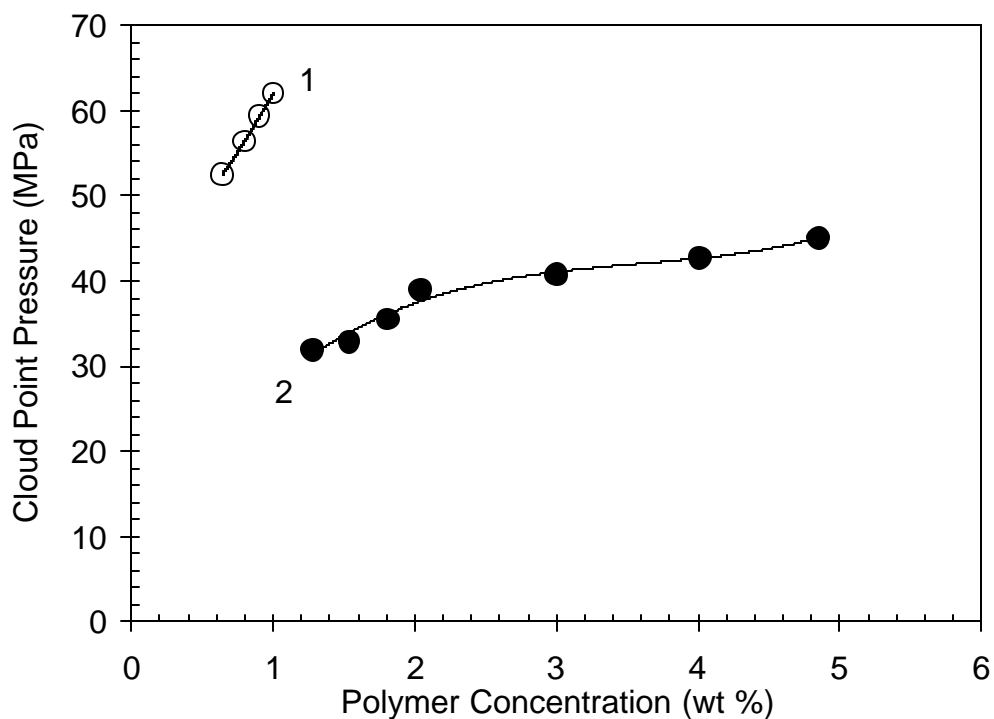


**Figure 7.7** Phase behavior of (1) PPO-DME 3500 (2) PVVEE 3800<sup>124</sup> at 295 K.

As mentioned earlier, recent ab initio calculations suggest that the ether oxygen could be as effective as the carbonyl oxygen in facilitating miscibility of a polymer with CO<sub>2</sub>.<sup>111</sup> It was reported earlier that the ether oxygen has a higher electron donating capacity than the carbonyl

oxygen.<sup>114</sup> Figure 7.8 compares the phase behavior of PVEE with PVAc's at two different molecular weights. As seen in the Table 7.1, both polymers have the same cohesive energy density value, but the Tg of PVAc is much higher than the Tg of PVEE. In this case, one would expect higher cloud point pressures for PVAc. However, experimentally it was observed that miscibility of PVAc with CO<sub>2</sub> is more favorable than that of PVEE. It is believed that favorable Lewis acid-base interactions between CO<sub>2</sub> and carbonyl oxygen are responsible for the superior miscibility of PVAc compared to PVEE. Moreover, aforementioned ab initio calculations also suggested that CO<sub>2</sub> can interact with ester oxygen to the same degree as ether oxygen. It is possible that observed differences in phase behaviors are due to PVAc having two points to interact with CO<sub>2</sub>. However, it is also likely that interaction of CO<sub>2</sub> with both ether oxygen in PVEE and ester oxygen in PVAc may not be as strong as carbonyl oxygen-CO<sub>2</sub> interactions due to steric hindrance from the long polymer backbone chain. Furthermore, it is also possible that the ester oxygen of PVAc provides rotational freedom to the carbonyl group, enhancing carbonyl-CO<sub>2</sub> interactions, as discussed in chapter 5 for propyl acetate functional-siloxane. Either or all factors can be operative here to explain the superior miscibility of PVAc as compared to PVEE.

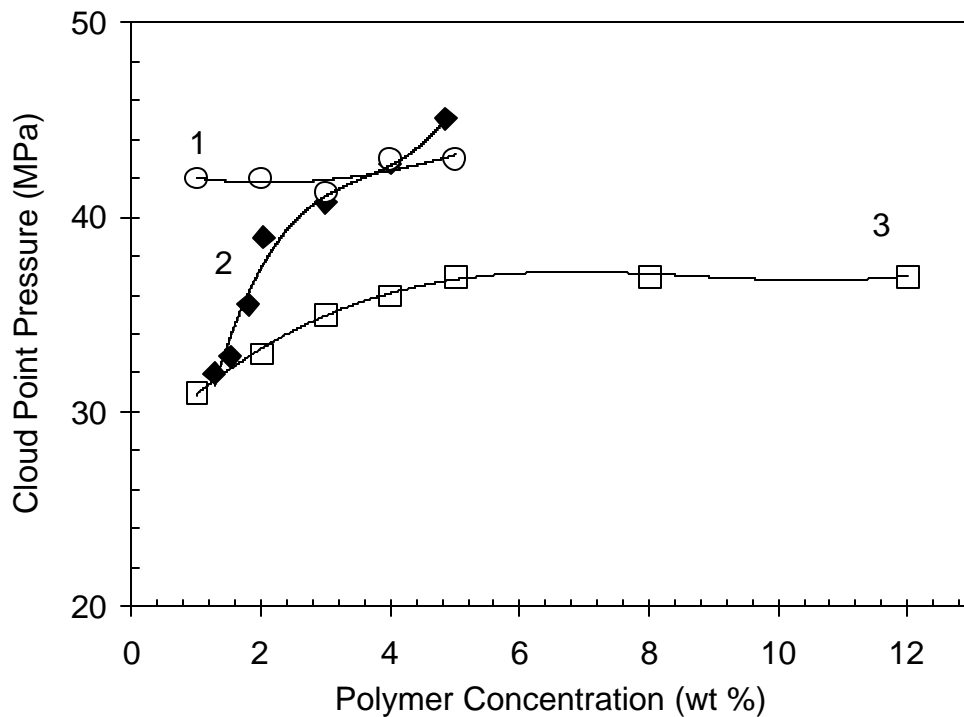


**Figure 7.8** Comparison of phase behavior of 1) PVAc-7700,<sup>56</sup> 2) PVEE-3800,<sup>124</sup> 3) PVAc-3090,<sup>56</sup> at 295 K.

It is worth to mention here that PVAc with a molecular weight of 193,000 (2244 number of repeat units) exhibits miscibility with CO<sub>2</sub> at 67.6 MPa at ~5 wt%,<sup>56</sup> on the other hand, PVEE with approximate molecular weight of 120,000 (1667 number of repeat units) did not exhibit any miscibility with CO<sub>2</sub> at 3.5 wt% and a pressure of 241 MPa and elevated temperatures.<sup>130</sup>

## 7.4 CONCLUSIONS

A series of oxygen containing polymers were tested to probe the effect of oxygen on the phase behavior of polymers. The change in the series was created by incremental structural changes, such as presence and absence of oxygen in the polymers and placement of oxygen in the backbone versus side chain in the polymer and increase in the length of side chain.

Results revealed that the effect of oxygen on phase behavior is more pronounced if it is situated in the side chain rather than in the backbone of a polyether. Miscibility behavior of the polymer was affected positively by the presence of oxygen, and this effect was attributed to Lewis acid-Lewis base interactions between ether oxygen and CO<sub>2</sub> and enhanced entropy of mixing gained by presence of oxygen in the structure.

Poly(vinyl ethyl ether) was found to be the most CO<sub>2</sub>-philic ether-based polymer (polyether). Finally, the miscibility behavior of poly(vinyl ethyl ether) was compared to poly(vinyl acetate), which is the most CO<sub>2</sub>-philic, non-fluorous vinyl polymer known to date. The results showed that the miscibility of poly(vinyl acetate) with CO<sub>2</sub> is more favorable than that of poly(vinyl ethyl ether). Since recent ab initio calculations suggest that interaction between CO<sub>2</sub> and ether/ester oxygen should be as favorable as interactions between CO<sub>2</sub> and carbonyl oxygen, it is surmised that the differences in miscibility results from presence of an extra oxygen (ester oxygen) in poly(vinyl acetate). There is a possibility that this extra oxygen of poly(vinyl acetate) may serve both as a Lewis base for a possible interaction with CO<sub>2</sub>, and auxiliary for rotational freedom of carbonyl group, facilitating the carbonyl-CO<sub>2</sub> interactions.

## 8.0 SUMMARY

Experimental results showed that the relative viscosity of neat CO<sub>2</sub> can be enhanced via dissolution of aromatic acrylate-fluoroacrylate copolymers. It is believed that association of the aromatic rings plays the primary role for the viscosity enhancement. Degree of enhancement was found to be strongly dependent on type and content of aromatic acrylate unit in the copolymer. Maximum viscosity enhancement was obtained with PHA-FA copolymer. 29 mole% of PHA in the copolymer was found to be the optimum. Observation of an optimum can be explained phenomenologically as follows: as content of aromatic acrylate unit increases in the copolymer, number of contacts for association and thus the relative viscosity increases. However, a point is reached beyond which the relative viscosity increases to a lesser extent. This is because CO<sub>2</sub> becomes poorer solvent for the copolymer with the increasing content of aromatic acrylate unit in the copolymer. In this case, polymer coils swell to a lesser degree (i.e. hydrodynamic volume decreases) and the association of aromatic rings become more likely intramolecularly than intermolecularly.

Unlike expected, spacer length has a detrimental effect on viscosity enhancement for the copolymers possessing single aromatic ring in the aromatic acrylate unit. Increasing size of the aromatic ring did not cause expected raise in the relative viscosity. This was attributed to obstruction for the association of the bulky naphthyl rings due to long backbone chain. All the

copolymers studied were found to be miscible with CO<sub>2</sub> at ambient temperature. Miscibility pressure curve of the copolymer did not increase dramatically with the increasing content of aromatic acrylate unit in the copolymer. This was ascribed to CO<sub>2</sub>-philic fluoroacrylate unit to be dominant in dissolution process, governing the miscibility of the copolymers in CO<sub>2</sub>.

Efforts to explore inexpensive, environmentally friendly, non-fluorous polymers showed that one needs to consider the enthalpic and entropic contributions to the Gibbs free energy of the solution for the design of CO<sub>2</sub>-philic polymers. As hypothesized, the results showed that there is a delicate balance between the forces acting against miscibility (e.g. increased cohesive energy density and factors suppressing the entropy of mixing) and those favoring miscibility, such as enhanced specific cross interactions, increased chain flexibility or free volume.

To probe the impact of different factors on the miscibility, such as type of backbone, type and number of Lewis base groups, and those effecting entropy of mixing, a series of polymers were prepared. Change in the series was created systematically by incremental steps. The results can be summarized as follows:

- 1) Propyl acetate and methyl butyrate functional silicone polymers exhibited different phase behaviors in CO<sub>2</sub>, although they are isomeric. This behavior was attributed to the rotational freedom gained by the oxygen in propyl acetate, causing more favorable carbonyl-CO<sub>2</sub> interactions.

- 2) Propyl ethyl ether-functionalized silicone polymer results showed that ether oxygen serves also as a Lewis base, interacting with CO<sub>2</sub>.
- 3) Results obtained with both the silicone polymers and the ethyleneimine polymers showed that trialkyl amine-CO<sub>2</sub> interactions are not favorable to mixing. It is believed that steric hindrance due to alkyl chains is responsible for the unfavorable interactions.
- 4) It is believed that ethyleneimine polymers could be a new class of polymers exhibiting good miscibility character in CO<sub>2</sub> if the functionalization on the ethyleneimine backbone is carried out more judiciously.
- 5) Interactions between CO<sub>2</sub> and acetate functionality were found to be more favorable to mixing compared to other Lewis base groups. This was ascribed to the interaction of CO<sub>2</sub> with the acetate at two points (e.g. ester oxygen and carbonyl oxygen), plus rotational freedom gained by the ester oxygen situated between carbonyl group and the backbone chain. However, results revealed that chain topology is very important. For instance, substitution of acetate functionality onto a polyether and allyl backbone has a detrimental effect on miscibility, whereas substitution on a vinyl backbone has the superb effect. It is believed that the oxygen situated between the carbonyl and the backbone in poly(vinyl acetate) serves as an auxiliary facilitating the carbonyl-CO<sub>2</sub> interactions as well as acting as a Lewis base.
- 6) Interactions between ether oxygen and CO<sub>2</sub> were found to be more favorable if oxygen is situated in the side chain rather than backbone.

## 9.0 FUTURE WORK

It was shown that aromatic rings can provide the necessary interaction for molecular association to increase the viscosity of neat CO<sub>2</sub>. However, high cost of fluoroacrylates used to maintain the miscibility of the polymer reduces economic viability of EOR process. Therefore, fluoroacrylate portion of the polymer should be replaced by inexpensive, environmentally friendly a non-fluorous polymer. Having shown that PVAc is the most CO<sub>2</sub>-philic non-fluorous vinyl polymer known to date, we suggest that a poly(vinyl acetate-co-aromatic acrylate) would be a good choice as a potential CO<sub>2</sub>-thickener (Figure 9.1.(a)). This polymer may be synthesized by bulk copolymerization of vinyl acetate and aromatic acrylate. However, if chain transfer reactions create problem during the synthesis, it is suggested to prepare the polymer in Figure 9.2.(b), which can be prepared by grafting functional groups onto poly(vinyl alcohol). The optimum conditions for the maximum viscosity enhancement (x, y, n, m) will need to be investigated. The effect of substitution on the strength of the association and thus viscosity enhancement also needs to be investigated.

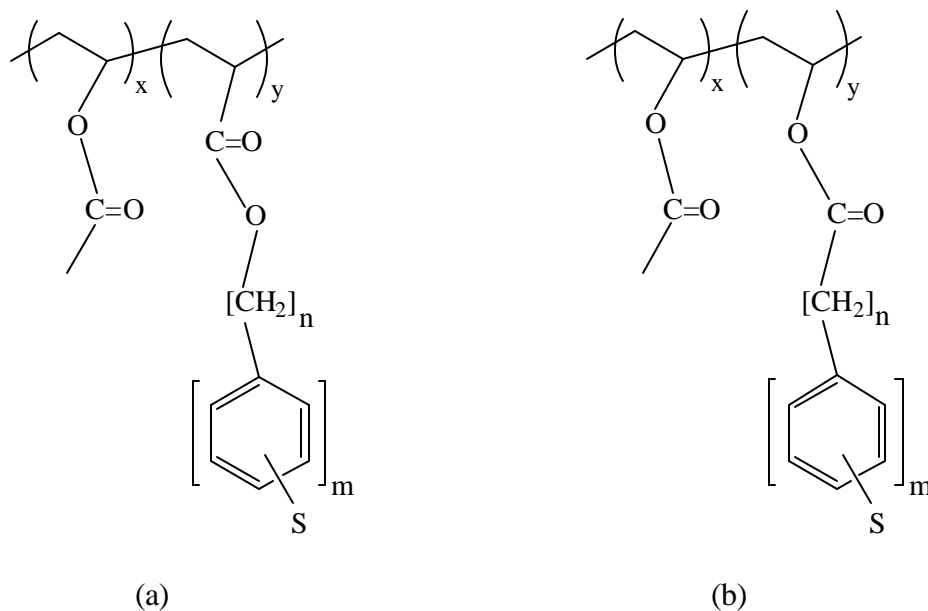


**Figure 9.1** (a) Poly(vinyl acetate-co-aromatic acrylate), (b) Poly(vinyl acetate-co-aromatic acetate)

It is believed that the cost of EOR process can be reduced further by discovery of new, non-fluorous, more CO<sub>2</sub>-philic polymers than poly(vinyl acetate). It has been shown that vinyl ether polymers also exhibit relatively good miscibility behavior in CO<sub>2</sub>. At present, it seems that poly(vinyl ethyl ether) is the second best non-fluorous CO<sub>2</sub>-philic polymer after poly(vinyl acetate). In this regards, it would be beneficial to see the miscibility behavior of poly(isobutylene oxide) (Figure 9.2). It is hypothesized that symmetric disubstitution of larger groups for H-atoms on backbone will lower the glass transition temperature of the polymer.<sup>83</sup> It is likely that poly(isobutylene oxide) would have a lower glass transition temperature than even poly(propylene oxide). In addition, poly(isobutylene oxide) has a lower surface tension, and thus cohesive energy density, than both poly(propylene oxide) and poly(vinyl ethyl ether).<sup>68,126</sup>

Therefore, it would be worth testing the miscibility behavior of poly(isobutylene) in CO<sub>2</sub>, despite the fact that oxygen is situated in the backbone.

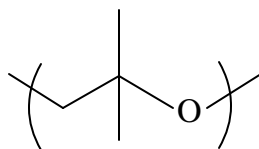


**Figure 9.2** Structure of poly(isobutylene oxide)

Poly(vinyl acetate) has a relatively high cohesive energy density (CED) and glass transition temperature (T<sub>g</sub>). However, we believe that the outstanding miscibility character of poly(vinyl acetate) in CO<sub>2</sub> results from favorable cross interactions of the carbonyl with CO<sub>2</sub>, which compensates for the negative effect of cohesive energy density and glass transition temperature. It is anticipated that a good balance of high cohesive energy density, glass transition temperature and cross interactions can be obtained if one could make the copolymer of vinyl acetate and vinyl ethyl ether or that of vinyl acetate and isobutylene oxide (Figure 9.3). In the copolymer, it is expected that vinyl ethyl ether or isobutylene oxide would increase chain flexibility while the ether oxygen adds relatively less to the cohesive energy density of the polymer and creates Lewis acid-Lewis base cross interactions with CO<sub>2</sub>, promoting miscibility. The vinyl acetate part imparts miscibility through interactions with CO<sub>2</sub> at two points: the carbonyl oxygen and the ester oxygen. Compositional parameters (x and y) need to be optimized.

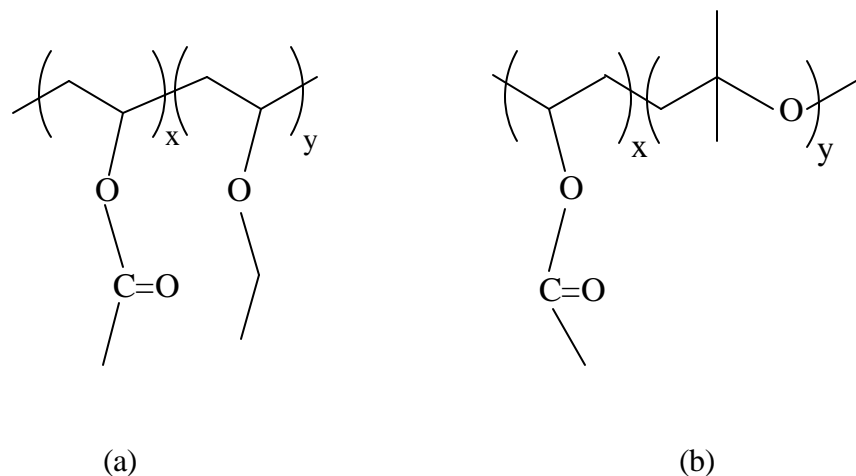


**Figure 9.3** Structure of (a) poly(vinyl acetate-co-vinyl ethyl ether), (b) poly(vinyl acetate-co-isobutylene oxide).

Previously, it was shown that the binding between -S=O group and CO<sub>2</sub> is much stronger than between -C=O and CO<sub>2</sub>.<sup>49</sup> As an analogy to poly(vinyl acetate), it would be worth probing the phase behavior of poly(vinyl sulfonate) (Figure 9.4). However, according to group contribution model, sulfonate group adds relatively high to the cohesive energy density of a polymer. Therefore, one should not be surprised if the polymer exhibits immiscibility with CO<sub>2</sub>. However, it is hypothesized that the copolymer of vinyl sulfonate with vinyl ethyl ether or with isobutylene oxide would exhibit favorable miscibility simply due to balancing effect among cohesive energy density, glass transition temperature and cross interactions (Figure 9.5).

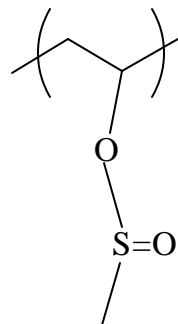


**Figure 9.4** Structure of Poly(vinyl sulfonate)

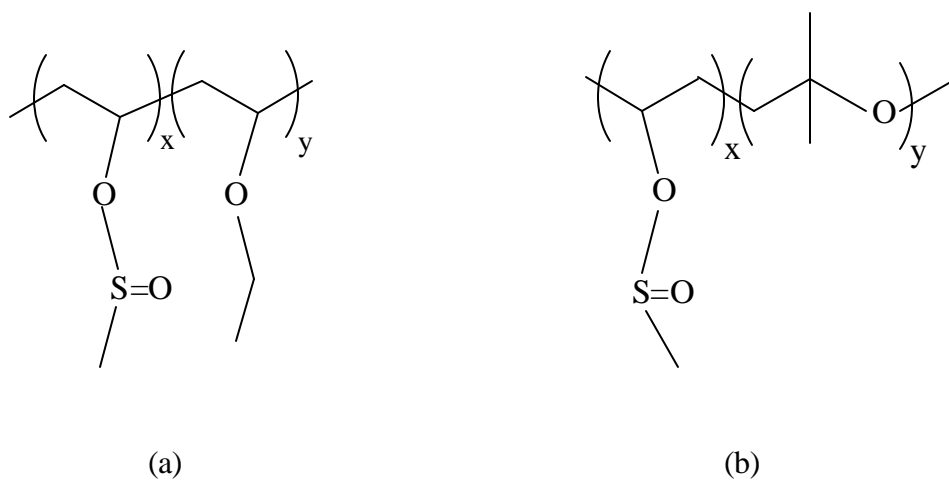


**Figure 9.5** Structure of (a) Poly(vinyl sulfonate-co-vinyl ethyl ether), (b) Poly(vinyl sulfonate-co-isobutylene oxide).

To determine whether the ester oxygen of poly(vinyl acetate) and ether oxygen of poly(vinyl ethyl ether) are accessible by CO<sub>2</sub> and Lewis acid-Lewis base interactions contribute to miscibility, it would be beneficial to assess the miscibility behavior of poly(vinyl ethyl ketone), since it is an analog to poly(vinyl ethyl ether), in that oxygen is replaced with carbonyl moiety (Figure 9.6).

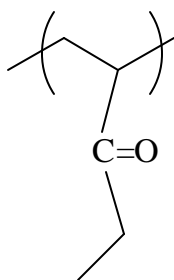


**Figure 9.6** Poly(vinyl ethyl ketone)

Proposing initially that the oxygen in the backbone increases chain flexibility and that Lewis base groups in the side chain promote Lewis acid-Lewis base interactions with CO<sub>2</sub>, the acetate and the ether substituted PPO's were earlier synthesized. However, the polymers were found to be poorly miscible with CO<sub>2</sub>. It is suspected that the extra methylene group situated between the backbone and the Lewis base group is responsible for the unfavorable mixing. To clarify this point and also test our initial hypothesis, it would be worth synthesizing and testing miscibility of the acetate or sulfinate-substituted poly(oxetane)s, in which the Lewis base groups are attached directly to the backbone (Figure 9.7). Substituted poly(oxetane)s can be synthesized

via modification of poly(3-hydroxyoxetane) or poly(3-chlorooxetane), which could be synthesized following the procedure described in the literature.<sup>131,132,133</sup> The effect of type and the extent of substitution on miscibility could be compared the miscibility of base polymer, namely poly(oxetane) (Figure 9.8). One can synthesize poly(oxetane) with controlled molecular weight according to an earlier procedure.<sup>134</sup>

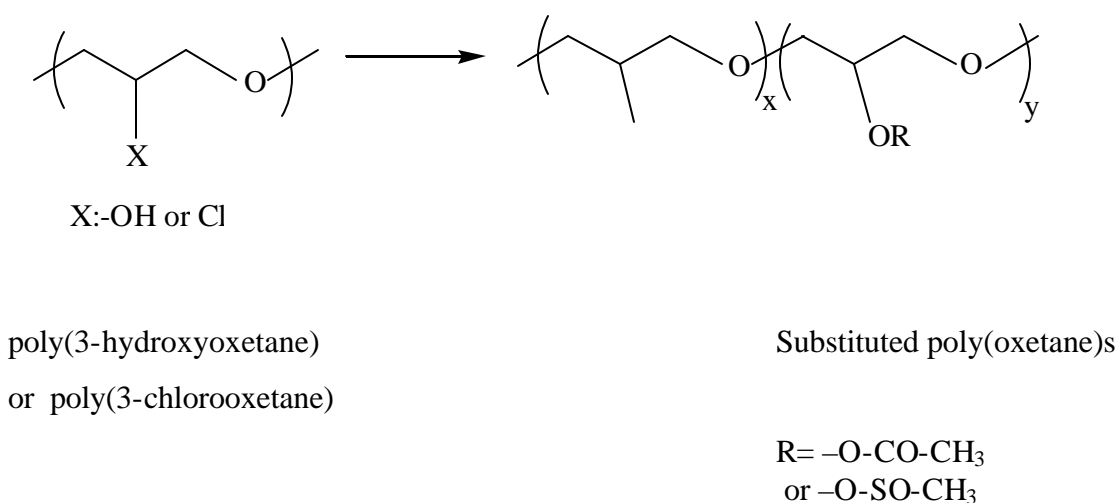


**Figure 9.7** Reaction scheme for synthesis of substituted poly(oxetane)s.

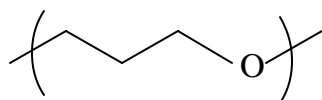


**Figure 9.8** Structure of Poly(oxetane)

As mentioned before, polyethyleneimines exhibit cohesive energy densities as low as polydimethyl siloxanes. Also, polyethyleneimines have relatively low glass transition temperature, though not as low as polydimethyl siloxanes. From the lessons learned from the functionalized siloxane copolymers in chapter 5, it is believed that one can get better or at least comparable miscibility of polyethyleneimines in CO<sub>2</sub> compared to that of polydimethyl siloxanes, provided that the polymer is partially functionalized and functional groups are integrated in the structure prudently. Incorporation of acetate groups would be a good start in probing the phase behavior of functionalized polyethyleneimines (Figure 9.9).

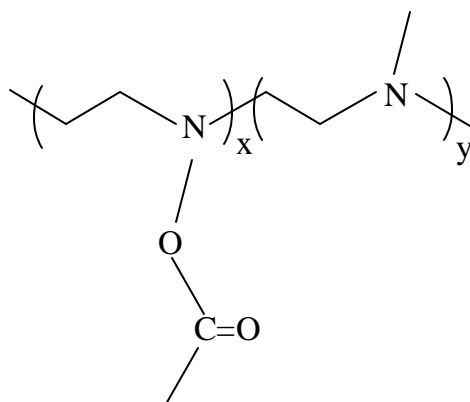


**Figure 9.9** Poly(methylated ethyleneimine-co-acetylated ethyleneimine)

## **APPENDICES**

# A $^1\text{H-NMR}$ SPECTRA OF COPOLYMERS IN CHAPTER 4

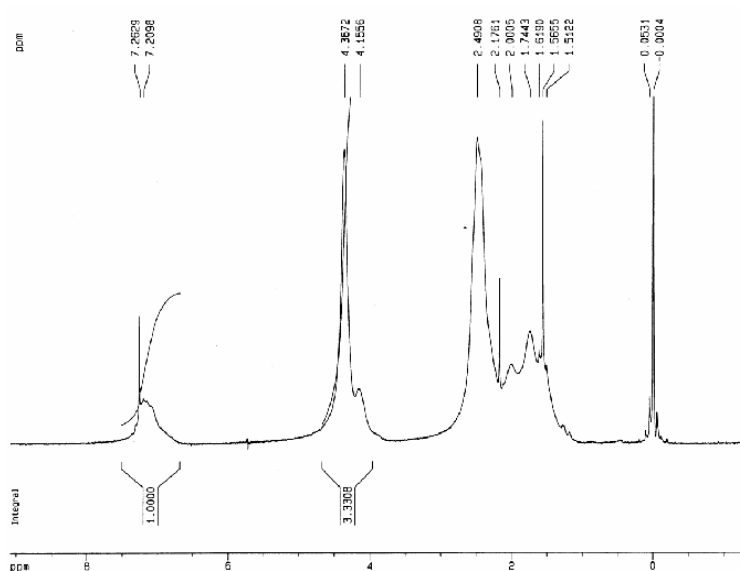


Figure A.1  $^1\text{H-NMR}$  spectrum of St-FA Copolymer in Freon.

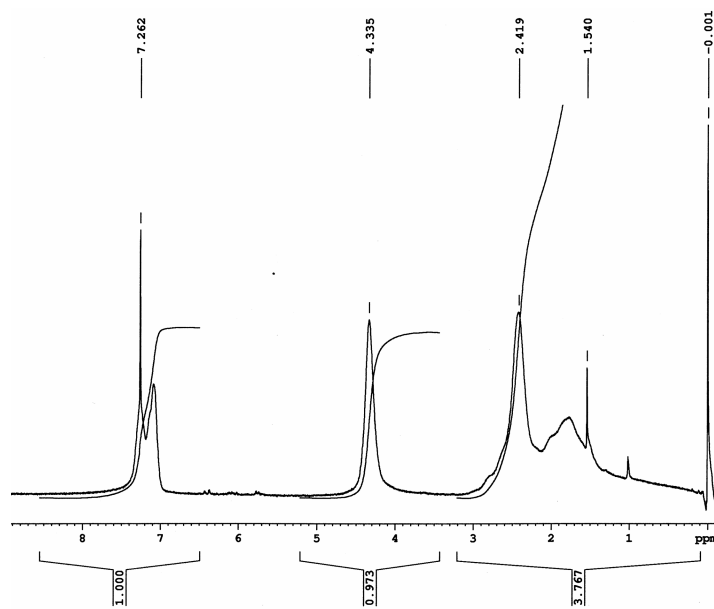
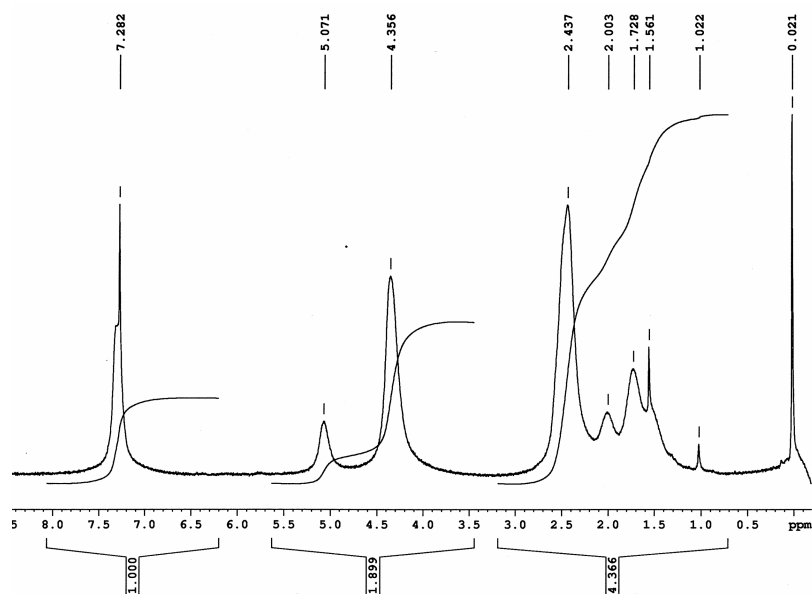
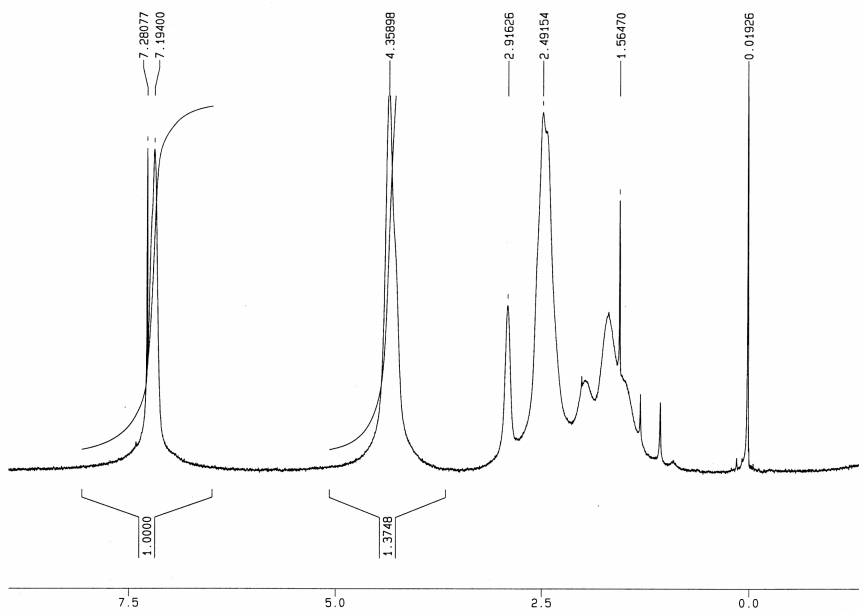


Figure A.2  $^1\text{H-NMR}$  spectrum of 29%PHA-71% Copolymer in Freon



**Figure A.3**  $^1\text{H-NMR}$  spectrum of 21%BEA-79%FA Copolymer in Freon



**Figure A.4**  $^1\text{H-NMR}$  spectrum of 29%PEA-71%FA Copolymer in Freon

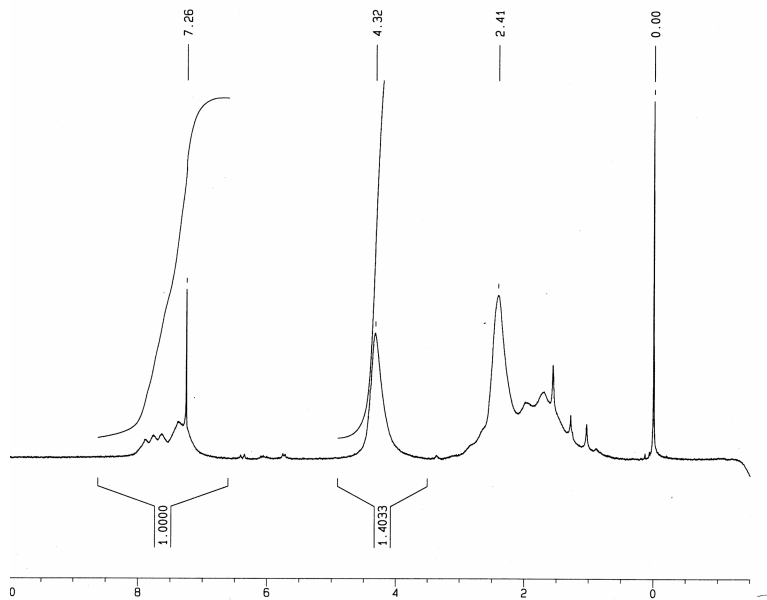


**Figure A.5**  $^1\text{H}$ -NMR spectrum of 17%NA-83%FA Copolymer in Freon

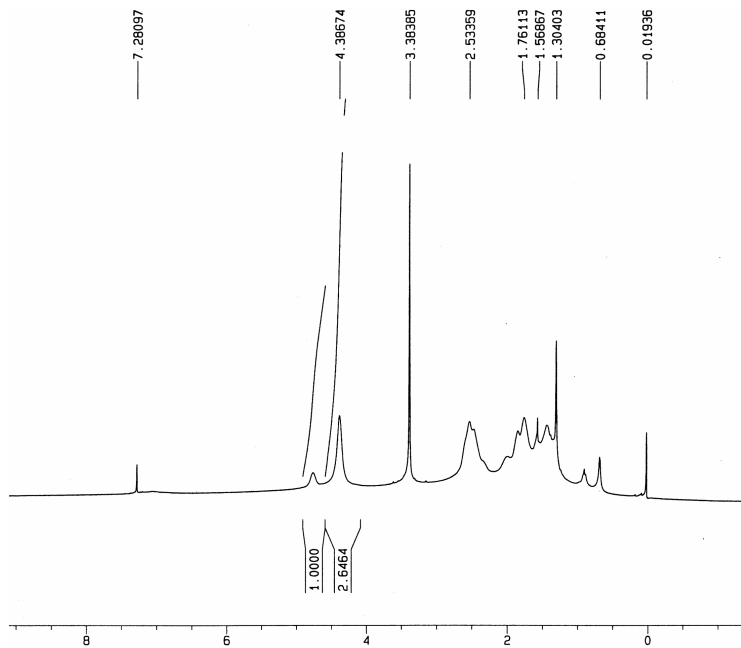


**Figure A.6**  $^1\text{H}$ -NMR spectrum of 27%CHA-73%FA Copolymer in Freon

## B $^1\text{H-NMR}$ AND FT-IR SPECTRA OF SILICONE POLYMERS (CHAPTER 5)

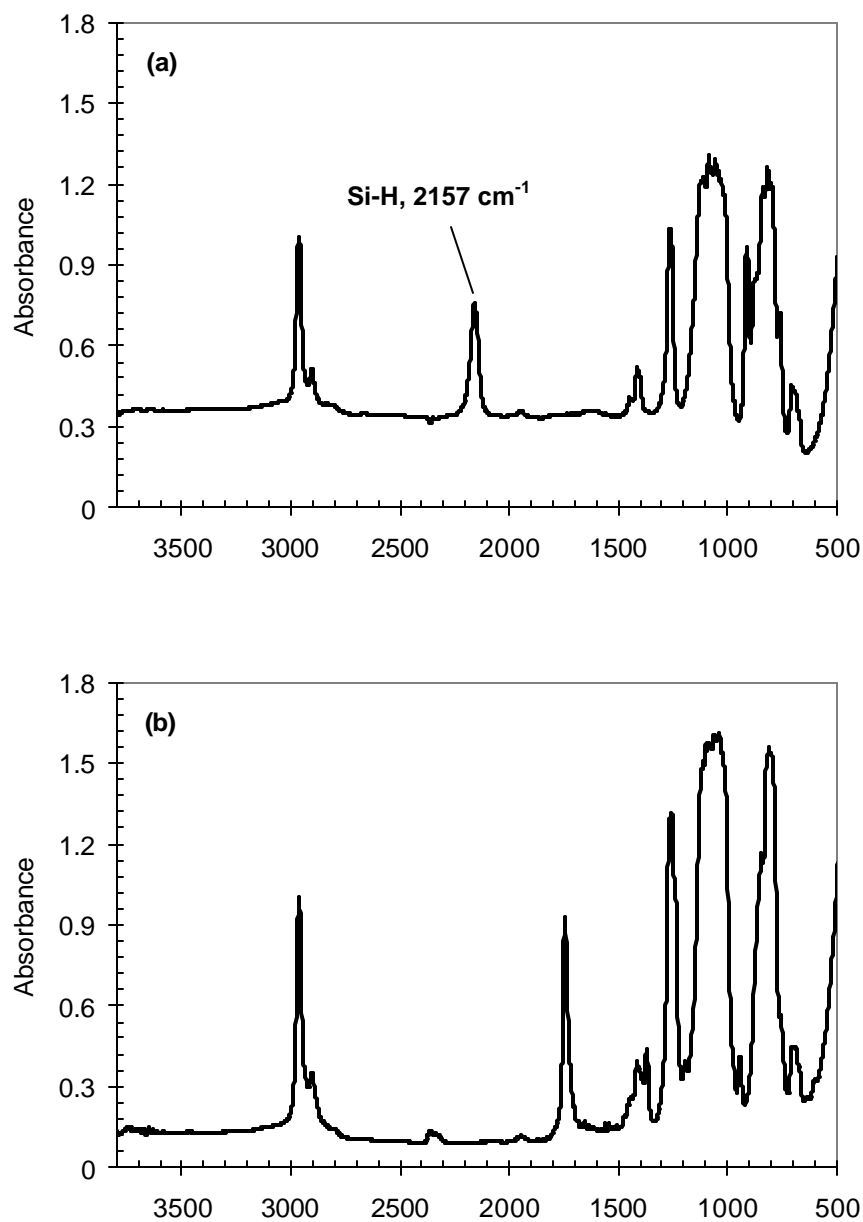


**Figure B.1** FT-IR spectrum for a) methylhydrosiloxane (16.5mole %)-dimethylsiloxane (83.5mole%) copolymer, b) Propyl acetate functionalized siloxane copolymer. The peak at 2157 cm<sup>-1</sup> in Figure 1.a corresponds to Si-H stretching.

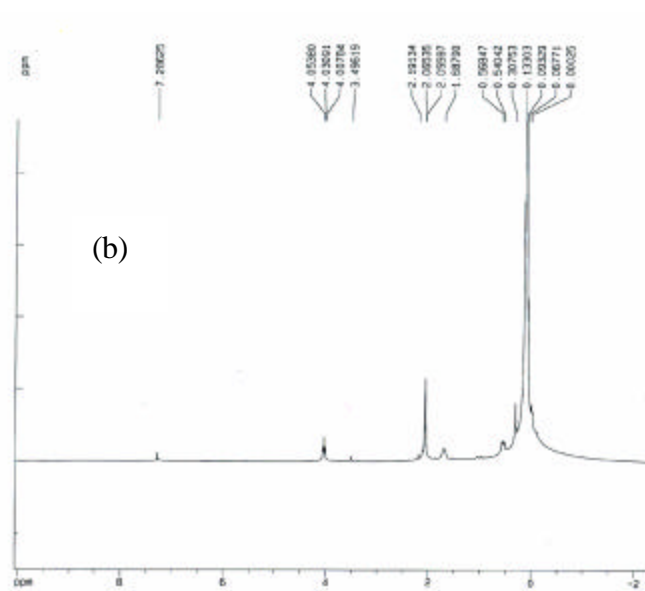
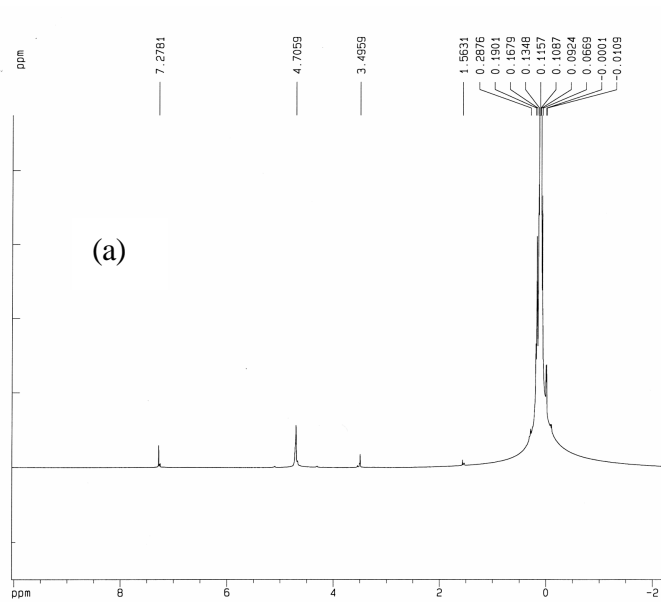


**Figure B.2**  $^1\text{H}$  NMR spectrum (300 MHz,  $\text{CDCl}_3$ ) of a) MethylHydrosiloxane (16.5mole %) - Dimethylsiloxane (83.5mole%) copolymer, The peak at 4.7 ppm corresponds to Si-H. b) (z=5) PA-functionalized siloxane copolymer

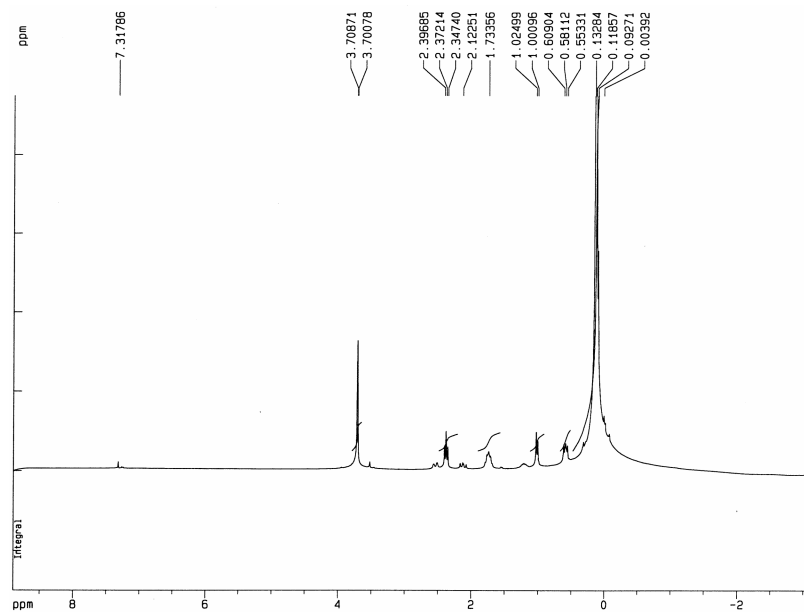


**Figure B.3**  $^1\text{H-NMR}$  spectrum of ( $z=5$ ) MB-functional siloxane copolymer in  $\text{CDCl}_3$

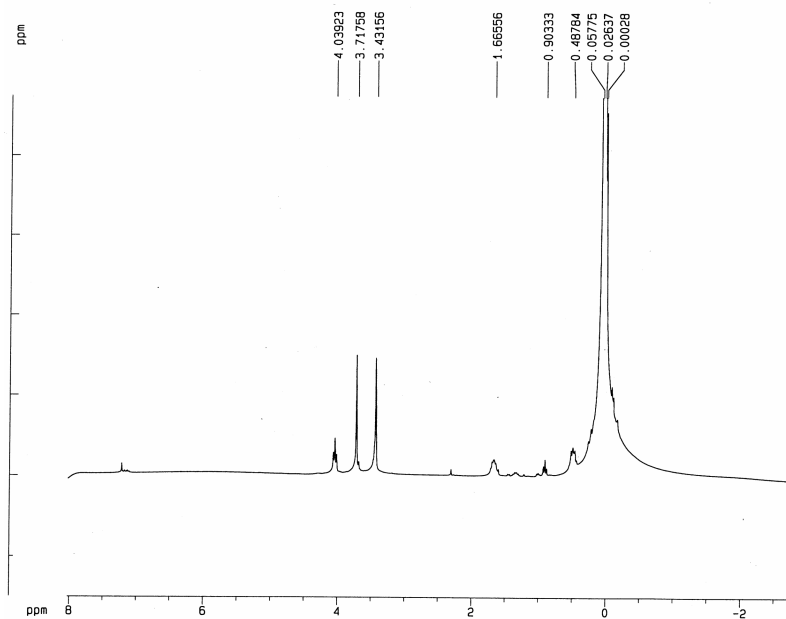


**Figure B.4**  $^1\text{H-NMR}$  spectrum of ( $z=5$ ) PMC-functional siloxane copolymer in  $\text{CDCl}_3$

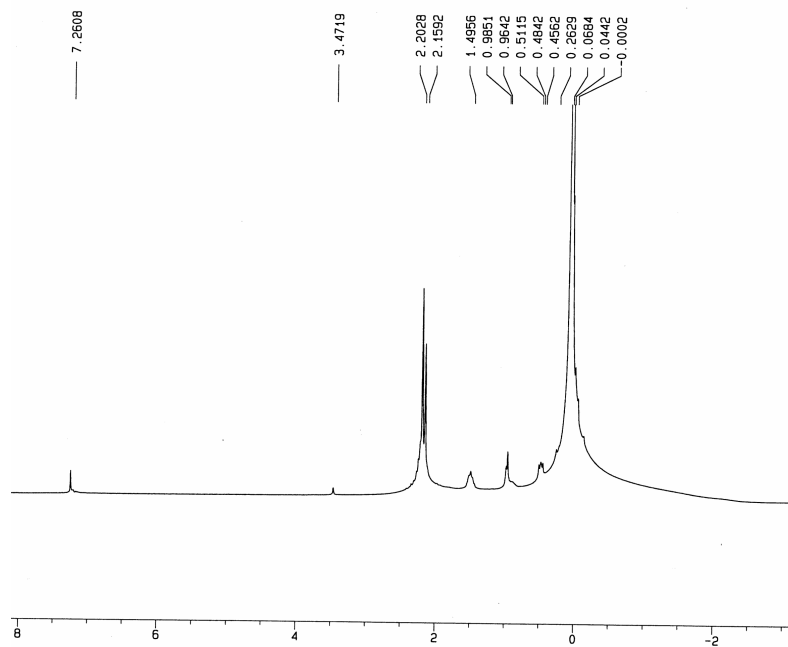


**Figure B.5**  $^1\text{H-NMR}$  spectrum of (z=5) PDA-functional siloxane copolymer in  $\text{CDCl}_3$

## C $^1\text{H-NMR}$ SPECTRA OF NITROGEN CONTAINING POLYMERS (CHAPTER 6)

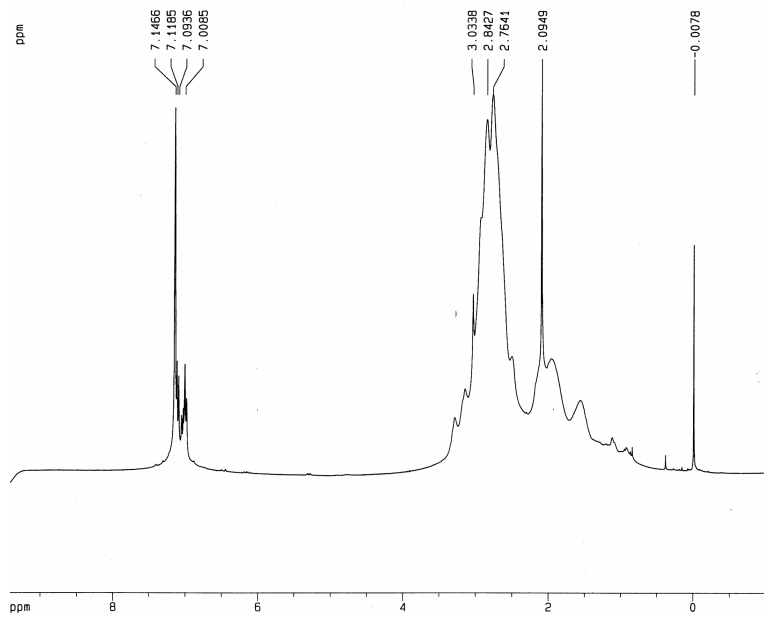


**Figure C.1**  $^1\text{H-NMR}$  Spectrum of Poly(N,N-dimethyl acrylamide) in  $\text{C}_6\text{D}_6$

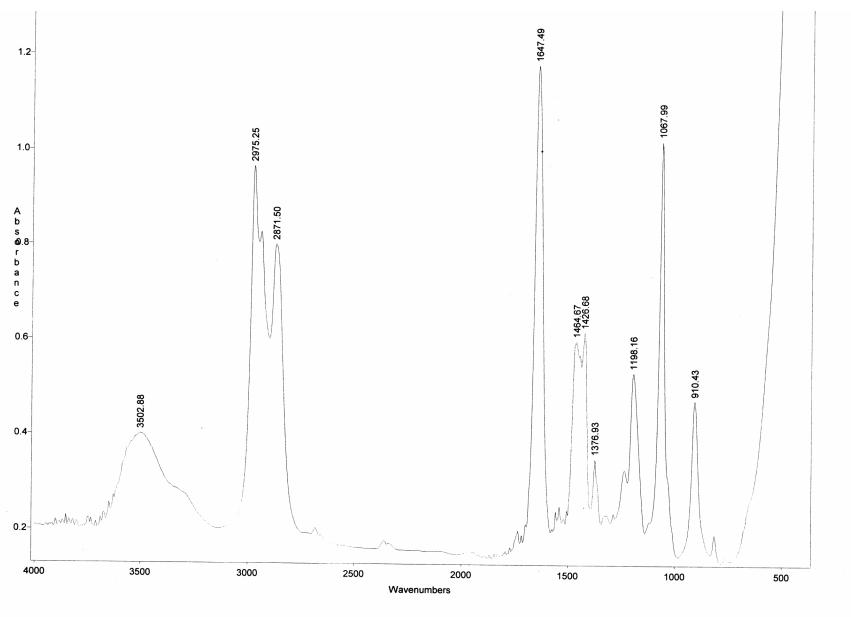


**Figure C.2** FT-IR spectrum of Poly(2-ethyl-2-oxazoline), Mw=5000 (Scientific Polymers, Inc.)

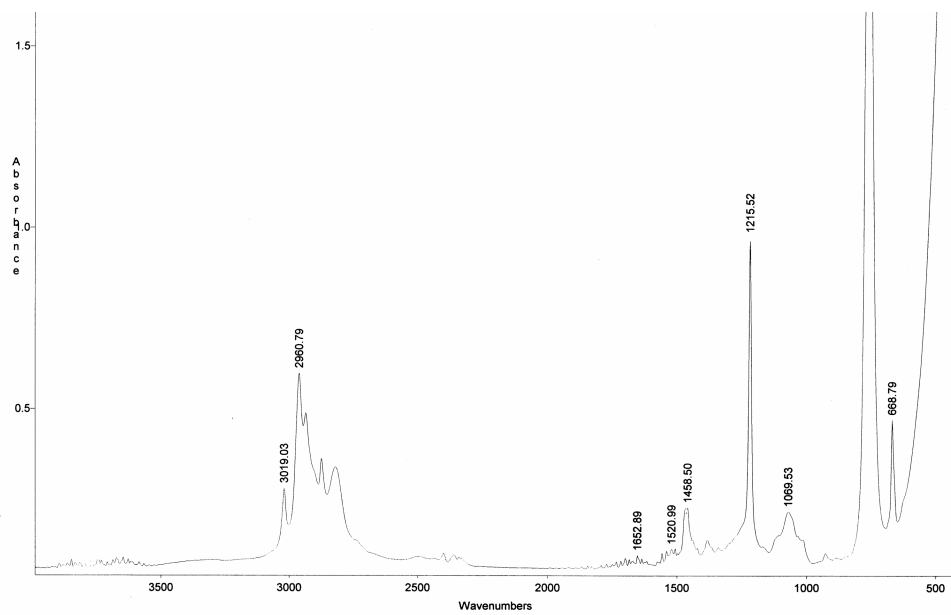


**Figure C.3** FT-IR spectrum of Poly(propylethyleneimine)

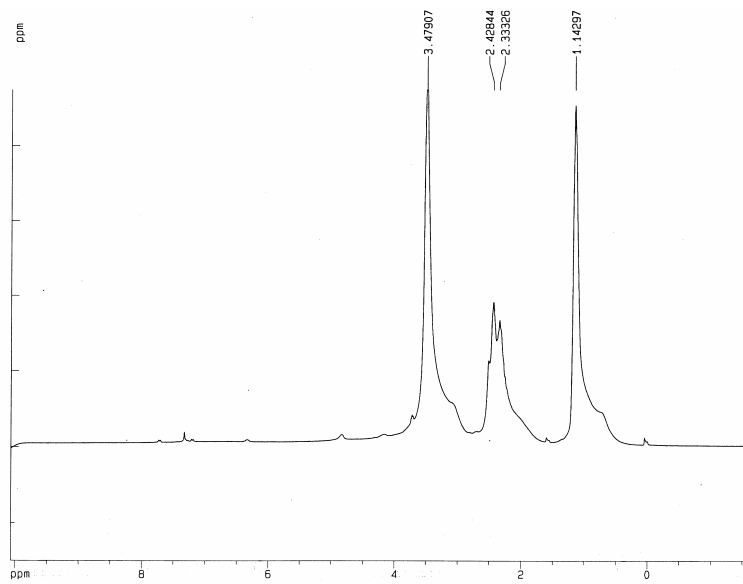


**Figure C.4**  $^1\text{H-NMR}$  spectrum of Poly(2-ethyl-2-oxazoline), Mw=5000 (SP<sup>2</sup> Inc.)

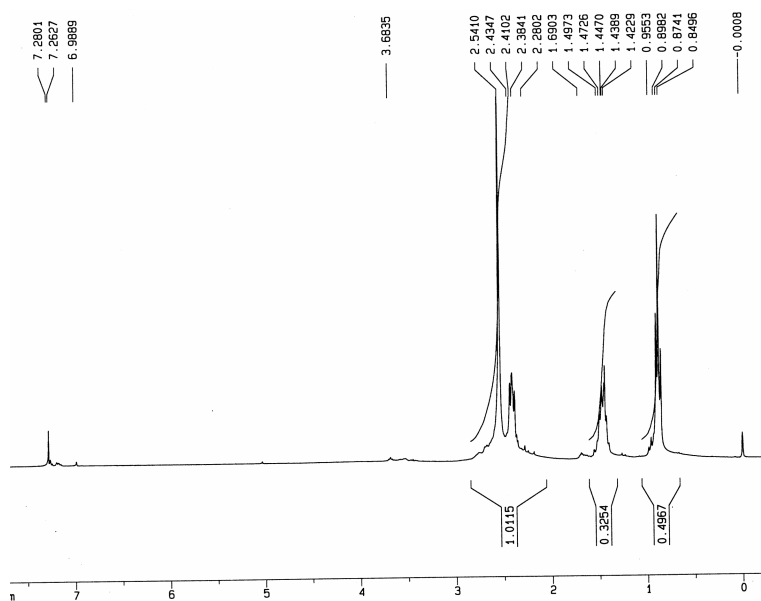


**Figure C.5**  $^1\text{H-NMR}$  spectrum of Poly(propyleneimine) in  $\text{CDCl}_3$

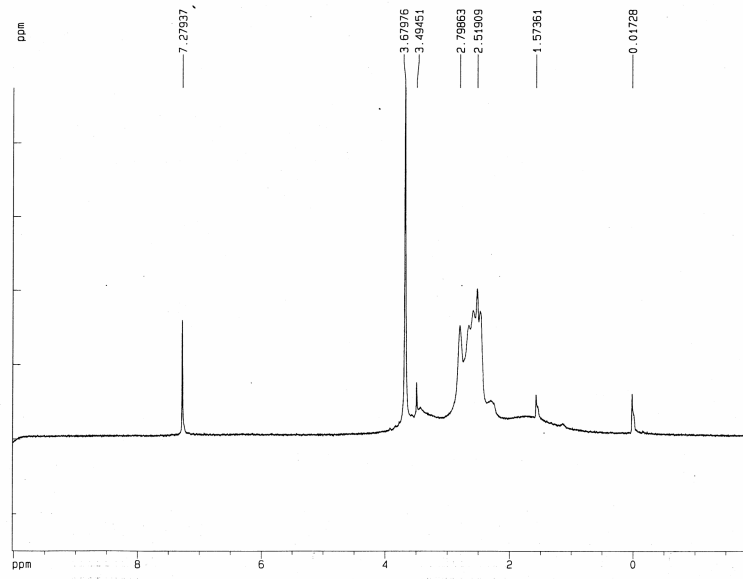


**Figure C.6** <sup>1</sup>H-NMR spectrum of PPMAEI in CDCl<sub>3</sub>

## D $^1\text{H-NMR}$ SPECTRA OF THE POLYMERS IN CHAPTER 7

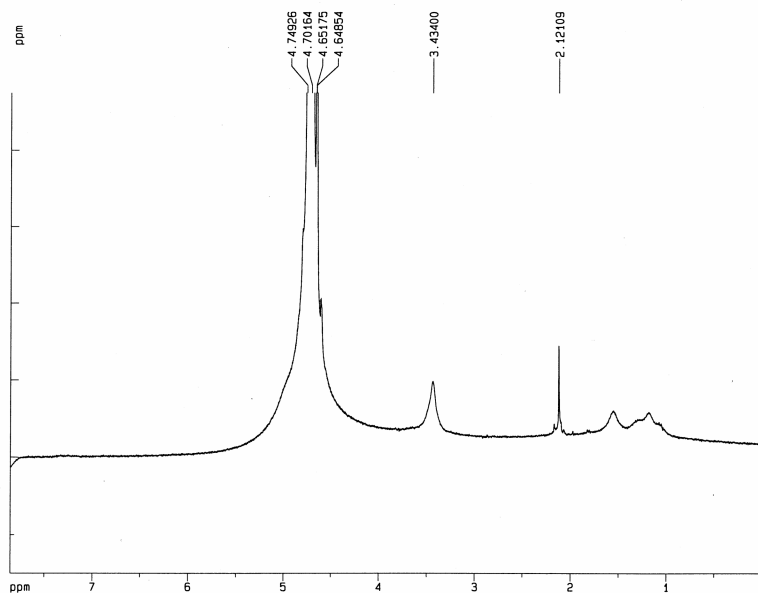


**Figure D.1**  $^1\text{H-NMR}$  spectrum of poly(allyl alcohol) in  $\text{D}_2\text{O}$

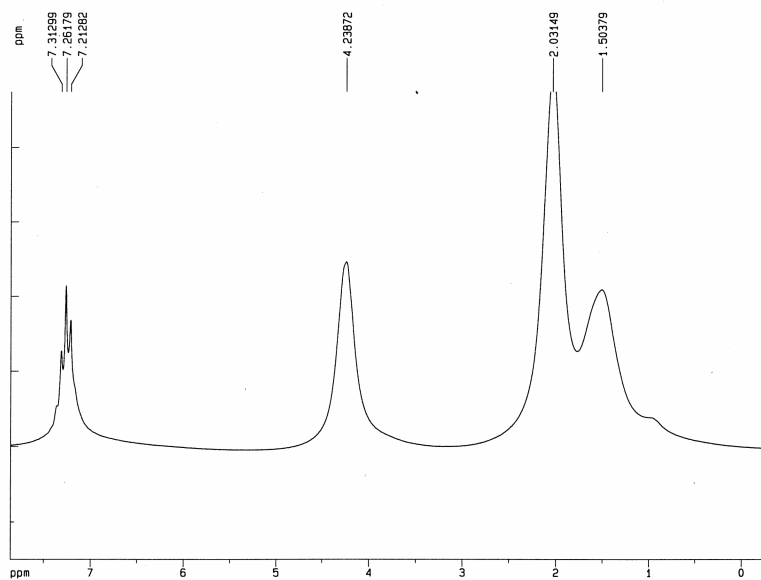


**Figure D.2**  $^1\text{H-NMR}$  spectrum of poly(allyl acetate) in  $\text{C}_6\text{D}_6$

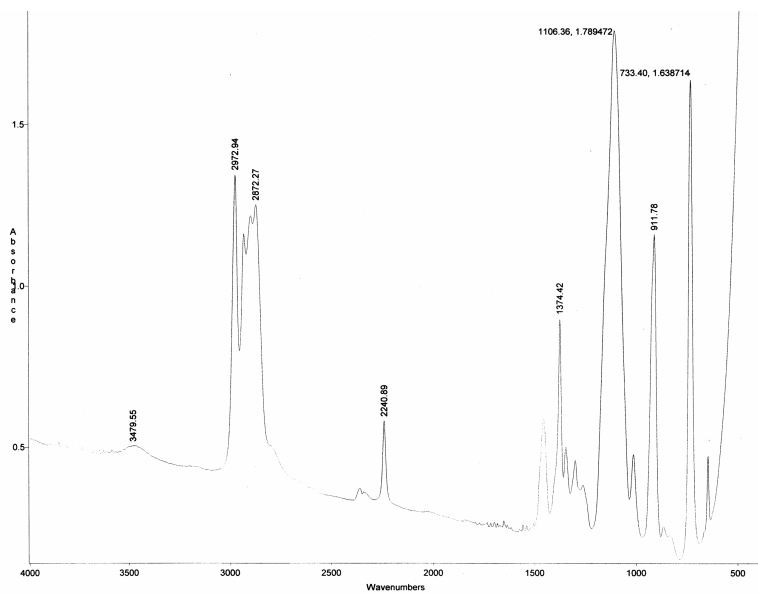


**Figure D.3** FT-IR spectrum of poly(propylene glycol), Mw=3500 (Aldrich)

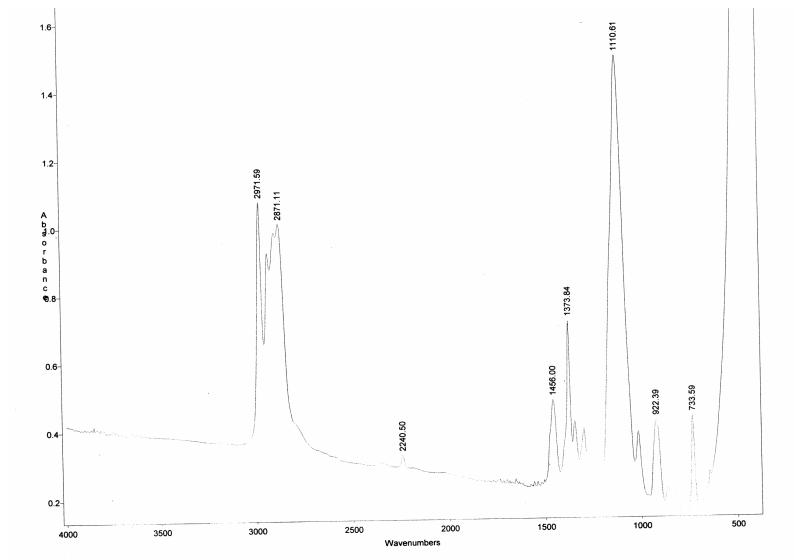


**Figure D.4** FT-IR spectrum of poly(propylene oxide) dimethylether

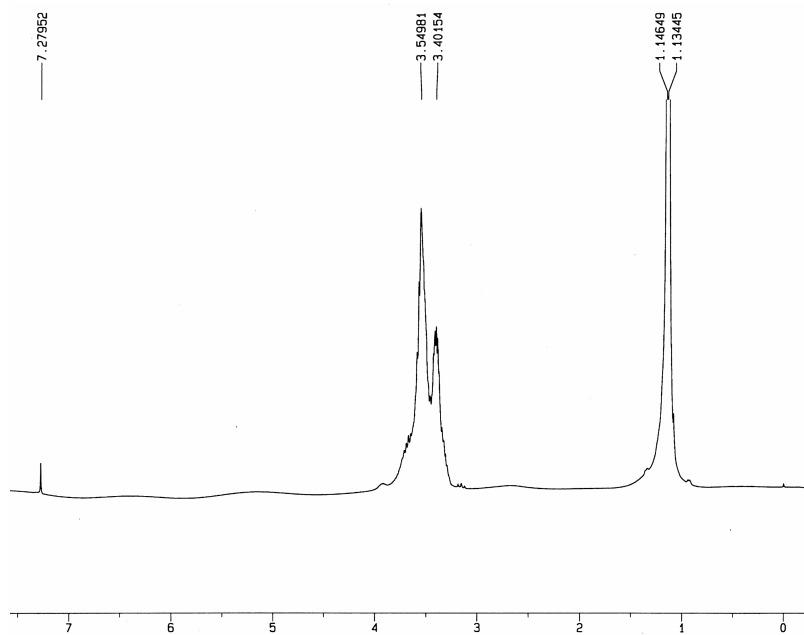


**Figure D.5** <sup>1</sup>H-NMR (CDCl<sub>3</sub>) spectrum of poly(propylene glycol), Mw=3500

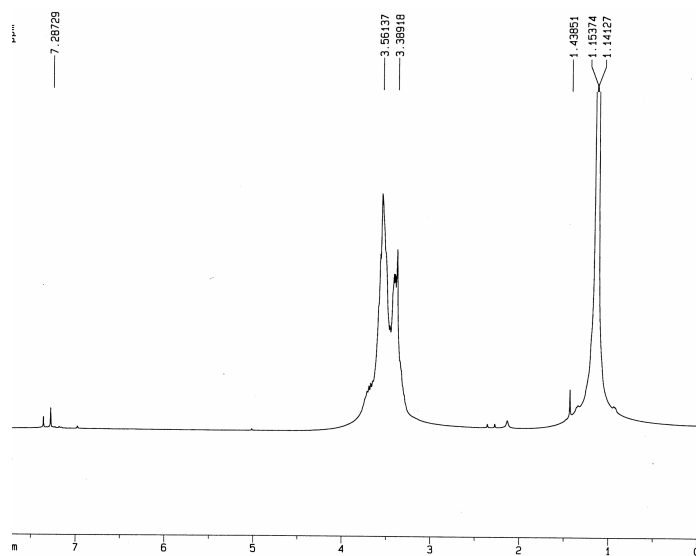


**Figure D.6** <sup>1</sup>H-NMR (CDCl<sub>3</sub>) spectrum of poly(propylene oxide) dimethylether

## BIBLIOGRAPHY

- <sup>1</sup> Vesovic et al., *J. Phys. Chem. Ref. Data* **1990**, 19, 765.
- <sup>2</sup> Beckman, E. J., Unpublished.
- <sup>3</sup> Heller, J. P., Donaruma, L. G., Dandge, D. K., *Poly. Preprints*, **1981**, 22, 59.
- <sup>4</sup> Heller, J. P., Dandge, D. K. Card, R. J., Donaruma, L. G., *SPE J.* **Oct. 1985**, 679.
- <sup>5</sup> Heller, J. P., Dandge, D. K., Card, R. J., Donaruma, L. G., *SPE J.* 11789 **1983**, 173.
- <sup>6</sup> Martin, F., Heller, J. P., PRRC 90-34, Sept. 1990.
- <sup>7</sup> Llave, F. M., Chung, F. T. H., Burchfield, T. E., *SPE Reservoir Eng.* **Feb. 1990**, 47.
- <sup>8</sup> Llave, F. M., Chung, F. T. H., Burchfield, T. E., *SPE/DOE* 17344.
- <sup>9</sup> Bae, J. H., Irani, C. A., *SPE J.* 20467 **Sept. 1990**, 73.
- <sup>10</sup> Harris, T., Irani, C., Pretzer, W., US Patent 4,913,235 **1990**.
- <sup>11</sup> Irani, C., Harris, T., Pretzer, W., US Patent 4,945,990 **1990**.
- <sup>12</sup> Iezzi, A., Enick, R., Brady, J., *Supercritical Fluid. Sci. Tech., ACS Symp. Series*, **1989**, 122.
- <sup>13</sup> Hoefling, T. A., Stofesky, D., Reid, M., Beckman, E., Enick, R. M., *J. Supercritical Fl.* **1992**, 5, 237.
- <sup>14</sup> Vikramanayake, R., Turberg, M., Enick, R., *Fl. Phase Equil.* **1991**, 70, 107.
- <sup>15</sup> Enick, M., *SPE J.*, 21016 **1991**, 149.
- <sup>16</sup> Dunn, P., Oldfield, D. J., *J. Macromol. Sci. Chem.* **1970**, A4(5), 1157.
- <sup>17</sup> Iezzi, A., Bendale, P., Enick, R., Turberg, M., Brady, J., *Fluid Phase Equil.* **1989**, 52, 307.

- <sup>18</sup> Gullapalli, P., Tsau, J., Heller, J. P., *SPE J.* 28979 **1995**, 349.
- <sup>19</sup> Terry, R. E., Zaid, A., Angelos, C., Whitman, D. L., *SPE J.* 16270 **1987**, 289
- <sup>20</sup> DeSimone, J., Guan, Z., Combes, J., Menciloglu, Y., *Macromolecules* **1993**, 26, 2663.
- <sup>21</sup> DeSimone, J., U.S. Patent 5,496,901 **1996**.
- <sup>22</sup> DeSimone, J. M. et al., *Science* **1992**, 257, 945.
- <sup>23</sup> Guan, Z., DeSimone, J. M., *Macromolecules* **1994**, 27, 5527.
- <sup>24</sup> McClain, J. B., Betts, D. E., DeSimone, J. M., *Poly. Preprints* **1996**, 74, 234.
- <sup>25</sup> Enick, R. M.; Beckman, E. J.; Shi, C.; Karmana, E., *J. Supercrit. Fl.* **1998**, 13, 127.
- <sup>26</sup> Huang, H., Shi, C., Xu, J., Kilic, S., Enick, R. M., Beckman, E. J., *Macromolecules* **2000**, 33, 5437.
- <sup>27</sup> Eckert, C. A.; Knutson, B. L.; Debenedetti, P.G.; *Nature* **1996**, 373, 313.
- <sup>28</sup> Consani, K. A.; Smith, R. D.; *J. Supercrit. Fluids* **1990**, 3, 51.
- <sup>29</sup> O'Shea, K. E.; Kirmse, K. M.; Fox, M. A.; Johnston, K. P.; *J. Phys. Chem.* **1991**, 95, 7863.
- <sup>30</sup> Johnston, K. P.; Lemert, R. M.; in *Encyclopedia of Chemical Processing and Design*; ed. J. J. McKetta, Dekker, N.Y., **1996**.
- <sup>31</sup> Francis, A.; *J. Phys. Chem.* **1954**, 58, 1099.
- <sup>32</sup> Hyatt, J. A.; *J. Org. Chem.* **1984**, 49, 5097.
- <sup>33</sup> McClain, J. B.; Londono, D.; Combes, J. R.; Romack, T. J.; Canelas, D. A.; Betts, D. E.; Wignall, G. D.; Samulski, E. T.; DeSimone, J. M.; *J. Am. Chem. Soc.* **1996**, 118, 917.
- <sup>34</sup> Mertdogan, C. A.; Byun, H.; McHugh, M. A.; Tuminello, W. H.; *Macromolecules* **1996**, 29, 6548.
- <sup>35</sup> McHugh, M. A.; Mertdogan, C. A.; DiNoia, T. P.; Anolick, C.; Tuminello, W. H.; Wheland, R.; *Macromolecules* **1998**, 31, 2252.
- <sup>36</sup> Mertdogan, C. A.; DiNoia, T. P.; McHugh, M. A.; *Macromolecules* **1997**, 30, 7511.
- <sup>37</sup> DeSimone, J. M.; Guan, Z.; Elsbernd, C. S.; *Science* **1992**, 267, 945.

- <sup>38</sup> Hoefling, T.; Stofesky, D.; Reid, M.; Beckman, E. J.; Enick, R.M.; *J. Supercrit. Fluids* **1992**, 5, 237.
- <sup>39</sup> Hasio, Y.L.; Maury, E. E.; DeSimone, J. M.; Mawson, S. M.; Johnston, K. P.; *Macromolecules* **1995**, 28, 8159.
- <sup>40</sup> Adamsky, F. A.; Beckman, E. J.; *Macromolecules* **1994**, 27, 312.
- <sup>41</sup> Ghenciu, E. G.; Russell, A. J.; Beckman, E. J.; Steele, L.; Becker, N. T.; *Biotech. Bioeng.* **1998**, 58, 572.
- <sup>42</sup> Johnston, K. P. et al.; *Science* **1996**, 271, 624.
- <sup>43</sup> Yazdi, A. V.; Beckman, E. J.; *Ind. Eng. Chem. Res.* **1997**, 36, 2368.
- <sup>44</sup> Kirby, C. F.; McHugh, M. A.; *Chem. Rev.* **1999**, 99, 565.
- <sup>45</sup> McHugh, M. A.; Park, H.; Reisinger, J. J.; Ren, Y.; Lodge, T. P.; Hillmyer, M. A.; *Macromolecules* **2002**, 35(12), 4653.
- <sup>46</sup> McHugh, M. A.; Garach-Domech, A.; Park, H.; Li, D.; Barbu, E.; Graham, P.; Tsibouklis, J.; *Macromolecules* **2002**, 35 (17), 6479.
- <sup>47</sup> Kazarian, S. G.; Vincent, M. F.; Bright, F. V.; Liotta, C. L.; Eckert, C. A.; *J. Am. Chem. Soc.* **1996**, 118, 1729.
- <sup>48</sup> Nelson, M. R.; Borkman, R. F.; *J. Phys. Chem.* **1998**, 102, 7860.
- <sup>49</sup> Raveendran, P.; Wallen, S. L.; *JACS* **2002**, 124, 12590.
- <sup>50</sup> Sarbu, T.; Styranec, T. J.; Beckman, E. J.; *Ind. Eng. Chem. Res.* **2000**, 39, 4678.
- <sup>51</sup> Sarbu, T.; Styranec, T. J.; Beckman, E. J.; *Nature* **2000**, 405, 165.
- <sup>52</sup> Hu, Y.; Chen, W.; Xu, L.; Xiao, J.; *Organometallics* **2001**, 20, 3206.
- <sup>53</sup> Raveendran, P.; Wallen, S. L.; *JACS* **2002**, 124, 7274.
- <sup>54</sup> Potluri, V. K.; Xu, J.; Enick, R.; Beckman, E.; Hamilton, A. D.; *Org. Letters* **2000**, 4, 2333.
- <sup>55</sup> Rindfleisch, F.; DiNoia, T. P.; McHugh, M. A.; *J. Phys. Chem.* **1996**, 100, 15581.
- <sup>56</sup> Shen, Z.; McHugh, M. A.; Xu, J.; Belardi, J.; Kilic, S.; Mesiano, A.; Bane, S.; Karnikas, C.; Beckman, E. J.; Enick, R. M.; *Polymer* **2003**, 44, 1491.

- <sup>57</sup> Desiraju, G. R., *The Crystal as a Supramolecular Entity*, John Wiley & Sons: Chichester, **1995**
- <sup>58</sup> Hunter, C. A., Sanders, J. K. M., *J. Am. Chem. Soc.* **1990**, 112, 5525.
- <sup>59</sup> Cozzi, F.; Cinquini, M.; Annuziata, R.; Siegel, J. S.; *J. Am. Chem. Soc.* **1993**, 115, 5330
- <sup>60</sup> Petsko, G. A., Burley, S. K., *J. Am. Chem. Soc.* **1986**, 108, 7995.
- <sup>61</sup> Gould, R. O., Gray, A. M., Taylor, P., Walkinshaw, M. D., *J. Am. Chem. Soc.* **1985**, 107, 5921.
- <sup>62</sup> Weber, E., *Topics in Current Chemistry: Design of Organic Solids*, Springer: Germany, **1998**
- <sup>63</sup> Heard, G. L.; Boyd, R. J.; *J. Phys. Chem.* **1997**; 101, 5374.
- <sup>64</sup> Trujillo, J. H.; Vela, A.; *J. Phys. Chem.* **1996**; 100, 6524.
- <sup>65</sup> Kool, E. T. et al., *J. Am. Chem. Soc.* **1996**, 118, 8182.
- <sup>66</sup> Taylor, D. K.; Keiper, J. S.; DeSimone, J. M., *Ind. Eng. Chem. Res.* **2002**, 41, 4451.
- <sup>67</sup> Allada, S. R. *Ind. Eng. Chem. Process Des. Dev.* **1984**, 23, 344.
- <sup>68</sup> O'Neill, M. L., Cao, Q., Fang, M., Johnston, K. P. et al., *Ind. Eng. Chem., Res.* **1998**, 37, 3067.
- <sup>69</sup> Kauffman, J. F., *J. Phys. Chem. A* **2001**, 105, 3433.
- <sup>70</sup> Hoefling, T. A.; Newman, D. A.; Enick, R. M.; Beckman, E. J., *J. Supercrit. Fluids* **1993**, 6, 165.
- <sup>71</sup> Yee, G. G.; Fulton, J. L.; Smith, R. D. *J. Phys. Chem.* **1992**, 96, 6172.
- <sup>72</sup> Dardin, A.; DeSimone, J. M.; Samulski, E. T.; *J. Phys. Chem. B* **1998**, 102, 1775.
- <sup>73</sup> Bothner-By, A. A.; Glick, R. E.; *J. Am. Chem. Soc.* **1958**, 78, 1071.
- <sup>74</sup> Yonker, C. R.; Palmer, B. J.; *J. Phys. Chem. A* **2001**, 105, 308.
- <sup>75</sup> Cece, A.; Jureller, S. H.; Kerscher, J. L.; Moschner, K. F., *J. Phys. Chem.* **1996**, 100, 7435.
- <sup>76</sup> Diep, P.; Jordan, K. D.; Johnson, J. K.; Beckman, E. J., *J. Phys. Chem. A* **1998**, 102, 2231.
- <sup>77</sup> Raveendran, P.; Wallen, S. L. *J. Phys. Chem. B.* **2003**, 107, 1473.

- <sup>78</sup> Fried, J. R.; Hu, N., *Polymer* **2003**, 44, 4363.
- <sup>79</sup> Rindfleisch, F., DiNoia, T. P., McHugh, M. A., *J. Phys. Chem.* **1996**, 100, 15581.
- <sup>80</sup> Dobrowolski, J. C.; Jamroz, M. H. *J. Mol. Struct.* **1994**, 275, 211.
- <sup>81</sup> Reilly, J. T.; Bokis, C. P.; Donohue, M. D. *Int. J. Thermophys.* **1995**, 16, 599.
- <sup>82</sup> Meredith, J. C.; Johnston K. P.; et al., *J. Phys. Chem.* **1996**, 100, 10837.
- <sup>83</sup> Bicerona, J.; *Prediction of Poly. Properties*; 2<sup>nd</sup> Ed., Marcel Dekker, Inc., New York, **1996**.
- <sup>84</sup> Charlet, G., Ducasse, R., Delmas, G., *Polymer* **1981**, 22, 1190.
- <sup>85</sup> Lepilleur, C., Beckman, E.J., Schonemann, H., Krukonis, V. J., *Fluid Phase Equil.* **1997**, 134, 285.
- <sup>86</sup> Makowski, H. S., Lundberg, R. D., Singhal, G. H., US Patent 3,870,841.
- <sup>87</sup> Storey, R. F., Lee, Y., *J. Polym. Sci.: Part A: Poly. Chem.* **1993**, 31, 31.
- <sup>88</sup> Orler, E. B., Yontz, D. J., Moore, R. B., *Macromolecules* **1993**, 26, 5157.
- <sup>89</sup> Azukizawa, M., Yamada, B., Hill, D. J. T., Pomery, P. J., *Macromol. Chem. Phys.* **2000**, 201, 774.
- <sup>90</sup> Yamada, B., Azukizawa, M., Yamazoe, H., Hill, D. J. T., Pomery, P. J., *Polymer* **2000**, 41, 5611.
- <sup>91</sup> Ahmad, N. M., Heatley, F., Lovell, P. A., *Macromol* **1998**, 31, 2822.
- <sup>92</sup> Britton, D., Heatley, F., Lovell, P. A., *Macromol.* **1998**, 31, 2828.
- <sup>93</sup> Sen, Y. L.; Kiran, E. J.; *J. Supercrit. Fluids* **1990**, 3, 91.
- <sup>94</sup> Sutterby, J. L., *AIChE* **1966**, 12, 63.
- <sup>95</sup> Mecozzi, S.; West, A. P.; Dougherty, D. A.; *J. Am. Chem. Soc.* **1996**, 118, 2307.
- <sup>96</sup> D. Quinonera, C. Garau, C. Rotger, A. Frontera, P. Ballester, A. Costa, P. M. Deya; *Angew. Chem. Int. Ed.* **2002**, 41, 3389.
- <sup>97</sup> Ma, J. C.; Dougherty, D. A.; *Chem. Rev.* **1997**, 97, 1303.

- <sup>98</sup> Dougherty, D. A., *Science* **1996**, 271, 163.
- <sup>99</sup> Norman, R.; Coxon, J. M.; *Principles of organic synthesis; 3<sup>rd</sup> Ed.*, N.Y.: Blackie Academic & Professional, **1993**
- <sup>100</sup> McDaniel, D. H.; Brown, H. C.; *J. Org. Chem.* **1958**, 23, 420.
- <sup>101</sup> Buhler, E., Dobrynin, A. V., DeSimone, J. M., Rubinstein, M.; *Macromolecules* **1998**, 31, 7347.
- <sup>102</sup> Barcenas, G., Meredit, J. C., Sanchez, I. C., Johnston, K. P., et al., *J. Chem. Phys.* **1997**, 107, 10782.
- <sup>103</sup> Fink, R.; Hancu, D.; Valentine, R.; Beckman, E. J.; *J. Phys. Chem. B.* **1999**, 103, 6441.
- <sup>104</sup> Zhao, X.; Watkins, R.; Barton, S. W.; *J. Appl. Poly. Sci.* **1995**, 55, 773.
- <sup>105</sup> Bunnell, J.; Ford, T. A.; *J. Mol. Spect.* **1983**, 100, 215.
- <sup>106</sup> Abraham, R. J.; Grant, G. H., *J. Comp. Chem.* **1988**, 9, 709.
- <sup>107</sup> Walsh, R., *Acc. Chem. Res.* **1981**, 14, 246.
- <sup>108</sup> Margrave, J. L.; Wilson, P. W., *Acc. Chem. Res.* **1971**, 4, 145.
- <sup>109</sup> Sigman, M. E.; Lindley, S. M.; Leffler, J. E.; *J. Am. Chem. Soc.* **1985**, 107, 1471.
- <sup>110</sup> Phillips, J. H.; Robey, R. J.; *J. Chromat.* **1989**, 465, 177.
- <sup>111</sup> Kilic, S.; Michalik, S.; Wang, Y.; Johnson, K. J.; Enick, R. M., Beckman, E. J.; *Ind. Eng. Chem. Res.*, in press.
- <sup>112</sup> Streitwieser, A.; Heathcock, C. H.; *Intro. Org. Chem.*; MacMillan Publishing Co., N.Y., **1976**
- <sup>113</sup> Drohman, C.; Beckman, E. J.; *J. Supercrit. Fluids* **2002**, 22, 103.
- <sup>114</sup> Gutmann, V.; *Coord Chem. Rev.* **1976**, 18, 225.
- <sup>115</sup> Van Krevelen, D. W.; *Prop. Polym.*; Elsevier Sci. Publishers, Netherlands, **1990**.
- <sup>116</sup> Li, D.; Brittain, W. J.; *Macromolecules* **1998**, 31, 3852.
- <sup>117</sup> Smith, M. B.; March, J.; *March's Advanced Organic Chemistry: Reactions, Mechanisms, and Structure*, Wiley, John & Sons, **2000**.

- <sup>118</sup> Kwiatkowski, S.; Jeganathan, A.; Tobin, T.; Watt, D. S.; *Syn. Commun.* **1989**, 946.
- <sup>119</sup> Farahani, M.; Antonucci, J. M.; Karam, L. R.; *J. Appl. Polym. Sci.* **1998**, 67, 1545.
- <sup>120</sup> Sauer, B. B.; Dee, G. T.; *Macromolecules* **2002**, 35, 7024.
- <sup>121</sup> Rosa, A. D.; Heux, L.; Cavaille, J. Y.; *Polymer* **2000**, 41, 7547.
- <sup>122</sup> Cohen, H. L.; Borden, D. G.; Minsk, L. M.; *J. Org. Chem.* **1960**, 26, 1274.
- <sup>123</sup> Quach, L.; Otsu, T.; *J. Poly. Sci. Poly. Chem. Ed.* **1982**, 20, 2501.
- <sup>124</sup> Michalik, Stephen J. *M.S. Thesis*, University of Pittsburgh, August **2003**.
- <sup>125</sup> Brown, C. A.; Barton, D.; *Synthesis* **1974**, 434.
- <sup>126</sup> Berins, M. L.; *SPI Plastics Engineering Handbook of the Society of the Plastics Industry, Inc.*, 5<sup>th</sup> Ed., Kluver Academic Publishers, Norwell, MA, **1991**.
- <sup>127</sup> Brandup, J.; Immergut, E. H.; Grulke, E. A.; *Polymer Handbook*, 4<sup>th</sup> Ed., New York : Wiley, **1999**.
- <sup>128</sup> Knovel Engineering and Scientific Online References Database
- <sup>129</sup> Lora, M.; Rindfleisch, F.; McHugh, M. A.; *J. App. Poly. Sci.* **1999**, 73, 1979.
- <sup>130</sup> Phase behavior of the polymer was tested by a fellow at Virginia Commonwealth University
- <sup>131</sup> Vandenberg, E. J.; Mullis, J. C.; Juvet, R. S.; Miller, T.; Nieman, R. A.; *J. Poly. Sci. Poly. Chem.* **1989**, 27, 3113.
- <sup>132</sup> Wicks, D. A.; Tirrell, D. A.; *Poly. Prep.* **1985**, 26, 155.
- <sup>133</sup> Wojtowicz, J. A.; Polak, R. J.; *J. Org. Chem.* **1973**, 38, 2061.
- <sup>134</sup> Takeuchi, D.; Aida, T.; *Macromolecules* **1996**, 29, 8096.